On Receptor Kinase Interactions and Complex Formations

Inauguraldissertation
zur Erlangung des Doktorgrades
der Mathematisch-Naturwissenschaftlichen Fakultät
der Heinrich-Heine-Universität Düsseldorf

vorgelegt von

Marc Somssich

aus Freiburg im Breisgau

Düsseldorf, August 2014

Aus dem Institut für Entwicklungsgenetik
der Heinrich-Heine-Universität Düsseldorf

Gedruckt mit der Genehmigung der
Mathematisch-Naturwissenschaftlichen Fakultät der
Heinrich-Heine-Universität Düsseldorf

Referent: Professor Dr. Rüdiger Simon
Korreferent: Professor Dr. Georg Groth

Tag der mündlichen Prüfung: 18.11.2014

I. Eidesstattliche Erklärung:

Eidesstattliche Erklärung zur Dissertation mit dem Titel:
„On Receptor Kinase Interactions and Complex Formations"

Hiermit erkläre ich, dass ich diese Dissertation selbstständig verfasst und keine anderen als die angegebenen Hilfsmittel genutzt habe. Alle wörtlich oder inhaltlich übernommenen Stellen habe ich als solche gekennzeichnet.
Ich versichere außerdem, dass ich diese Dissertation nur in diesem und keinem anderen Promotionsverfahren eingereicht habe und, dass diesem Promotionsverfahren kein gescheitertes Promotionsverfahren vorausgegangen ist.

_____ _____

Ort, Datum Unterschrift

II. Index:

III. Aims of this Study:

The aim of this study is a detailed analysis of the interactions between the CLAVATA receptors of *Arabidopsis thaliana*.

In *A. thaliana*, stem cell homeostasis is regulated through the CLAVATA (CLV) - WUSCHEL (WUS) negative feedback loop. The homeobox transcription factor WUS is a positive regulator of stem cell fate and is negatively regulated by the small signaling peptide CLAVATA3 (CLV3). CLV3 signals through the plasmamembrane (PM)-localized receptor-like proteins CLAVATA1 (CLV1), CLAVATA2 (CLV2) and CORYNE (CRN). From previous studies it is known that all three of these proteins can interact with themselves to form homomers. Furthermore, it was shown that CRN forms heteromers with both CLV1 and CLV2, while CLV1 and CLV2 cannot directly interact. These interactions have been shown in static experiments, lacking the temporal dimension. Therefore it was not possible to monitor changes in the interacting state or the intracellular localizations of the receptors in response to ligand availability. These temporal and spatial dynamics are to be explored in this study.

To do this, multi-parameter fluorescence imaging spectroscopy (MFIS) will be applied to monitor the fluorescent protein tagged receptors intracellular localizations and their interacting state following treatment with the ligand CLV3 over time in single living plant cells. As this has never been done before in living plant cells the development and establishment of a suitable MFIS setup will be the first step in this study. Once the setup is established, the measurements will be performed and the data analyzed.

In a second experiment to closer examine the CLV-pathway a functional analysis of the CRN protein kinase will be performed. Of the three receptor-like proteins in the CLV-pathway the function of CRN remains obscure. CLV1 is a full receptor-like kinase, which has been shown to bind CLV3 and autophosphorylate following ligand perception. CLV2 is a receptor-like protein that possesses the capability to bind CLV3. CRN is a protein kinase, which appears to be a signaling inactive pseudokinase. Accordingly it does not autophosphorylate in response to CLV3 availability. CLV2 and CRN must interact in order for the two proteins to get exported from the endoplasmic reticulum (ER) to the PM, where CLV2 can act as a (co-) receptor. The function of CRN at the PM however is not understood so far.

To examine the role of CRN and its predicted protein domains in the CLV-pathway, several manipulated variants of this protein will be constructed and probed for their ability to interact with CLV2, relocalize from the ER to the PM and complement the *crn* mutant phenotype. This will help to assign specific functions to the CRN protein and its intramolecular domains.

The results obtained from these experiments will contribute to a better understanding of stem cell homeostasis in plants. The development of a MFIS setup to monitor receptor proteins and their interactions over time in single living plant cells additionally will open up new possibilities to the plant science community.

IV. Chapter 1: Dynamics of ligand dependent or independent assembly of flagellin and CLAVATA3 receptor complexes

1. Introduction:

In multicellular organisms growth and development is based on the coordination of cell proliferation and differentiation between single cells and within tissues. In every developmental step, communication between cells is essential. In plants, several signal transduction pathways have been described that play a major role in coordinating growth or responses to various stimuli. Many of those involve small signaling peptides, which are perceived by receptor-like kinase (RLK) proteins, which then transduce the signal into the cells. The flagellin (flg) and CLAVATA (CLV) pathways are two prominent examples of RLK-mediated peptide signal transduction in *Arabidopsis thaliana*.

In plant defense against bacterial pathogens, the leucin-rich repeat (LRR)-RLK FLAGELLIN-SENSING 2 (FLS2) and its co-receptor, the LRR-RLK BRI1-ASSOCIATED KINASE 1 (BAK1) aid to detect the presence of potential pathogens (Chinchilla et al., 2007). Both proteins consist of an extracellular LRR receptor domain, a transmembrane domain (TMD) that integrates into the plasmamembrane (PM) and an intracellular kinase domain, necessary for signal transduction within the cell (Li et al., 2002, Gomez-Gomez et al., 2000). While the FLS2 LRR receptor domain consists of 28 LRRs, the BAK1 LRR receptor domain is truncated to 5 LRRs, indicating that BAK1 may act as a co-receptor (Gomez-Gomez et al., 2001, Nam et al., 2002). In the absence of the ligand flg22, a 22 amino acid peptide of the bacterial flagellin (flg), BAK1 is sequestered by BAK1-Interacting RLK 2 (BIR2), thereby preventing interaction with FLS2 (Halter et al., 2014). BIR2, like BAK1, carries a truncated LRR receptor domain, and the BAK1-BIR2 complex is therefore not likely to bind a ligand independently of a full-size receptor. BIR2 appears to carry a non-functional kinase domain, since it lacks two of the three conserved glycines in the g-loop that are necessary for ATP-binding. BIR2 is probably not involved in active signaling, but could act as a negative regulator of BAK1 and prevent interaction with FLS2 until flg22 is detected. So far it is not clear if the BAK1/BIR2 complex is a heterodimer, containing one BAK1 and BIR2 molecule each, or if they form higher-order complexes. For FLS2, the interacting state prior to ligand binding is not fully understood. Sun et al. utilized co-immunoprecipitation (co-IP) experiments to show that some FLS2 molecules can participate in the formation of homomeric FLS2-FLS2 complexes. Ali et al. investigated FLS2 complex formation in

protoplasts using FRET and FRAP, but could not detect significant FLS2 homomeric complexes using this method. Both BAK1 and FLS2 interact with the cytoplasmic kinase BIK1 independent of flg22 (Lu et al., 2010). Upon perception of flg22, BAK1 is released from BIR2 and complexes with FLS2 at the PM (Ali et al., 2007, Sun et al., 2012). Transphosphorylation between the FLS2/BAK1 complex and BIK1 allows release of BIK1 from the complex to initiate downstream signal propagation.

A similar mechanism, also involving BAK1 as a co-receptor, has been described for the brassinosteroid (BR) signaling pathway. Here, the main BR receptor BRASSINOSTEROID INSENSITIVE 1 (BIR1), a PM localized LRR-RLK, can bind BR via its LRR receptor domain (Clouse et al., 1996, Kinoshita et al., 2005). This binding leads to a conformational change in the receptor-domain of BRI1, enabling BRI1 to recruit BAK1 (Nam et al., 2002, Wang et al., 2005). The formed BRI1-BAK1 complex then becomes signaling active through transphosphorylation of the receptor kinase domains (Wang et al., 2008).
It both cases, it is suggested that binding of the ligand results in the formation of signaling active receptor complexes, with the ligand acting as a molecular glue to fix the receptors in an active state. However, it is not known if this is a general mechanism how all LRR-RLKs are activated. Alternatively, preformed receptor complexes may already exist, as was indicated already for FLS2, that are only activated by ligand binding. Investigation of the behaviour of further LRR-RLKs could help to resolve this question.

The CLAVATA (CLV) pathway is the key regulatory pathway for stem cell homeostasis in floral and shoot apical meristems (SAM) of *A. thaliana*. CLAVATA3 (CLV3) encodes a precursor protein that is processed into a 13 amino acid peptide, which is further modified by addition of sugar moieties to hydroxyproline residues. The mature CLV3 peptide is secreted from stem cells, and perceived by the CLAVATA1 (CLV1), CLAVATA2 (CLV2) and CORYNE (CRN) receptor-like proteins in underlying cells of the organizing center (OC) (Clark et al., 1997, Clark et al., 1995, Kayes et al., 1998, Müller et al., 2008, Fletcher et al., 1999). There, the signal is transmitted intracellularly to control and repress the expression of the stem cell regulatory transcription factor WUSCHEL (WUS) (Brand et al., 2000, Mayer et al., 1998). *CLV1* encodes an RLK with an extracellular LRR-receptor domain that can bind the peptide CLV3 (Ogawa et al., 2008), a TMD that integrates into the PM and an intracellular kinase domain for downstream signaling. Protein interaction studies showed that CLV1 preferentially forms homomers at the PM (Bleckmann et al., 2010). CLV2 PM-localizes via a TMD and carries an extracellular LRR-receptor domain which can interact with a range of different peptides of the CLV3-related CLE family (Guo et al., 2010). CLV2

carries a short juxtamembrane domain on the intracellular side, but lacks a kinase domain. CRN is also PM-localized through its TMD, but lacks an extracellular LRR-receptor domain. CRN was described to be a pseudokinase, since the kinase domain does not have the conserved g-loop which is required for ATP-binding. Additionally, the activation segment is truncated and the Mg^{2+} binding motif is not conserved (Nimchuk et al., 2011). Accordingly, CRN was suggested to act as a co-receptor for CLV2. CLV2 and CRN were shown to physically interact via their TMDs, and this interaction was found to be required for the export of both proteins from the ER towards the PM. Genetic data indicate that the CLV2/CRN complex functions in parallel with and independently from CLV1 in the perception of the CLV3 signal. However, the two pathways also appear to crosstalk, which could be mediated by a direct interaction between CRN and both CLV1 and CLV2. Previous interaction studies using Förster (Fluorescence) Resonance Energy Transfer (FRET) between fluorescently labelled receptor proteins had shown that CRN might act as the central component in a multimeric complex consisting of CLV1, CLV2 and CRN, which can be already detected in the absence of CLV3. Noteworthy, CLV1 and CLV2 are not able to interact directly with each other (Bleckmann et al., 2010, Müller et al., 2008). Thus, in contrast to the flagellin or brassinosteroid perceiving receptors, the receptors for CLV3 (and related CLE peptides) appear to be already preassembled at the PM. Whether the composition of these complexes, their localization or stoichiometry changes upon ligand availability has not been investigated so far.

The observations described above demonstrate that receptor localizations, complex-arrangements and interaction dynamics are of central importance for these proteins to execute their functions. However, information on the spatial and temporal dynamics of these interactions is not available. Previous studies mainly employed methods such as co-immunoprecipitation (co-IP) experiments, genetic interaction studies, FRET-Acceptor PhotoBleaching (APB) measurements and the structure analysis of protein crystals. A major drawback of these methods is that they only reflect the static situation at the specific time point when the experiment is performed, but lack any temporal dimension. Therefore, interaction dynamics over time could not be recorded. Furthermore, since most of these experiments are not performed in the intact living cell, all positional information is lost. For example, experiments such as co-IPs are usually performed with cell extracts that do not allow to discriminate between interactions taking place at the PM, in specific sub-domains of the PM, or even in other membraneous compartments such as the ER or vesicles formed during receptor recycling. To enable us to collect all of this information, we used a

multiparameter fluorescence imaging spectroscopy (MFIS) approach, combining fluorescence lifetime imaging with fluorescence polarization/anisotropy microscopy. This allowed us to measure changes in protein concentration and both homomeric and heteromeric interactions simultaneously with pixel-wise resolution. We are thus moving from a static view on the receptors interaction-state to a live-imaging view with high spatial and temporal resolution to monitor the receptors interaction-states over time in a single living plant cell and in response to peptide treatments, which allows us to detect also rapid or transient changes in complex formation, arrangement and intracellular localization. Taking the ligand induced interaction between FLS2 and BAK1 as a paradigm, we then asked if the related LRR-RLKs signaling in the CLV pathway behave in a similar manner. Importantly, we could now compare changes in the distribution and formation of receptor complexes from a defence and a developmental pathway upon ligand stimulation over time.

Using live imaging in plant cells, we could show that BAK1-FLS heteromeric complexes assemble upon flg22 treatment at the PM. Furthermore, we found that BAK1-FLS2 heteromers are not present prior to ligand perception, and that also BAK1-BAK1 or FLS2-FLS2 homomers are lacking at the PM. We monitored the formation of the FLS2-BAK1 receptor complex over the course of one hour after flg22-treatment and observed that the BAK1-FLS2 complex does not only consist of a heterodimer, but forms a higher-order complex with at least two BAK1 molecules, probably connecting two FLS2 molecules.

In the case of the CLAVATA pathway, we were able to show that the CLV receptors are already organized in pre-formed complexes prior to CLV3 being present, in a ready-state to perceive the signal. In this situation, the CLV1 homodimers and the CLV2-CRN heterodimers are evenly distributed along the PM, while larger multimers, consisting of all three receptors, accumulate in small clusters along the PM. Once the ligand is detected, the receptors aggregate to form active signaling super-complexes, again in specific domains along the cells plasmamembrane.

We conclude here that the CLV and flg signalling pathways provide examples of two different principles of signaling pathways: in the CLV pathway, which is constitutively active throughout plant growth and development, the receptor complexes are pre-assembled in a ready-state to receive the signal. Signal perception leads to a rapid re-arrangement of the existing complexes. For the flg pathway, which is activated when a pathogen attacks, receptors are kept separate at the PM and interact only when their ligand is present. Thus, the fundamental differences between a continuously active developmental and a pathogen triggered signalling pathway are already encoded in the assembly behaviour of their receptors.

2. Results:

2.1 BAK1 and FLS2 are monomeric before ligand perception

We first tested if BAK1 and FLS2 are already assembled in BAK1-BAK1 or FLS2-FLS2 homomers before flg22 is perceived. For this we performed FRET-APB measurements with GFP- and mCherry-tagged versions of the proteins. BAK1-GFP and BAK1-mCherry (or FLS2-GFP and FLS2-mCherry) were transiently co-expressed in *Nicotiana benthamiana*. We chose an inducible system to avoid overexpression artifacts. If the receptors interact, FRET would take place between the GFP and the mCherry which we would be able to measure as donor-dequenching (E%) after mCherry-photobleaching. As negative control we measured the E% of BAK1-GFP (or FLS2-GFP) expressed without the mCherry fusion protein and as positive control a version of BAK1 (or FLS) tagged with both, GFP and mCherry fused directly together. These control measurements resulted in an E% of ~ -2,5 for the negative, and ~ 18 for the positive control. In the case of BAK1-BAK1 interaction we measured an E% of 0.7 (St.Dev. = 1.7), which, compared to the controls, indicates no FRET and therefore no interaction. For FLS2, the E% was 0.7 (St.Dev. = 1.3), again indicating no interaction (Suppl. Fig. S1).

To obtain a higher, pixelwise resolution, we then applied *fluorescence polarization*/anisotropy (FPA) (r) measurements of BAK1-GFP. The anisotropy reflects the rotational freedom of a fluorophore. Free GFP in an aqueous solution is free to rotate at all angles, which results in an anisotropy r of about 0.32, derived from the Perrin equation (Perrin, 1929). If a protein is fused to the GFP, its rotational freedom is impaired and the value for r is higher. FRET between the GFP and another GFP (homo-FRET) reduces the anisotropy to the value of free GFP or lower. Because of these properties, anisotropy measurements provide additional information about the FRET-state of a fluorophore. BAK1-GFP had an anisotropy r of 0.35. Since this is higher than the anisotropy value of free GFP, there is no homo-FRET between two or more GFPs, and hence no BAK1-GFP multimer formation (Suppl. Fig. S2 lowermost row and Fig. 2, black dots and dotted line). This confirms our FRET-APB results, in that BAK1 does not interact with itself prior to complex formation with FLS2.

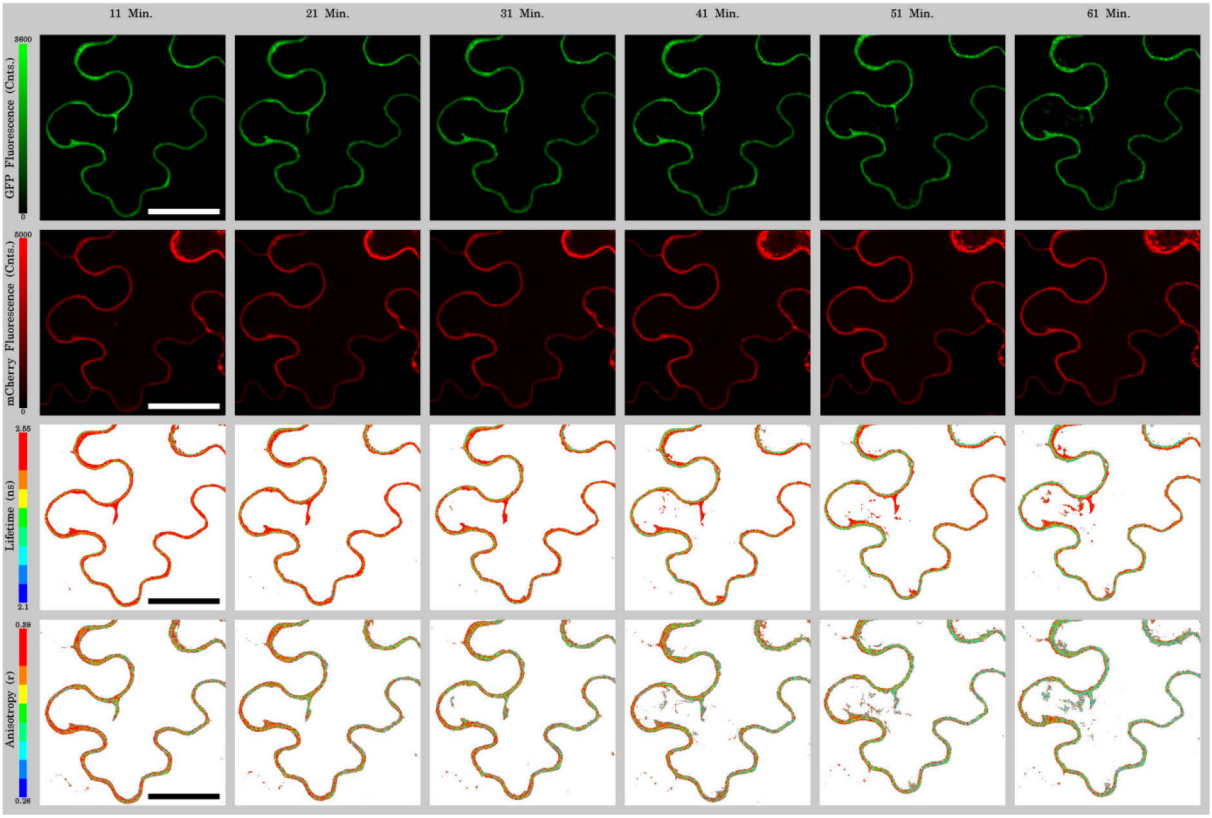

Fig. 1: Fluorescence intensity and lifetime and anisotropy projections on a cell expressing BAK1-GFP and FLS2-mCherry and treated with flg22

Time series of a cell expressing BAK1-GFP and FLS2-mCherry treated with flg22. While the average fluorescence intensities are unchanged over the course of one hour (top and second row), the average lifetime of BAK1-GFP (third row) drops from ~ 2.6 ns to ~ 2.43 ns over the course of one hour. The average anisotropy (lowermost row) is reduced from 0.35 to 0.325.

2.2 flg22 dependent formation of multimeric BAK1-FLS2 complexes at the PM

We then treated the plants with flg22 peptide and again measured the anisotropy r over the course of one hour. Within this time range the anisotropy of BAK1-GFP decreased from 0.35 to 0.325, a value comparable to that of free GFP. This indicates homo-FRET between two BAK1-GFPs, and therefore the presence of at least two BAK1 molecules in the flg22-triggered BAK1-FLS2 complexes (Fig. 1 lowermost row and Fig. 2, red dots and dotted line).

To monitor the interaction between the BAK1-GFP and FLS2-mCherry molecules we then applied FLIM measurements to individual plant cells over time. We transiently co-expressed BAK1-GFP and FLS2-mCherry in *N. benthamiana* and treated the cells with the flg22 peptide (Fig. 1 top and second row). Subsequently we measured the GFP lifetime of individual cells every 10 minutes over the course of one hour. When complexes between BAK1-GFP and FLS2-mCherry are being formed, this will result in FRET taking place from the GFP to the

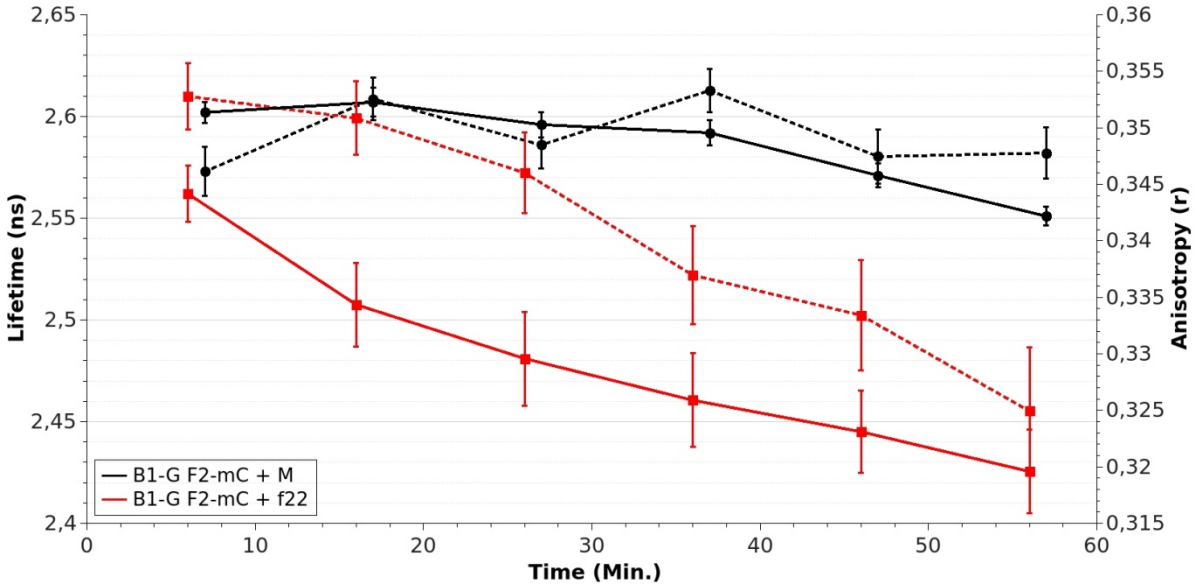

Fig. 2: Lifetime and Anisotropy of BAK1-GFP over time

The lifetime (τ) of BAK1-GFP (B1-G) is ~ 2.6 ns at the first time point. Mock treatment (M) of cells co-expressing of BAK1-GFP (B1-G) and FLS2-mCherry (F2-mC) does not lead to a significant change over time (black circles and continuous line). However, flg22 (f22) treatment leads to a continuous and significant reduction of BAK1-GFP lifetime to ~ 2.43 ns, 55 minutes after peptide-infiltration (red squares and continuous line).

The anisotropy (r) of BAK1-GFP (B1-G) co-expressed with FLS2-mCherry (F2-mC) is ~ 0.35 at the first time point. This does not change significantly over time when cells are mock (M) treated with a nonsense peptide (black circles and dotted line). Treatment with the flg22 (f22) peptide leads to a decrease in anisotropy to ~ 0.325, 57 minutes after peptide-infiltration (red squares and dotted line). This reduction in anisotropy points to homo-FRET between two or more GFPs and thereby to homomerization of two or more BAK1 molecules.

mCherry, which would be reflected in a steady decrease of GFP-lifetime in these cells. The initial lifetime of BAK1-GFP was 2.6 ns. After treating the cells with flg22 the lifetime decreased gradually to 2.43 ns one hour after treatment, showing the formation of BAK1-GFP/FLS2-mCherry complexes (Fig. 1, third row and Fig. 2, red squares and line). This decrease in GFP lifetime could not be observed in mock-treated cells (Suppl. Fig. S2, third row and Fig. 2, black dots and line). The fluorescence intensity of BAK1-GFP or FLS2-mCherry was unchanged during that time, indicating that more and more complexes are being formed between the proteins already present at the membrane. Also, the lifetime was homogenous along the entire membrane, indicating the same BAK1-FLS2 complexes being evenly distributed along the membrane. To quantify this even distribution of complexes, we determined how heterogeneous the measured lifetimes from all pixels of the FLIM images are. If treatment with the flg22 peptide would result in the same BAK1-FLS2 complexes

being formed everywhere along the PM, all the pixels will have comparable lifetimes and the heterogeneity of the sample will be low. If peptide-treatment would lead to different or unevenly distributed complexes, the lifetime-heterogeneity would increase over time after flg22-addition. The heterogeneity in a sample can be quantified as lifetime-heterogeneity theta (θ). We determined the change of θ in the time points after flg22-treatment relative to the first time point measured. Over the course of one hour the heterogeneity remained around 1, showing an even distribution of the same BAK1-FLS2 complexes along the entire plasmamembrane (Fig. 5 light blue downward triangles and line).

2.3 The receptors in the CLAVATA pathway form complexes prior to ligand-perception

For the CLV pathway we already know of some receptor complexes, which are formed independently of CLV3 peptide treatment: CLV1-CLV1 homomers, CLV2-CRN heteromers and bigger CLV1-CLV2-CRN multimers (Bleckmann et al., 2010). However, we do not know if they are formed at similar rates and at the same time, or if they evenly distribute along the PM. Furthermore, we do not know if CLV3-perception has any influence on these factors. Since CLV2 can bind CLV3 only with a weak affinity, it is not unlikely that the CLV2-CRN heteromer functions as a co-receptor with the CLV1 homomer, just like BAK1 is the co-receptor for FLS2. We first applied FLIM-measurements to show the interaction between the three receptors. Just as we did for BAK1 and FLS2, we transiently co expressed CRN-GFP, CLV2 and CLV1-mCherry in *N. benthamiana* (Fig. 3, top and second row). In this case, the lifetime of CRN-GFP was 2.37 ns, compared to 2.57 ns when CRN-GFP and CLV2 were expressed without CLV1-mCherry. This shorter lifetime reflects the presence of pre-assembled CLV1-CLV2-CRN receptor-complexes at the PM in the absence of the CLV3 peptide. We then treated the cells with the CLV3-peptide to measure the effects that ligand-perception might have on the existing receptor complexes. CLV3 treatment led to a weak but continuous decrease of GFP lifetime from 2.37 ns to 2.3 ns after one hour (Fig. 4, red squares and line). This continuous decrease could not be observed in mock-treated cells, where the lifetime varied in the region of 2.35 – 2.37 ns (Fig. 4, black dots and line). These lifetimes were determined as an average of all pixels in the image, which could account for the weak drop in lifetime. To obtain more detailed information, we performed a pixel-wise analysis next.

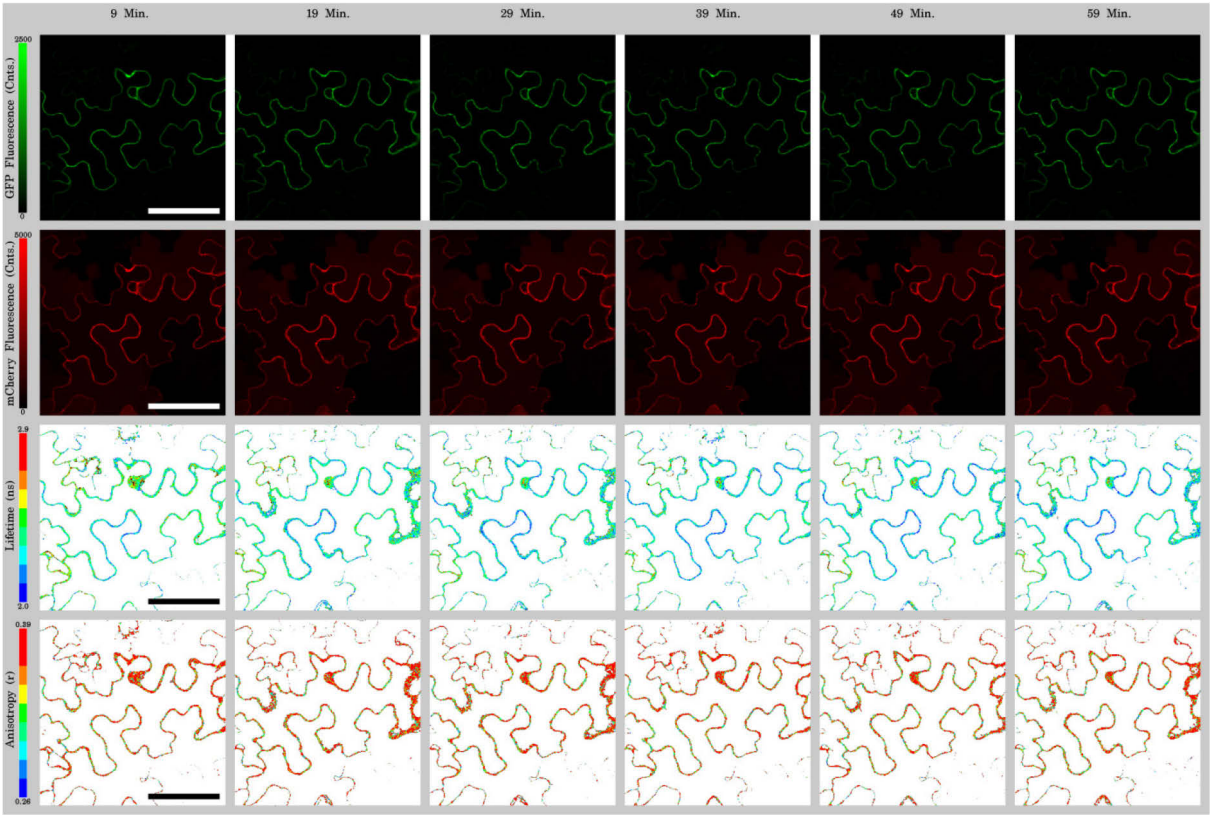

Fig. 3: Fluorescence intensity and lifetime and anisotropy projections on a cell expressing CRN-GFP, CLV2 and CLV1-mCherry and treated with CLV3

Time series of a cell expressing CRN-GFP, CLV2 and CLV1-mCherry treated with CLV3. While the average fluorescence intensities are unchanged over the course of one hour (top and second row), the average lifetime of CRN-GFP (third row) drops from ~ 2.35 ns to ~ 2.3 ns on average. However, in specific domains along the membrane the lifetime is strongly reduced to only ~ 2 ns. The anisotropy is unchanged over time (lowermost row).

2.4 The CLV3 peptide triggers the formation of receptor complex clusters along the PM

When the lifetimes of all collected photons were plotted back to the FLIM-image of the cells, we noticed the emergence of small regions along the PM that reacted to the peptide-treatment with severely reduced lifetimes after one hour (Fig. 3, third row). However, because the GFPs in the other areas of the PM had a relatively unchanged lifetime, the average lifetime of all pixels was only weakly affected by these regional differences. To quantify this effect of the CLV3-treatment we again determined the lifetime-heterogeneity theta (θ) of the samples. We first determined θ for cells expressing only CRN-GFP and CLV2-mCherry, but not CLV1. These proteins exhibited a smooth membrane distribution and no peptide-effect after CLV3-addition. Accordingly, the θ value was 1 on average (Fig. 5, green triangles and line). When we expressed CRN-GFP, CLV2 and CLV1-mCherry, but only added a mock-peptide, the

cells already showed an increase in lifetime-heterogeneity, but no effect over time, with θ varying in the range of 1 to 1.3 (Fig. 5, black dots and line). CLV3-treatment on the other hand resulted in a continuous increase in lifetime-heterogeneity to up to 1.5 after one hour (Fig. 5, red squares and line).

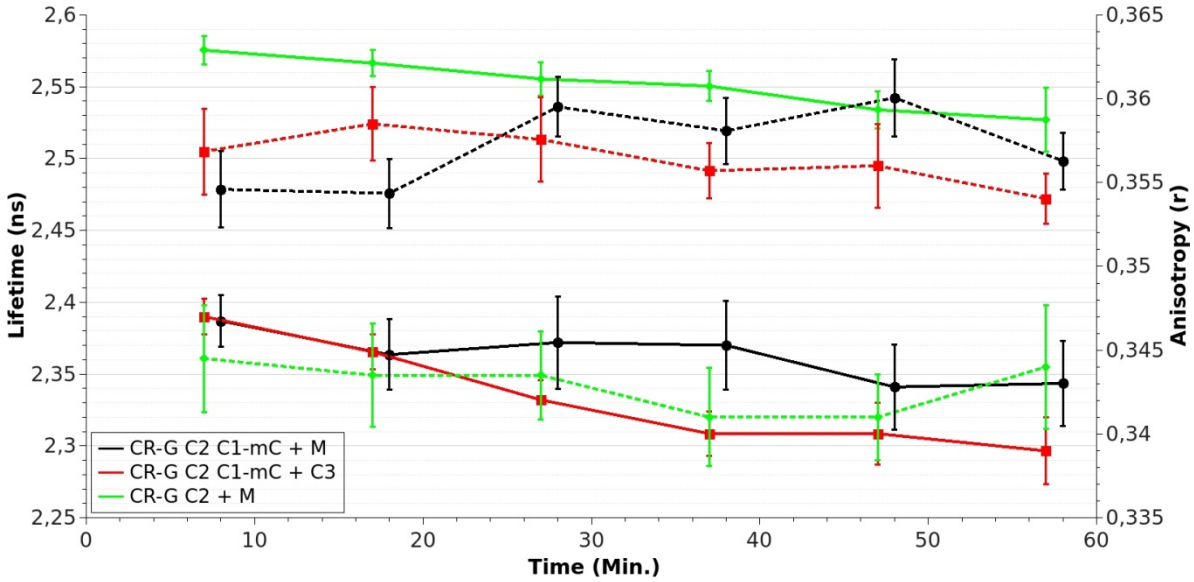

Fig. 4: Lifetime and Anisotropy of CRN-GFP

The lifetime (τ) of CRN-GFP (CR-G) is ~ 2.56 ns at the first time point. Mock-treatment of cells expressing CRN-GFP (CR-G) and CLV2 (C2) with a mock peptide (M) does not lead to a significant change in lifetime over the course of one hour (green rectangle and continuous line). Co-expression of CRN-GFP, CLV2 and CLV1-mCherry (C1-mC) and mock-treatment results in a decreased CRN-GFP lifetime of ~ 2.35 ns but no significant change over time (black dots and continuous line). CLV3 (C3) treatment of cells co-expressing CRN-GFP, CLV2 and CLV1-mCherry leads to a slight but continuous decrease of CRN-GFP lifetime to ~ 2.3 ns (red squares and continuous line) after one hour.

The anisotropy (r) of CRN-GFP (CR-G) co-expressed with untagged CLV2 (C2) is ~ 0.343 at the first time point. This does not change significantly over time when cells are mock (M) treated with a nonsense peptide (green triangle and dotted line). When CLV1-mCherry (C1-mC) is c-expressed, the anisotropy increases to 0,356 due to FRET, but neither mock (M) (black dots and continuous line) nor CLV3 (C3) (red squares and continuous line) treatment show further effects.

From these observations we concluded that the CLV2-CRN hetero-dimers are evenly distributed along the membrane (heterogeneity θ = 1 on average), while the CLV1-CLV2-CRN multimers seem to localize slightly more heterogeneous in specific domains of the membrane (θ = 1.15 on average). When the CLV3 peptide is bound by the receptor complexes, binding triggers the formation of more CLV1-CLV2-CRN clusters in specific domains of the PM, which leads to a stronger and continuously increasing heterogeneity (θ = up to 1.5 after one hour).

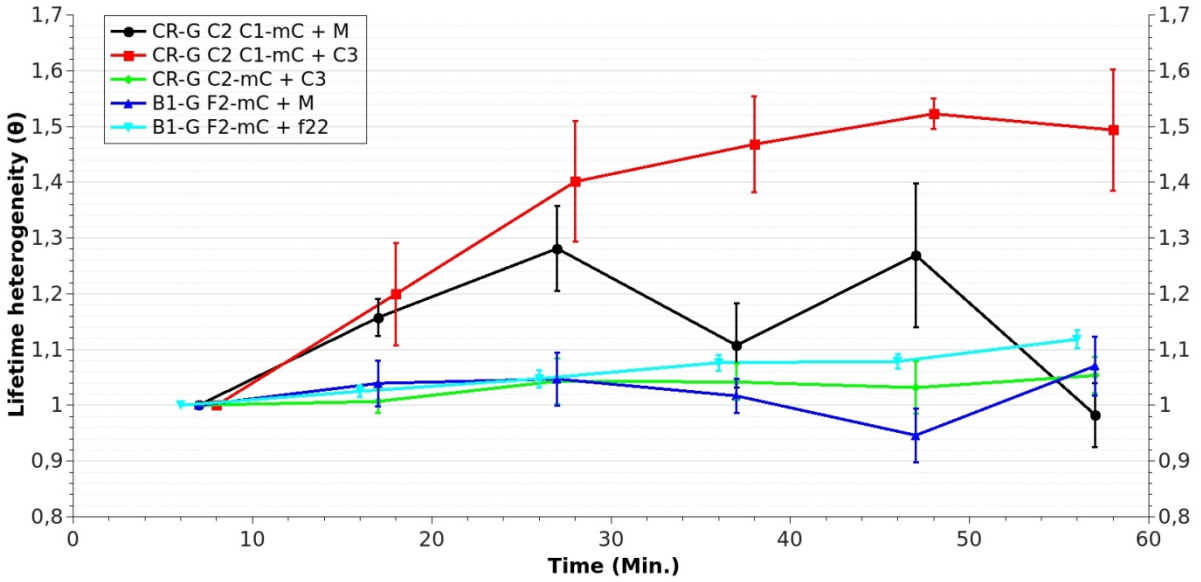

Fig. 5: Quantification of BAK1-GFP and CRN-GFP lifetime-heterogneity (θ)

In cells expressing BAK1-GFP (B1-G) and FLS2-mCherry (F2-mC), the lifetime-heterogeneity θ varies around the background level of ~ 1 and is not affected by mock (M) (dark blue upright triangle and line) or flg22 (f22) treatment (light blue downright triangle and line) over time. In cells expressing CRN-GFP (CR-G) and CLV2-mCherry (C2-mC), but not CLV1, the lifetime-heterogeneity θ varies around the background level of ~ 1 as well and is not affected by CLV3-treatment over time (green rectangles and line). Co-expressing CRN-GFP (CR-G), CLV2 (C2) and CLV1-mCherry (C1-mC) results in some multimeres being formed, and therefore a slightly increased θ of ~ 1 – 1.25, but treatment with a mock (M) peptide does not alter the heterogeneity over time (black dots and line). Treating CRN-GFP, CLV2 and CLV1-mCherry expressing cells with the CLV3 (C3) peptide leads to more multimeres being formed due to active signaling in specific regions of the cells, and hence θ increases to > 1.5 (red squares and line).

3. Discussion:

With our results we demonstrate that the CLAVATA and the flagellin pathway are examples for two different types of receptor-mediated signal transduction. In the flg pathway, FLS2 and BAK1 complex formation is completely dependent on the ligand flg22. Before that, the two receptors are localized to the PM without forming homo- or heteromers with each other (Fig. 6a). The finding that FLS2 does not interact with itself prior to flg22 binding is in the contrast to data published by Sun et al. (2012), but supported by Ali et al (2007). However, since the results of Sun et al. were obtained utilizing co-IP experiments with cell extracts, it is possible that the FLS2/FLS2 complexes they found were not from the PM, but possibly from vesicles, destined for receptor-recycling or degradation. In both, our work and the work of Ali et al., live cell imaging was applied to measure interactions in living cells and at the PM only. On the other hand, it is possible that a very small amount of the FLS2 molecules at the PM is already present in dimeric form, while the majority is monomeric. In this case, it is possible that in life imaging the stronger signal coming from the monomeric molecules could drown out the signal coming from the few dimers, while co-IPs could detect these few molecules.

However, we could also show that BAK1 does not interact with itself prior to flg22, which would imply that the BAK1/BIR2 complex is most likely a heterodimer. After ligand perception, the newly formed FLS2/BAK1 complex contains at least two BAK1 molecules. This signaling active complex likely consists of two BAK1 and FLS2 molecules each, with the two BAK1 molecules interacting with each other, and one FLS2 molecule on each of the flanks, forming a FLS2-BAK1-BAK1-FLS2 tetramer (Fig. 6a). Each of the two FLS2/BAK1 units would be active in both, extracellular signal perception and intracellular transduction. Their position on the flanks of the complex separates the FLS2 molecules considerably, which would also explain why Ali et al. were not able to detect FLS2-FLS2 homomers after flg22 treatment.

This functional principle, with only forming complexes when they are needed appears to be reasonable for the FLS2 and BAK1 proteins for several reasons. For one, the FLS2-BAK1 complex is only needed in the case of bacterial infection. Accordingly, producing and accumulating these complexes at the PM at all time would be a waste of material and energy. Furthermore, the diverse functions of the co-receptor BAK1 must be considered. BAK1 is not only the co-receptor for FLS2 in transmitting the flg signal. It is, for example, also involved in BR signaling, where it was first described as co-receptor for the BR receptor BRI1. As a co-

receptor in several pathways, it is unlikely that BAK1 forms constitutive complexes with all its possible co-receptors (Chinchilla et al., 2009).

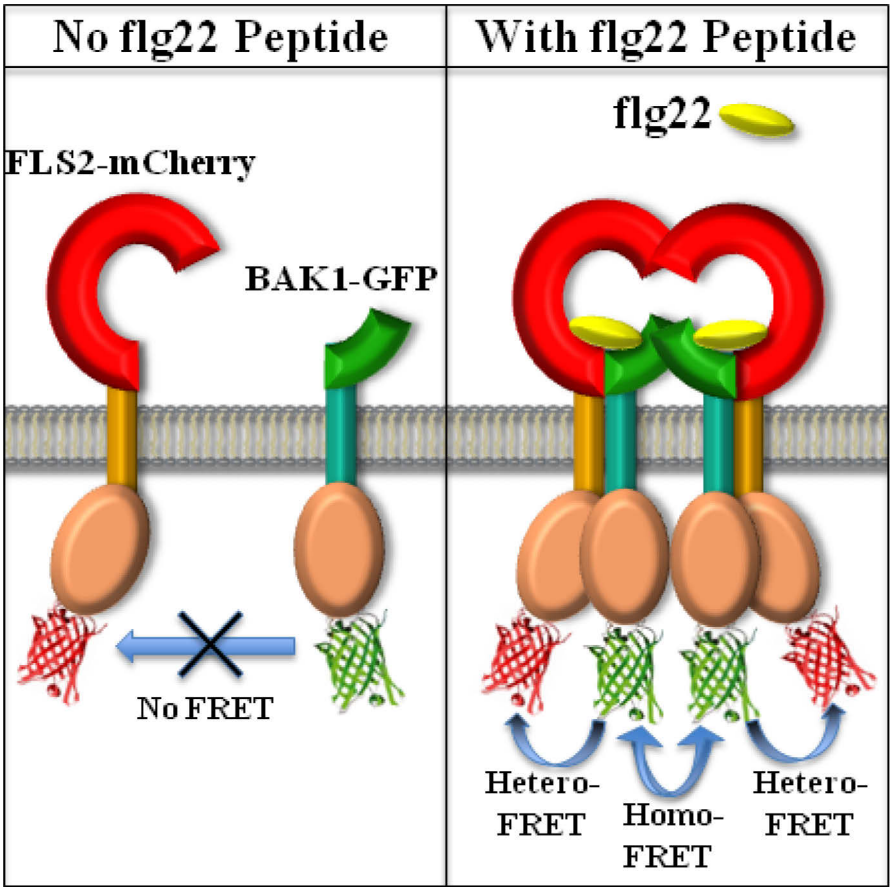

Fig. 6a: Model of the flg Pathway

Without flg22 present the two receptors FLS2-mCherry and BAK1-GFP do not interact and no FRET can be measured between the fluorophores. When flg22 is present, the two receptors form a complex consisting of two central BAK1 molecules with one FLS2 molecules on each flank. Homo-FRET can be measured between the two central BAK1-bound GFPs, and Hetero-FRET can be measured between one GFP and one FLS2-bound mCherry.

The CLAVATA pathway, on the other hand, is the key regulatory pathway in the plants stem cell homeostasis. Plants keep a constant number of stem cells in their primary above ground stem cell niche, which is the shoot apical meristem. The key to the maintenance of this pool of stem cells is a tight balance between stem cell proliferation and differentiation. If too many cells differentiate, the meristem is drained and the plant ceases all above ground growth. If too many stem cells are maintained, the plant produces supernumerary tissues and organs that stress the plants overall fitness. To keep this delicate and essential balance between cell division and differentiation, the CLV pathway evolved as a negative feedback loop, involving the stem cell fate promoting factor WUS and the stem cell fate repressing

factor CLV3. CLV3 is produced by the stem cells and represses WUS in the cells of the OC. When WUS is repressed, stem cells are no longer maintained and this in turn leads to CLV3 production being reduced. With a falling CLV3 level, WUS expression is reactivated and stem cell fate is propagated again and so on (Schoof et al., 2000, Brand et al., 2000). Since this negative feedback loop is active at all time and its function is essential to the plants survival, there must be at least some active receptor complexes at the membrane at any given moment (Fig. 6b). At the same time, the strength of the transmitted CLV3 signal can be varied by varying the abundance of receptor complexes at the PM, depending on the necessity of stronger or weaker WUS repression. A high concentration of CLV3, which we have simulated in our experiment by infiltrating 1 µM of CLV3 peptide, is an indicator of a strongly enlarged stem cell population, and accordingly WUS must be repressed rapidly to counteract this. For this, the plant quickly assembles higher order complexes that consist of several LRR-receptor and kinase molecules to enhance the magnitude of the CLV3 signal being transmitted (Fig. 6b).

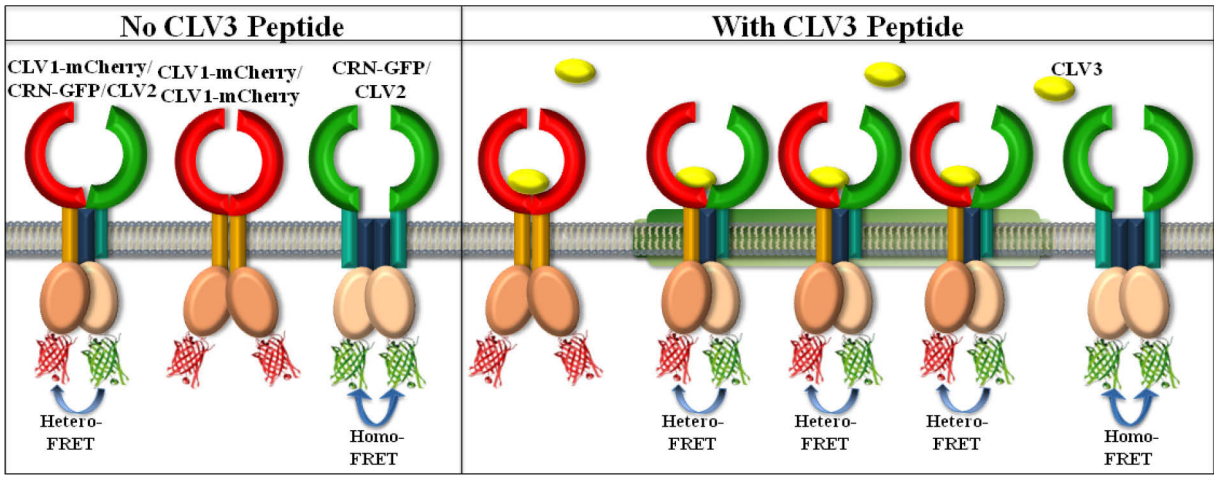

Fig. 6b: Model of the CLV pathway

Without CLV3 present, CLV1-mCherry forms preferentially homomers, CRN-GFP and CLV2 form heteromers and few CLV1/CLV2/CRN multimers are formed. Homo-FRET can be measured between the CRN-bound GFPs in the CLV/CRN heteromers, and Hetero-FRET can be measured between CRN-GFP and CLV1-mCherry in the multimers. When CLV3 is present, more CLV1/CLV2/CRN multimers are formed in clusters, resulting in stronger Hetero-FRET in these regions.

It is reasonable as well that this happens in specific hot spots, since there are many more components involved in signal transduction next to the peptide and the receptors. For one, the receptor-complex itself most likely involves many more proteins, just as it has been shown for the FLS2-BAK1 complex (Lin et al., 2014). The signal must then be transmitted on the intracellular side of the membrane. This is most likely happening through phosphorylation

events involving the receptors kinase domains and some downstream factors (Yu et al., 2003, Stone et al., 1998). The availability of these factors could be restricted to these specific domains of the cells, or they could be enriched there. Also, parts of the endoplasmic reticulum or the cytoskeleton could be involved, and they only attach to the membrane at some specific points. So far it is not clear how these hot spots are defined, but there are some hints towards them being lipid rafts in the membrane, since it has been recently published that the CLV receptors all localize to lipid rafts (Gish et al., 2013). Furthermore, one reason that many proteins involved in signaling pathways localize to lipid rafts is that through this sequestration of all involved factors they are kept in close proximity at all time and can form complexes much quicker than they would if they were scattered along the entire plasmamembrane (Simons et al., 2000).

Intriguingly, a similar functional principle has recently been proposed for the well-studied epidermal growth factor receptor (EGFR) in mammalian cells. So far it is not clear, whether cell signaling involving EGFR and its related receptors erbB2, erbB3 and erbB4 works through ligand-induced dimer-formation from the monomeric receptors, or a rearrangement of existing dimers. In an approach combining microscopy, image correlation spectroscopy (ICS), phosphorylation assays and computational modeling of mass-action kinetics, Kozer et al. now suggest that the EGF receptors are localized at the PM as pre-formed dimers, and that ligand-treatment then leads to the formation of higher-order oligomers from these dimers in clusters along the PM, which are then transphosphorylated (Kozer et al., 2013).

A scenario, in which the formation of the bigger CLV1-CLV2-CRN multimers is a negative response to enhanced CLV3 signaling is conceivable as well. In this case, the receptor proteins would be sequestered in these bigger complexes to dampen CLV3-signaling, either after a short time period of necessary enhancement, or accidental excess signaling. By being forced into huge aggregates, the membrane could be drained of active molecules, which would then lead to reduced signal being transmitted. In this scenario it would be likely that the CLV1-CLV1 homodimers function as one receptor complex, while the CLV2-CRN heteromer acts in another complex with a so far undefined interactor, such as the CLV1-related LRR-RLK RECEPTOR-LIKE PROTEIN KINASE2 (RPK2) (Kinoshita et al., 2010).

Clearly, one of the next goals for the research on this topic must be a closer examination of the nature of these hot spots. Also, we still lack downstream components of the CLAVATA receptors that close the gap between signal perception at the receptor level and WUS downregulation at the transcriptional level.

4. Supplementary Figures:

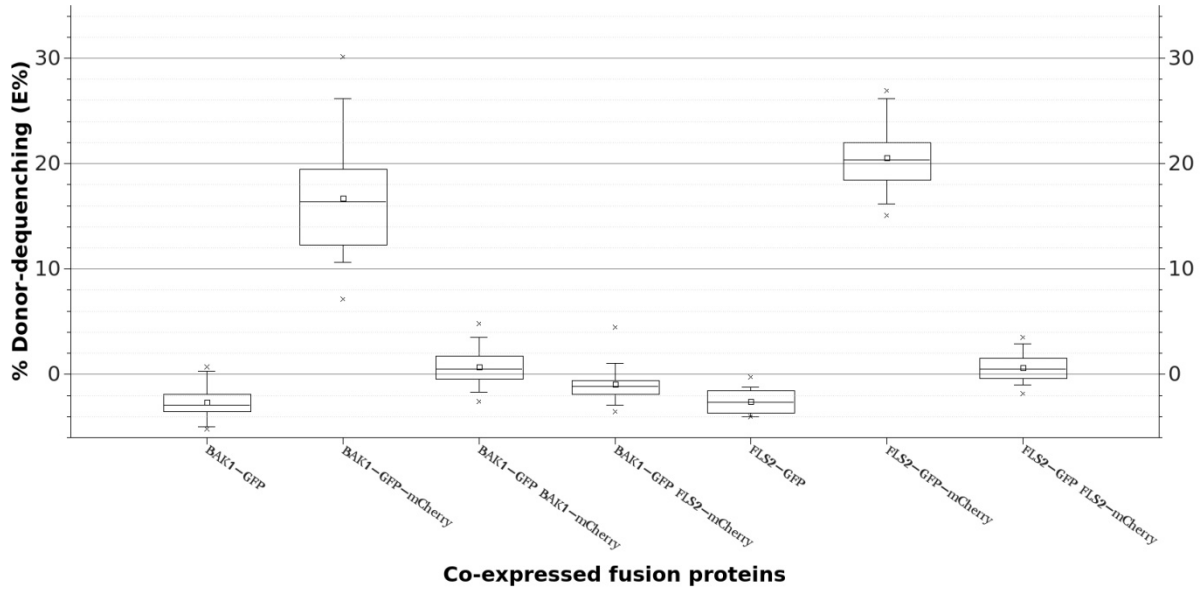

Fig. S1: FRET-APB results for BAK1-BAK1 and FLS2-FLS2 interactions

Measurements for BAK1-GFP or FLS2-GFP alone are negative controls and resulted in negative E% values. BAK1-GFP-mCherry and FLS2-GFP-mCherry measurements are positive controls and resulted in ~ 16 or 20 E% respectively. The values for the measured interactions, i.e. BAK1-GFP BAK1-mCherry, FLS2-GFP FLS2-mCherry and BAK1-GFP FLS2-mCherry all exhibited E% values of around 0, indicating no interaction between the proteins.

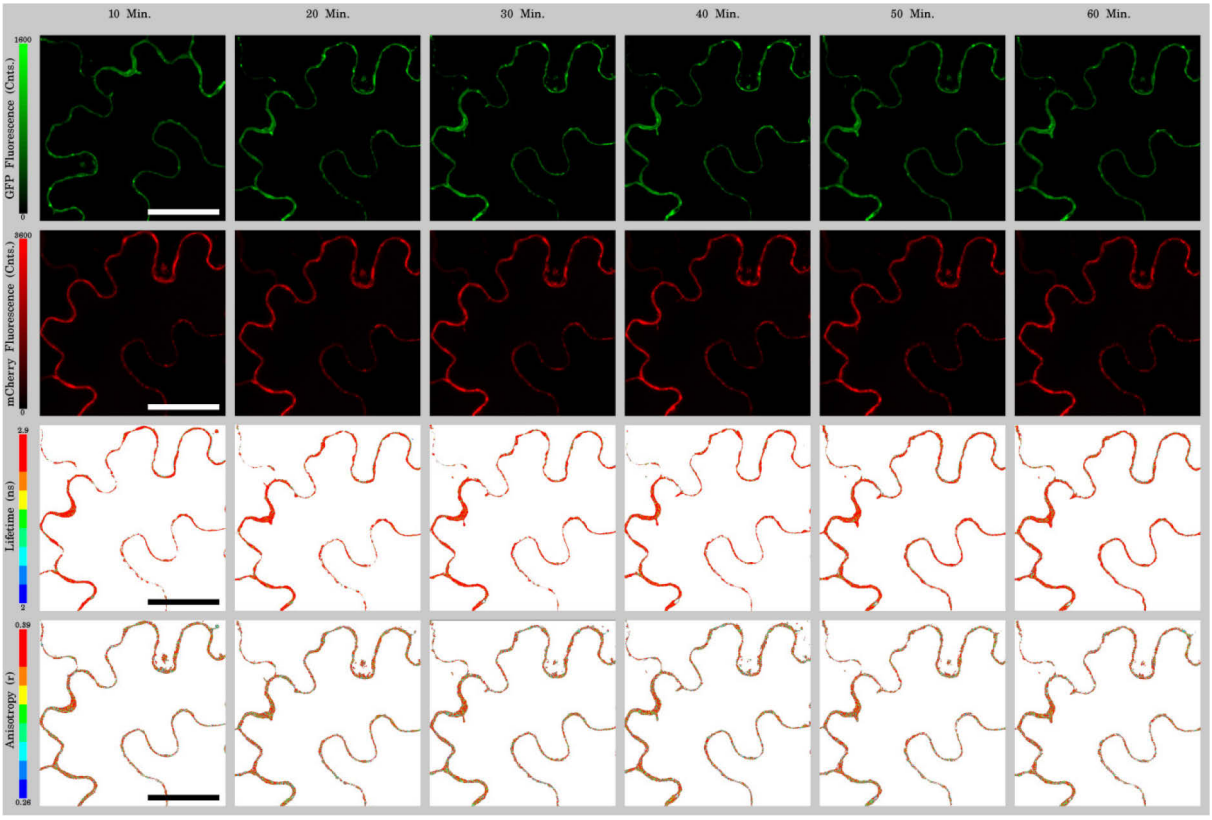

Fig. S2: Fluorescence intensity and lifetime and anisotropy projections on a mock-treated cell expressing BAK1-GFP and FLS2-mCherry

Time series of a cell expressing BAK1-GFP and FLS2-mCherry treated with a mock peptide. The average fluorescence intensities, lifetime and anisotropy are unchanged over the course of one hour (top to lowermost rows).

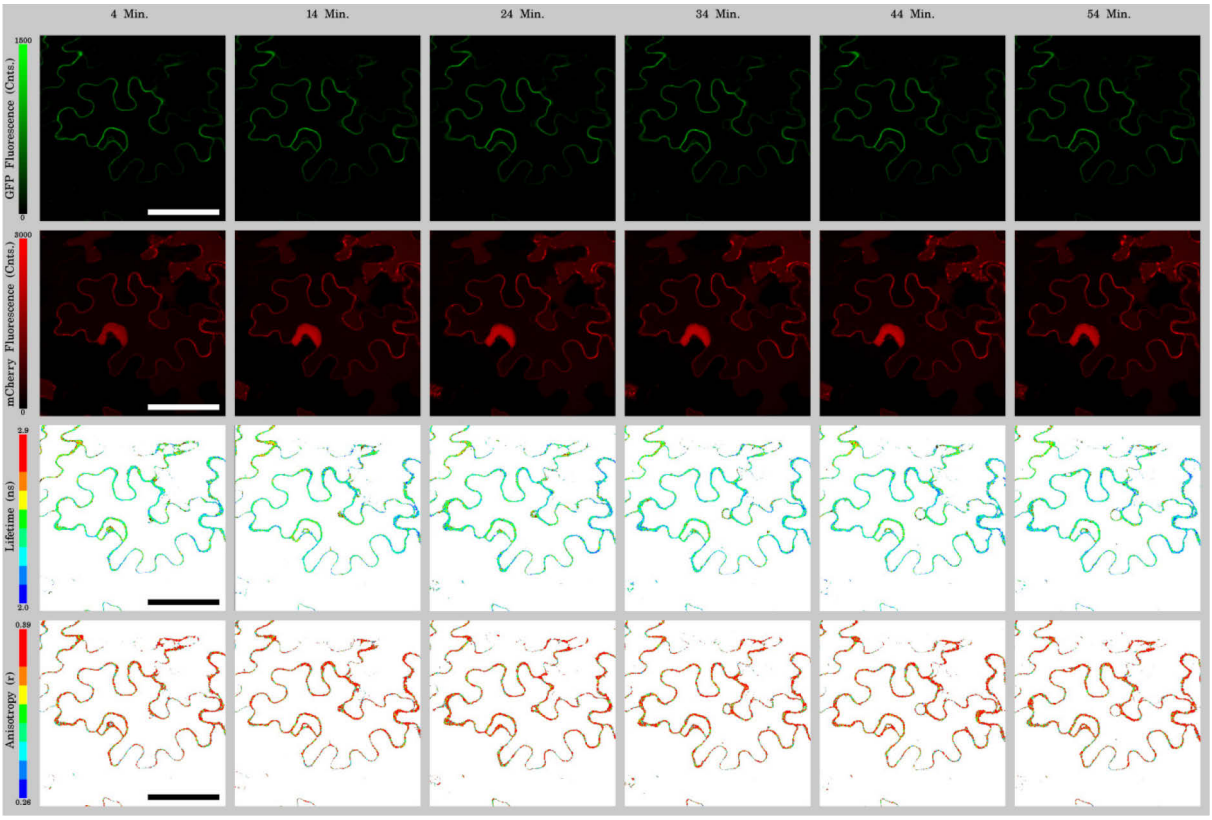

Fig. S3: Fluorescence intensity and lifetime and anisotropy projections on a mock-treated cell expressing CRN-GFP, CLV2 and CLV1-mCherry

Time series of a cell expressing CRN-GFP, CLV2 and CLV1-mCherry treated with a mock peptide. The average fluorescence intensities, lifetime and anisotropy are unchanged over the course of one hour (top to lowermost rows).

5. Methods:

Plant Reporter Lines

Nicotiana benthamiana plants were grown in the greenhouse for four weeks prior to transient transformation. Transformation and expression were described before (Bleckmann et al., 2010).

Construction of Inducible Receptor Fusions

The CLV1, CLV2, CRN and BAK1 expression vectors were described before before (Bleckmann et al., 2010). The FLS2 fusions were created from cDNA using the pENTR™/D-TOPO® and Gateway® LR Clonase® II Cloning Kits, as well as the destination vectors pABindGFP, pABindmCherry, and pABindFRET described previously (Bleckmann et al., 2010).

Peptides

The peptides flg22 (QRLSTGSRINSAKDDAAGLQIA), CLV3 (RTV[Hyp]SG[Hyp]DPLHHH) and Mock (LPQHPHGRSDVT) were ordered from ThermoFisher Scientific. They were infiltrated into the transformed plant leaves immediately before imaging at a concentration of 1 µM.

Microscopy

Measurements were performed using a multiparameter fluorescence detection setup as described previously (Weidtkamp-Peters et al., 2009, Kudryavtsev et al., 2007). Experiments were performed with a confocal laser scanning microscope (FV1000 Olympus, Hamburg, Germany) additionally equipped with a single photon counting device with picosecond time-resolution (Hydra Harp 400, PicoQuant, Berlin, Germany). GFP was excited at 485 nm with a linearly polarized, pulsed (32 MHz) diode laser (LDH-D-C-485, Pico-Quant, Berlin, Germany) at 0.8 µW at the objective (60x water immersion, Olympus UPlanSApo NA 1.2, diffraction limited focus). mCherry was excited at 559 nm with a continuous-wave laser (FV1000) at 5.6 µW at the objective. The emitted light was collected in the same objective and separated into its perpendicular and parallel polarization. GFP fluorescence was then detected by MPDs (PDM50-CTC, Micro Photon Devices, Bolzano, Italy) in a narrow range of its emission spectrum (bandpass filter: HC520/35, AHF, Tübingen, Germany). mCherry fluorescence was detected by HPDs(HPMC-100-40, Becker&Hickl, Berlin, Germany), of

which the detection wavelength range was set by the bandpass filters (HC 607/70, AHF). Images were taken with 20 µs pixel dwell time and a resolution of 103 nm/pixel. Series of 40 frames were merged to one image and further analyzed using custom-designed software (LabView).

FRET-APB measurements were done on a Zeiss LSM 780. GFP was excited with a continuous wave 480 nm argon laser at the objective (40x water immersion, Zeiss C-Apochromat 40x/1.20 W korr M27) and emission was detected at 498 - 524 nm by 32-Channel-GaAsP-Detectors. mCherry was excited using a 561 nm continuous wave diode laser and emission detected at 578 - 639 nm. A series of 12 256 x 256 pixel frames with 0.18 µM pixel size, 47 μm^2 image size and 1.27 µs pixel dwell time was recorded. After 5 frames, mCherry was photobleached in a region of interest along the PM by 80 iterations with 100 % laser power. E% was determined as GFP-intensity change after photobleaching by (GFPafter − GFPbefore)/GFPafter × 100.

Pixel-wise fluorescence-weighted lifetime analysis

The histograms presenting the decay of fluorescence intensity after the excitation pulse were built for each pixel with 128ps per bin. The fluorescence-weighted lifetime of donor molecule ($<\tau_D>_f$) in single pixel was determined using a model function containing only two variables ($<\tau_D>_f$) and scatter contribution (for details see (Stahl et al., 2013)), with maximum likelihood estimator (MLE). The instrument response function was measured with the back-reflection of the laser beam and used for iterative reconvolution in the fitting process.

Pixel-wise anisotropy analysis

The steady-state anisotropy is given by $r_G = \frac{F_{\parallel} - G \cdot F_{\perp}}{F_{\parallel} + 2 \cdot G \cdot F_{\perp}}$, where $F_{\parallel}$ and $F_{\perp}$ are the average fluorescence count rates within a pixel, with a polarization parallel and perpendicular to that of the excitation light, respectively. Both were corrected for dead time of the detection electronics (Becker, 2005) and mixing of polarization in the high numerical aperture objective (Schaffer et al., 1999) $F = F_{\parallel} + 2GF_{\perp}$ is the total fluorescence intensity. Calibration measurements with Rhodamine 110 delivered the G-factor to correct the signal for orientational sensitivity differences of the detection system.

Fluorescence lifetime heterogeneity analyses

With maximum likelihood estimator (MLE), the variance of fluorescence lifetime distribution σ_0^2 is inversely proportional to the number of photons in the decay histogram N under shot-noise limited conditions: $\theta_0 = \sigma_0^2 \cdot N$. The constant θ_0 that governs the width of the lifetime distribution can be calculated, for details see (Maus et al., 2001). But for the experiments in live cell, lifetime distribution is wider than what expected in the ideal condition due to the detector noise and the heterogeneous cellular environment in biological samples. This will be reflected by a larger θ value compared to θ_0. To quantify the lifetime broadening, for each image, its θ value is calculated according to: $\theta = \sigma^2 \cdot \overline{N}$, in which σ^2 is the variance of the lifetime distribution and $\overline{N}$ is the mean photon count. Considering that each individual cell may have different environment which results in different absolute θ, we normalized θ values of a set of k time-series measurements to that of the first measurement: $\overline{\theta^{(k)}} = \theta^{(k)} / \theta^{(1)}$. In this way, those time-independent factors that exist in all the measurements are excluded, which leaves only the time-dependent lifetime broadening due to peptide infiltration. After normalization, the starting normalized θ value is always unity, so that different sets of time-series measurements can also be compared.

This chapter is a manuscript in preparation for submission.

Authors:
Marc Somssich[1], Qijun Ma[3], Stefanie Weidtkamp-Peters[2], Claus A. M. Seidel[2, 3] and Rüdiger Simon[1, 2]

[1] Institute of Developmental Genetics
[2] Center for Advanced Imaging
[3] Institute for Molecular Physical Chemistry
Heinrich Heine University, 40225 Düsseldorf, Germany

The experiment was designed by Marc Somssich, Rüdiger Simon, Qijun Ma, Stefanie Weidtkamp-Peters and Claus Seidel. Molecular biology and plant work was done by Marc Somssich. Microscopy was done by Marc Somssich and Qijun Ma. Data analysis was done by Qijun Ma and Marc Somssich. The manuscript was written by Marc Somssich with help from Rüdiger Simon.

6. References:

ALI, G. S., PRASAD, K. V. S. K., DAY, I. & REDDY, A. S. N. 2007. Ligand-dependent reduction in the membrane mobility of FLAGELLIN SENSITIVE2, an Arabidopsis receptor-like kinase. *Plant and Cell Physiology,* 48**,** 1601-1611.

BECKER, W. 2005. *Advanced time-correlated single photon counting techniques,* Berlin ; New York, Springer.

BLECKMANN, A., WEIDTKAMP-PETERS, S., SEIDEL, C. A. & SIMON, R. 2010. Stem cell signaling in Arabidopsis requires CRN to localize CLV2 to the plasma membrane. *Plant Physiol,* 152**,** 166-76.

BRAND, U., FLETCHER, J. C., HOBE, M., MEYEROWITZ, E. M. & SIMON, R. 2000. Dependence of stem cell fate in Arabidopsis an a feedback loop regulated by CLV3 activity. *Science,* 289**,** 617-619.

CHINCHILLA, D., SHAN, L., HE, P., DE VRIES, S. & KEMMERLING, B. 2009. One for all: the receptor-associated kinase BAK1. *Trends in Plant Science,* 14**,** 535-541.

CHINCHILLA, D., ZIPFEL, C., ROBATZEK, S., KEMMERLING, B., NURNBERGER, T., JONES, J. D., FELIX, G. & BOLLER, T. 2007. A flagellin-induced complex of the receptor FLS2 and BAK1 initiates plant defence. *Nature,* 448**,** 497-500.

CLARK, S. E., RUNNING, M. P. & MEYEROWITZ, E. M. 1995. Clavata3 Is a Specific Regulator of Shoot and Floral Meristem Development Affecting the Same Processes as Clavata1. *Development,* 121**,** 2057-2067.

CLARK, S. E., WILLIAMS, R. W. & MEYEROWITZ, E. M. 1997. The CLAVATA1 gene encodes a putative receptor kinase that controls shoot and floral meristem size in Arabidopsis. *Cell,* 89**,** 575-585.

CLOUSE, S. D., LANGFORD, M. & MCMORRIS, T. C. 1996. A brassinosteroid-insensitive mutant in Arabidopsis thaliana exhibits multiple defects in growth and development. *Plant Physiology,* 111**,** 671-678.

FLETCHER, L. C., BRAND, U., RUNNING, M. P., SIMON, R. & MEYEROWITZ, E. M. 1999. Signaling of cell fate decisions by CLAVATA3 in Arabidopsis shoot meristems. *Science,* 283**,** 1911-1914.

GISH, L. A., GAGNE, J. M., HAN, L. Q., DEYOUNG, B. J. & CLARK, S. E. 2013. WUSCHEL-Responsive At5g65480 Interacts with CLAVATA Components In Vitro and in Transient Expression. *Plos One,* 8.

GOMEZ-GOMEZ, L., BAUER, Z. & BOLLER, T. 2001. Both the extracellular leucine-rich repeat domain and the kinase activity of FLS2 are required for flagellin binding and signaling in arabidopsis. *Plant Cell,* 13**,** 1155-1163.

GOMEZ-GOMEZ, L. & BOLLER, T. 2000. FLS2: An LRR receptor-like kinase involved in the perception of the bacterial elicitor flagellin in Arabidopsis. *Molecular Cell,* 5**,** 1003-1011.

GUO, Y. F., HAN, L. Q., HYMES, M., DENVER, R. & CLARK, S. E. 2010. CLAVATA2 forms a distinct CLE-binding receptor complex regulating Arabidopsis stem cell specification. *Plant Journal,* 63**,** 889-900.

HALTER, T., IMKAMPE, J., MAZZOTTA, S., WIERZBA, M., POSTEL, S., BUCHERL, C., KIEFER, C., STAHL, M., CHINCHILLA, D., WANG, X., NURNBERGER, T., ZIPFEL, C., CLOUSE, S., BORST, J. W., BOEREN, S., DE VRIES, S. C., TAX, F. & KEMMERLING, B. 2014. The leucine-rich repeat receptor kinase BIR2 is a negative regulator of BAK1 in plant immunity. *Curr Biol,* 24**,** 134-43.

KAYES, J. M. & CLARK, S. E. 1998. CLAVATA2, a regulator of meristem and organ development in Arabidopsis. *Development,* 125**,** 3843-3851.

KINOSHITA, A., BETSUYAKU, S., OSAKABE, Y., MIZUNO, S., NAGAWA, S., STAHL, Y., SIMON, R., YAMAGUCHI-SHINOZAKI, K., FUKUDA, H. & SAWA, S. 2010. RPK2 is an essential receptor-like kinase that transmits the CLV3 signal in Arabidopsis (vol 137, pg 3911, 2010). *Development,* 137**,** 4327-4327.

KINOSHITA, T., CANO-DELGADO, A. C., SETO, H., HIRANUMA, S., FUJIOKA, S., YOSHIDA, S. & CHORY, J. 2005. Binding of brassinosteroids to the extracellular domain of plant receptor kinase BRI1. *Nature,* 433**,** 167-171.

KOZER, N., BARUA, D., ORCHARD, S., NICE, E. C., BURGESS, A. W., HLAVACEK, W. S. & CLAYTON, A. H. A. 2013. Exploring higher-order EGFR oligomerisation and phosphorylation-a combined experimental and theoretical approach. *Molecular Biosystems,* 9**,** 1849-1863.

KUDRYAVTSEV, V., FELEKYAN, S., WOZNIAK, A. K., KONIG, M., SANDHAGEN, C., KUHNEMUTH, R., SEIDEL, C. A. & OESTERHELT, F. 2007. Monitoring dynamic systems with multiparameter fluorescence imaging. *Anal Bioanal Chem,* 387**,** 71-82.

LI, J., WEN, J. Q., LEASE, K. A., DOKE, J. T., TAX, F. E. & WALKER, J. C. 2002. BAK1, an Arabidopsis LRR receptor-like protein kinase, interacts with BRI1 and modulates brassinosteroid signaling. *Cell,* 110**,** 213-222.

LIN, W. W., LI, B., LU, D. P., CHEN, S. X., ZHU, N., HE, P. & SHAN, L. B. 2014. Tyrosine phosphorylation of protein kinase complex BAK1/BIK1 mediates Arabidopsis innate immunity. *Proceedings of the National Academy of Sciences of the United States of America,* 111**,** 3632-3637.

MAUS, M., COTLET, M., HOFKENS, J., GENSCH, T., DE SCHRYVER, F. C., SCHAFFER, J. & SEIDEL, C. A. M. 2001. An experimental comparison of the maximum likelihood estimation and nonlinear least squares fluorescence lifetime analysis of single molecules. *Analytical Chemistry,* 73**,** 2078-2086.

MAYER, K. F. X., SCHOOF, H., HAECKER, A., LENHARD, M., JURGENS, G. & LAUX, T. 1998. Role of WUSCHEL in regulating stem cell fate in the Arabidopsis shoot meristem. *Cell,* 95**,** 805-815.

MÜLLER, R., BLECKMANN, A. & SIMON, R. 2008. The receptor kinase CORYNE of Arabidopsis transmits the stem cell-limiting signal CLAVATA3 independently of CLAVATA1. *Plant Cell,* 20**,** 934-46.

NAM, K. H. & LI, J. M. 2002. BRI1/BAK1, a receptor kinase pair mediating brassinosteroid signaling. *Cell,* 110**,** 203-212.

NIMCHUK, Z. L., TARR, P. T. & MEYEROWITZ, E. M. 2011. An Evolutionarily Conserved Pseudokinase Mediates Stem Cell Production in Plants. *Plant Cell,* 23**,** 851-854.

OGAWA, M., SHINOHARA, H., SAKAGAMI, Y. & MATSUBAYASHI, Y. 2008. Arabidopsis CLV3 peptide directly binds CLV1 ectodomain. *Science,* 319**,** 294-294.

SCHAFFER, J., VOLKMER, A., EGGELING, C., SUBRAMANIAM, V., STRIKER, G. & SEIDEL, C. A. M. 1999. Identification of single molecules in aqueous solution by time-resolved fluorescence anisotropy. *Journal of Physical Chemistry A,* 103**,** 331-336.

SCHOOF, H., LENHARD, M., HAECKER, A., MAYER, K. F. X., JURGENS, G. & LAUX, T. 2000. The stem cell population of Arabidopsis shoot meristems is maintained by a regulatory loop between the CLAVATA and WUSCHEL genes. *Cell,* 100**,** 635-644.

SIMONS, K. & TOOMRE, D. 2000. Lipid rafts and signal transduction. *Nature Reviews Molecular Cell Biology,* 1**,** 31-39.

STAHL, Y., GRABOWSKI, S., BLECKMANN, A., KÜHNEMUTH, R., WEIDTKAMP-PETERS, S., PINTO, K. G., KIRSCHNER, G. K., SCHMID, J. B., WINK, R. H., HÜLSEWEDE, A., FELEKYAN, S., SEIDEL, C. A. M. & SIMON, R. 2013.

Moderation of Arabidopsis Root Sternness by CLAVATA1 and ARABIDOPSIS CRINKLY4 Receptor Kinase Complexes. *Current Biology,* 23**,** 362-371.

STONE, J. M., TROTOCHAUD, A. E., WALKER, J. C. & CLARK, S. E. 1998. Control of meristem development by CLAVATA1 receptor kinase and kinase-associated protein phosphatase interactions. *Plant Physiology,* 117**,** 1217-1225.

SUN, W. X., CAO, Y. R., LABBY, K. J., BITTEL, P., BOLLER, T. & BENT, A. F. 2012. Probing the Arabidopsis Flagellin Receptor: FLS2-FLS2 Association and the Contributions of Specific Domains to Signaling Function. *Plant Cell,* 24**,** 1096-1113.

WANG, X. F., KOTA, U., HE, K., BLACKBURN, K., LI, J., GOSHE, M. B., HUBER, S. C. & CLOUSE, S. D. 2008. Sequential transphosphorylation of the BRI1/BAK1 receptor kinase complex impacts early events in brassinosteroid signaling. *Developmental Cell,* 15**,** 220-235.

WANG, X. L., LI, X. Q., MEISENHELDER, J., HUNTER, T., YOSHIDA, S., ASAMI, T. & CHORY, J. 2005. Autoregulation and homodimerization are involved in the activation of the plant steroid receptor BRI1. *Developmental Cell,* 8**,** 855-865.

WEIDTKAMP-PETERS, S., FELEKYAN, S., BLECKMANN, A., SIMON, R., BECKER, W., KUHNEMUTH, R. & SEIDEL, C. A. 2009. Multiparameter fluorescence image spectroscopy to study molecular interactions. *Photochem Photobiol Sci,* 8**,** 470-80.

YU, L. P., MILLER, A. K. & CLARK, S. E. 2003. POLTERGEIST encodes a protein phosphatase 2C that regulates CLAVATA pathways controlling stem cell identity at Arabidopsis shoot and flower meristems. *Current Biology,* 13**,** 179-188.

V. Chapter 2: A functional analysis of the CORYNE (CRN) protein

1. Introduction:

In *Arabidopsis thaliana*, all above ground tissue is produced from the stem cell population of the shoot apical meristem (SAM). In the SAM, stem cell homeostasis is dependent on the activity of the CLAVATA (CLV) – WUSCHEL (WUS) negative feedback loop (Schoof et al., 2000). WUS, a homeobox transcription factor, is a positive regulator of stem cell fate which is expressed in a small group of cells called the organizing center (OC), residing just beneath the central stem cell domain of the SAM (Laux et al., 1996, Mayer et al., 1998). *WUS* expression is negatively regulated by the small signaling peptide CLAVATA 3 (CLV3), which signals through the receptor-like proteins CLAVATA 1 (CLV1), CLAVATA 2 (CLV2) and CORYNE (CRN) to repress *WUS* expression. As CLV3 is expressed in the stem cells, repression of WUS results in an indirect repression of CLV3, since less *CLV3*-expressing stem cells can be maintained when WUS abundance declines (Schoof et al., 2000). Plants carrying mutations in either gene of the *CLV*/*CRN* receptor-like proteins, exhibit increased stem cell numbers due to unrestricted *WUS* expression, which results in bigger meristems and subsequently more organs being generated. A reliable readout for the severity of a mutation is the number of carpels fusing to form a silique. In the wild type situation, a silique is formed by two fused carpels. This number is significantly enhanced in the different CLV mutants, according to the severity of impairment (Dievart et al., 2003).

Based on this readout and the underlying genetic data, it has been assumed that CLV1 and CLV2/CRN act in parallel via two independent pathways to regulate stem cell fate. In contrast to the strong *clv3* mutant carpel phenotypes, the single mutants of the receptors show only intermediate phenotypes. *clv1*/*clv2* or *clv1*/*crn* double mutants however show an additive phenotype as strong as the *clv3* mutant, which *clv2*/*crn* double mutants do not. Accordingly, CLV2 and CRN have been proposed to act together in the same pathway, while CLV1 acts independently (Müller et al., 2008, Okada et al., 1989, Kayes et al., 1998, Clark et al., 1995). This is supported by the molecular properties of these proteins. *CLV1* encodes a full leucin-rich repeat (LRR) receptor-like kinase (RLK) with an extracellular LRR receptor and an intracellular kinase domain, localized to the plasmamembrane (PM) via a transmembrane domain (TMD) (Clark et al., 1997). CLV2 is also localized to the PM through a TMD and

carries a LRR receptor domain, but lacks an intracellular kinase (Jeong et al., 1999). CRN on the other hand is a kinase protein lacking a receptor domain, but is localized to the PM via a TMD as well (Müller et al., 2008). Thus, CLV1 could potentially perceive and transmit the CLV3 signal independently, while CLV2 and CRN would have to interact to form a full receptor kinase. Interaction data further supports this notion. Based on live cell imaging and Förster (Fluorescence) Resonance Energy Transfer (FRET) Acceptor PhotoBleaching (APB) experiments, it has been shown that CLV2 and CRN strongly interact with each other and are only exported from the endoplasmic reticulum (ER) to the PM as a heteromer. CLV1 preferentially forms homomers, which led to the conclusion that CLV1/CLV1 homomers signal in parallel to CRN/CLV2 heteromers. Furthermore, in the same interaction studies it could be shown that CLV1 and CRN also possess the capability to interact with each other, hinting towards the formation of larger complexes consisting of all three receptors. This indicates that, while the two pathways are separated, they are not fully independent. Instead, they seem to be interconnected with crosstalk between them (Bleckmann et al., 2010).
If CLV1 and CLV2/CRN function independently to transmit the CLV3 signal, this would implicate that CLV2 should be able to perceive the CLV3 signal and CRN should be able to transmit it to downstream effectors. This, however, does not hold true according to more recent studies. While the binding of CLV3 to the LRR receptor domain of CLV1 has been shown experimentally, CLV2 does not exhibit a specific affinity to bind CLV3 (Ogawa et al., 2008, Guo et al., 2010). Furthermore, the kinase domain of CRN contains several features that are typical for signaling inactive pseudokinases: It is missing the essential aspartic acid in the HRD motif of the catalytic loop and the G-loop, necessary for ATP-binding. Furthermore, the DFG motif in the Mg^{2+} binding loop is not fully conserved, and its activation segment is truncated. Accordingly it did not exhibit any autophosphorylation activity in an *in vitro* kinase assay (Nimchuk et al., 2011).

All of this makes it unlikely that the CLV2/CRN complex is actively involved in signaling without a co-receptor and raises the question which function the CRN protein exerts. To examine the role of CRN in the CLV pathway in closer detail, several deletion variants of the protein were constructed to test for their capability to interact with CLV2, localize to the PM and complement the *crn* mutant phenotype.

The variants constructed are based on the predicted protein domain structure:

The CRN protein carries three main domains: A small extracellular domain (EC), a transmembrane domain (TMD) and an intracellular kinase domain (Ki). Prior to protein processing and intracellular transport, it also carries a signal peptide (Fig. 1, A).

The TMD (24 amino acids (aa)): The first described *CRN* mutant in *Arabidopsis*, *crn-1*, carries a point mutation in the TMD (Müller et al., 2008). This already implies that the TMD plays an important role for CRN function. Previous studies have assigned two important functions to the TMD of the CRN protein. First, it localizes the protein to the PM. Second, the TMD mediates the interaction between the different receptor proteins of the CLV pathway. Deletion, or the exchange of the TMD against a TMD of a related LRR-RLK, strongly diminishes or abolishes the interaction between CRN and CLV1 or CLV2 (Bleckmann et al., 2010).

The EC (41 aa): The EC has no apparent conserved motifs, it could however be involved in the facilitation or regulation of ER retention or export. Furthermore it could be important for protein stability or the functionality of the directly adjacent TMD.

The Ki (308 aa): As the CRN kinase appears to be a pseudokinase, it is unlikely that it exerts its function via active signaling (Nimchuk et al., 2011). However, since the *crn-3* mutant phenotype is caused by a premature stop codon in the kinase domain, truncating the kinase by one third of its normal size, the kinase does seem to play a role in CRN functionality. This could be a more mechanistic role, acting as an adapter protein mediating interactions, stabilizing a bigger signaling complex and influencing the localization and re-localization of CLV2.

Furthermore, a potential RxR motif was identified in the juxtamembrane domain of CLV2. In the case of the $GABA_B$ receptor, an RxR motif prevents the export of the receptor from the ER (Pagano et al., 2001). This could be the case for CLV2 as well. In this case, the interaction with CRN would be necessary to disguise the motif and allow ER-export of CLV2.

2. Results:

2.1 Variants Constructed

To analyze CRN function, the following protein variants were constructed:

To analyze the function of the TMD, the described mutant version of *CRN*, *crn-1*, was cloned and expressed to analyze the effect of the mutation in closer detail (Fig. 1, B).

For the EC the following constructs were created:

CRΔEC	A deletion of the entire 41 aa of the EC (Fig. 1, C).
CRΔEC1	A deletion of the central 9 aa of the EC (Fig. 1, D).
CRΔEC2	A deletion of 14 aa adjacent to the TMD (Fig. 1, E).

Deleting parts of the EC (CRΔEC1, CRΔEC2) or the entire domain (CRΔEC) could have effects on either ER-retention (when CLV2 is not present), or ER-export (in the presence of CLV2). If this domain contains a concealed ER retention motif, deleting it would lead to constitutive ER-export, even in the absence of CLV2. On the other hand, the EC could contain a motif necessary for the CLV2-mediated export of CRN. In this case, the protein should be retained in the ER, even if CLV2 is co-expressed. Finally, if the EC is involved in maintaining protein stability or TMD function, CLV2-interaction could be impaired, if the EC is removed.

To analyze the function of the kinase domain the following constructs were created:

crn-3	The described mutant version of *CRN* (Fig. 1, F).
CRΔKi	A deletion of the entire kinase (Fig. 1, G).
CR(SD)	An exchange of the potentially phosphorylated serine (S) to an aspartic acid (D) (Fig. 1, H).
CR(KQ)	An exchange of the active site lysine (K) to a glutamine (Q) (Fig. 1, I).
CR(<>C1Ki)	A replacement of the entire kinase with the CLV1 kinase (Fig. 1, J).
C2(CRKi)	A chimeric protein of CLV2 with the intracellular CRN kinase (Fig. 2, D).

It has been shown that the CRN kinase is a pseudokinase. Since the *crn-3* mutant, which lacks one third of the kinase, is not fully functional though, it appears that the kinase domain does exert some kind of function. To see, which step is impaired in the *crn-3* mutant, the crn-3 protein was cloned and tested for its intracellular localization and CLV2-interaction. It is possible, that the kinase plays a more mechanistic or steric role. In this case, the presence of the kinase structure might be required, e.g. to facilitate ER-export, stabilize a bigger

complex or provide docking points for other factors. If this was true, removing it would diminish the remaining proteins functionality (CRΔKi).

To further test this possibility, another two constructs were built: First, a chimeric recombinant protein, consisting of the CLV2 LRR-receptor- and transmembrane domain (TMD) and the CRN kinase domain (C2(CRKi)) was created. With this protein it can be tested if only a full receptor-like kinase, containing both, a receptor and a kinase domain is necessary to facilitate ER-export of the protein and functionality. If this is the case, the protein should get exported, even though there is no interaction partner. Additionally, the CRN kinase was replaced with the CLV1 kinase (CR(<>C1Ki)) which has a similar structure but has been shown to be active. In this case, the CLV2 / CRN complex is still formed, but with a different kinase.

If the kinase does possess autophosphorylation activity, contrary to what has been shown, exchanging the active site lysine, necessary for ATP-binding, against a glutamine (Q) would prevent this and render the kinase constitutively inactive (CR(KQ)). Furthermore, even if the CRN kinase does not autophosphorylate, transphosphorylation of the CRN kinase by a kinase of an interacting protein could be necessary. To test this, a version of CRN with an exchange of the potentially phosphorylated serine (S) to an aspartic acid (D) was created (Nühse et al., 2004). This could result in a version of the kinase mimicking constitutive phosphorylation and hence activation (CR(SD)).

To test if the potential RxR motif (Pagano et al., 2001) in the CLV2 protein is responsible for ER-retention, two variants of CLV2 were created.

C2(RA) A replacement of the first conserved arginine (R) of the RxR motif with an alanine (A) (Fig. 2, B).

C2(708) A deletion of the potential RxR motif (Fig. 2, C).

Mutating the RxR motif should lead to constitutive export of CLV2 from the ER, independent of the presence of CRN. Therefore, the CLV2 protein should be at the PM, even if CRN is not present. They should also be able to rescue the *clv2* mutant phenotype, if the deletion does not influence protein stability or functionality.

Two assays were used to test the functionality of the different CRN variants. First the proteins ability to interact with their respective interaction partner was assayed (CLV2 for the CRN variants and vice versa) as well as their intracellular localization (ER or PM).
Second a complementation assay was performed, to test if the different protein variants are able to complement their respective mutants.

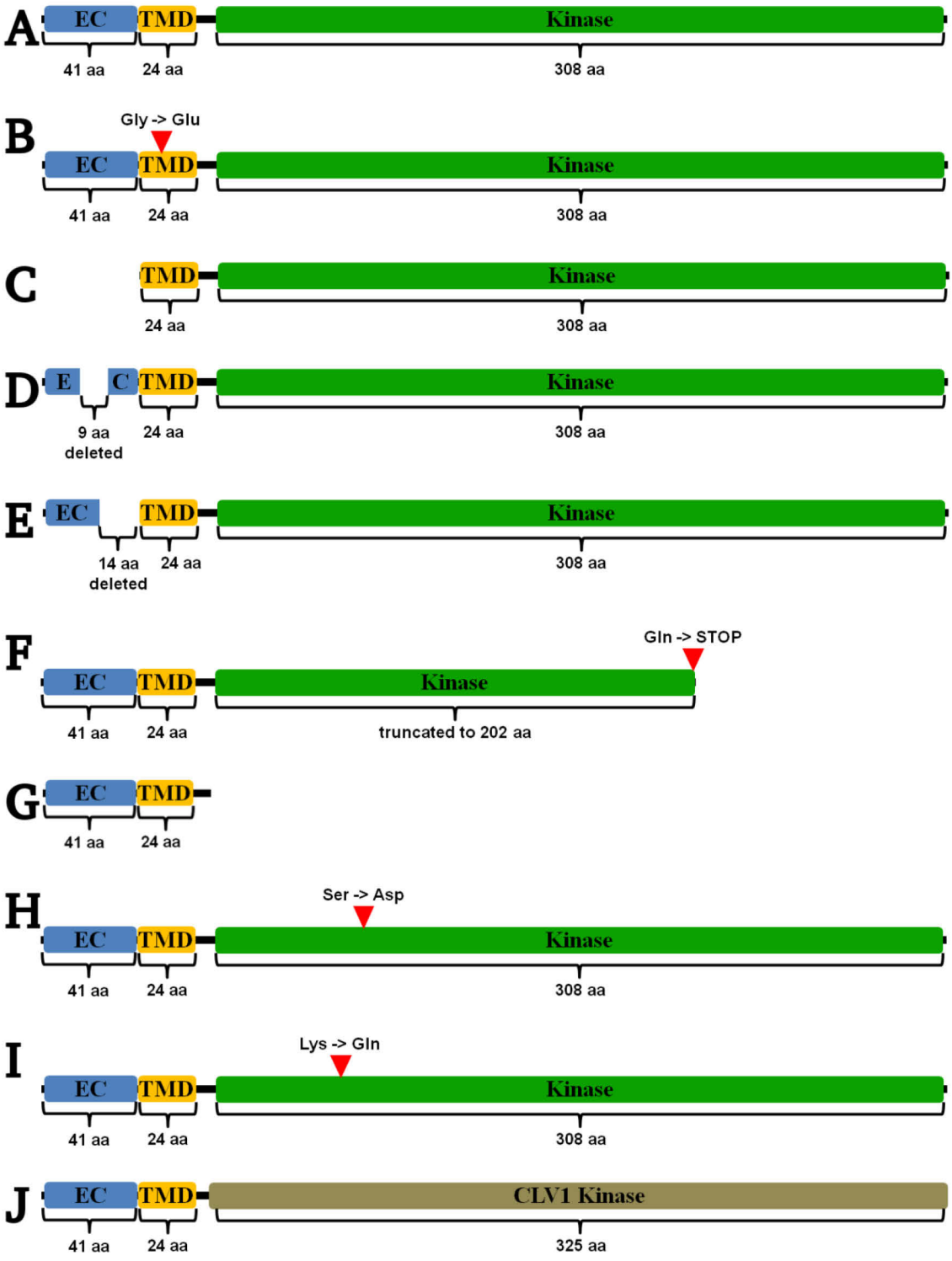

Fig. 1: Schematic representations of the CRN protein variants

A) CRN, B) crn-1, C) CRΔEC, D) CRΔEC1, E) CRΔEC2, F) crn-3, G) CRΔKi, H) CR(SD), I) CR(KQ), J) CR(<>C1Ki).

Blue = EC domain, Orange = TMD, Green = Kinase domain, Light Brown = CLV1 kinase domain. The red arrowheads in B, F, H and I represent the positions of amino acid exchanges.

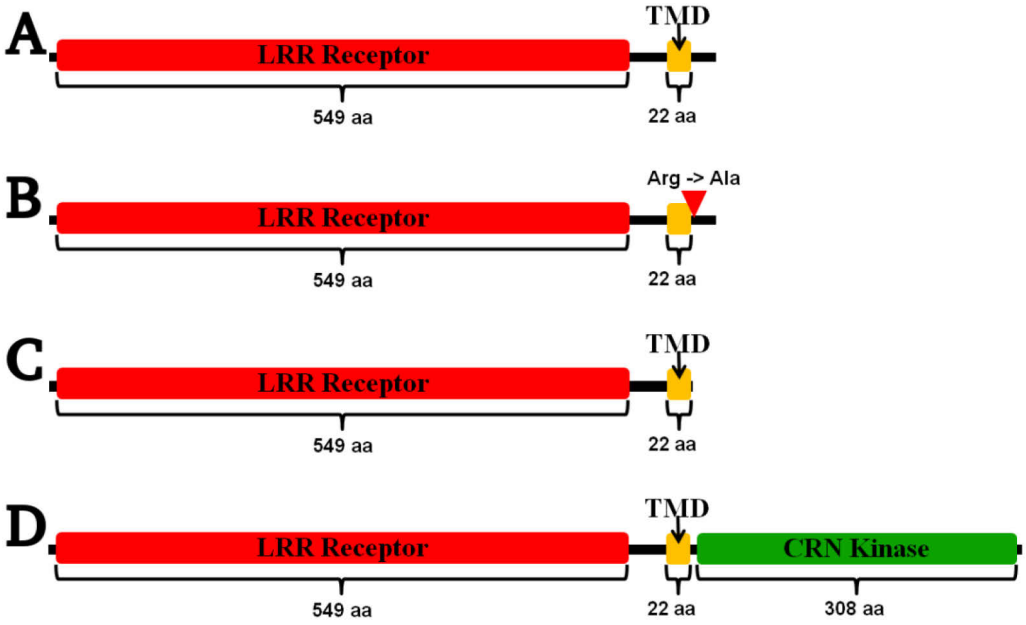

Fig. 2: Schematic representations of the CLV2 protein variants

A) CLV2, B) C2(RA), C) C2(708), D) C2(CRKi)

Red = LRR receptor domain, Orange = TMD, Green = CRN Kinase domain. The red arrowhead in B represents the positions of an amino acid exchange.

For the complementation assay the carpel phenotype was used as readout for the proteins functionality. The Columbia-*0* (Col-*0*) wild type plant produces siliques consisting of two carpels, while the *crn-3* mutant forms siliques with 2.4 carpels on average. This phenotype is stronger in Landsberg *erecta* background, where the L*er* wild type control already has 2.04 carpels on average and the *crn-1* mutant produces siliques with 3.6 carpels on average. The CLV2 variants were tested for their ability to rescue the *clv2-gk* mutant, which is in Col-*0* background and produces siliques with 2.4 carpels on average.

2.2 The Effects of the CRN and CLV2 Variations on Protein Interaction and Localization

The interaction- and localization-assay brought up two CRN variants with impaired interaction with CLV2 (Fig 3, Tab. 1). Those were the *crn-1* version and the CRΔEC variant, which is missing the entire extracellular domain. Interestingly, ER to PM transport was only blocked in the CRΔEC variant, while the *crn-1* variant was still exported from the ER, even though it seemed that some protein was retained in the ER. Hence, the impaired interaction with CLV2 seemed to impair ER export as well. From this experiment it seems that the

extracellular domain of CRN can be partially deleted. Deleting it in its entirety on the other hand, results in impaired CLV2-interaction and blocked ER to PM transport.

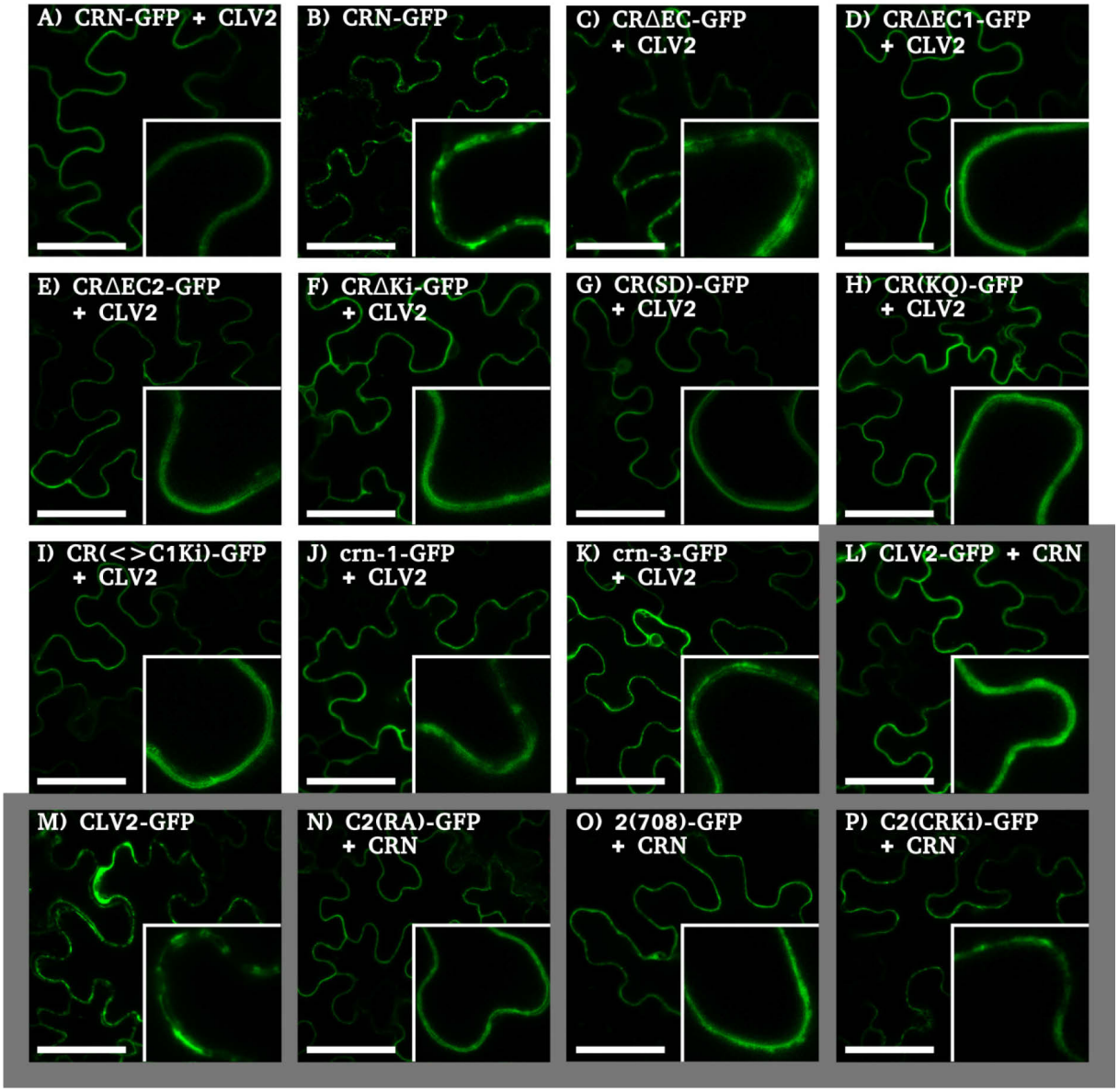

Fig. 3: Intracellular localization of the different CRN and CLV2 variants

GFP-reporter lines for the different CRN (white background) and CLV2 (grey background) variants. CRN-GFP (+/- CLV2) and CLV2-GFP (+/- CRN) are shown to demonstrate PM (with partner) or ER localization (without partner) of the wild type proteins. The patchy signal at the PM for the CRΔEC variant shows the blocked ER-export. The slightly more patchy signal at the PM for the crn-1, crn-3 and C2(CRKi) variants shows the impaired ER-export. All other lines show a smooth signal coming from the PM. The inserts are magnifications, taken from the same cells. Scale bars are 50 µM.

The *crn-3* variant showed impaired ER export as well, while it still seemed to fully interact with the CLV2 protein. This implies that CRN/CLV2-interaction and ER-to-PM transport are not always completely correlated, as *crn-3* appears to fully interact with CLV2,

but its ER-to-PM transport is impaired. Interestingly, the other variants with have a deleted, mutated or exchanged kinase domain exhibit no effects when it comes to CLV2-interaction and protein localization. Hence, it is possible that the remaining part of the kinase in the crn-3 variant is somehow misfolded or partially unfolded and thereby interferes with other proteins in the ER (Fig. 3, Tab. 1).

For CLV2, the C2(RA) and C2(708) variants still interact with CRN and are exported from the ER (Fig. 3, Tab. 1). Without CRN being present however, still none of them are exported. This shows that the potential RxR motif in the CLV2 protein, which could have been responsible for ER retention, is actually not functional. If it was, the two variants in which the motif is mutated or deleted should be exported, even in the absence of the CRN protein.

The C2(CRKi) variant was not exported in the absence of CRN as well, which shows that the presence of a kinase structure alone is not enough for the CLV2 protein to be exported. This variant did interacted with CRN however, but even in the presence of CRN ER-to-PM transport seemed to be impaired. This could imply that the added kinase interferes mechanistically, just as the bigger CLV1 kinase appeared to do in the CR(<>C1Ki) variant (Fig. 3, Tab. 1).

Variant	Interaction w/ CLV2	ER->PM w/ CLV2
CRN	Yes	Yes
CRΔEC	Impaired	✕
CRΔEC1	Yes	Yes
CRΔEC2	Yes	Yes
CRΔKi	Yes	Yes
CR(SD)	Yes	Yes
CR(KQ)	Yes	Yes
CR(<>C1Ki)	Yes	Yes
crn-1	Impaired	Impaired
crn-3	Yes	Impaired
Variant	**Interaction w/ CRN**	**ER->PM w/ CRN**
CLV2	Yes	Yes
C2(RA)	Yes	Yes
C2(708)	Yes	Yes
C2(CRKi)	Yes	Impaired

Tab. 1: Capability of the different CRN and CLV2 variants to interact with CLV2 and get exported from the ER to the PM

Interaction of CRΔEC and crn-1 with CLV2 is impaired. CRΔEC is not exported from the ER, while export is impaired for crn-1, crn-3 and C2(CRKi).

2.3 The Complementation Ability of the different CRN and CLV2 Variants

From the complementation assay three CRN variants were identified that could rescue the *crn* mutant phenotype (Fig. 4 and Tab. 2). For one this was the wild type CRN protein, which served as the positive control for this experiment. Furthermore, the CRΔEC2 and CR(SD) variants restored the carpel phenotype back to wild type. In the case of the CRΔEC2 variant this is especially interesting. This is the variant with a deletion of 14 aa of the EC removed from the TMD by 3 aa. In the interaction- and localization-assay, this variant gave the same results as the CRΔEC1 variant, in which the central 9 aa of the EC are deleted. Both interacted with CLV2 and got exported from the ER, while the variant in which the entire domain was deleted did not interact with CLV2 anymore and was not exported either. From this it seems that the central (CRΔEC) and / or more distal parts (CRΔEC) of the EC are important for the protein to function, while the 14 aa adjacent to the TMD seem to be of minor importance (CRΔEC2).

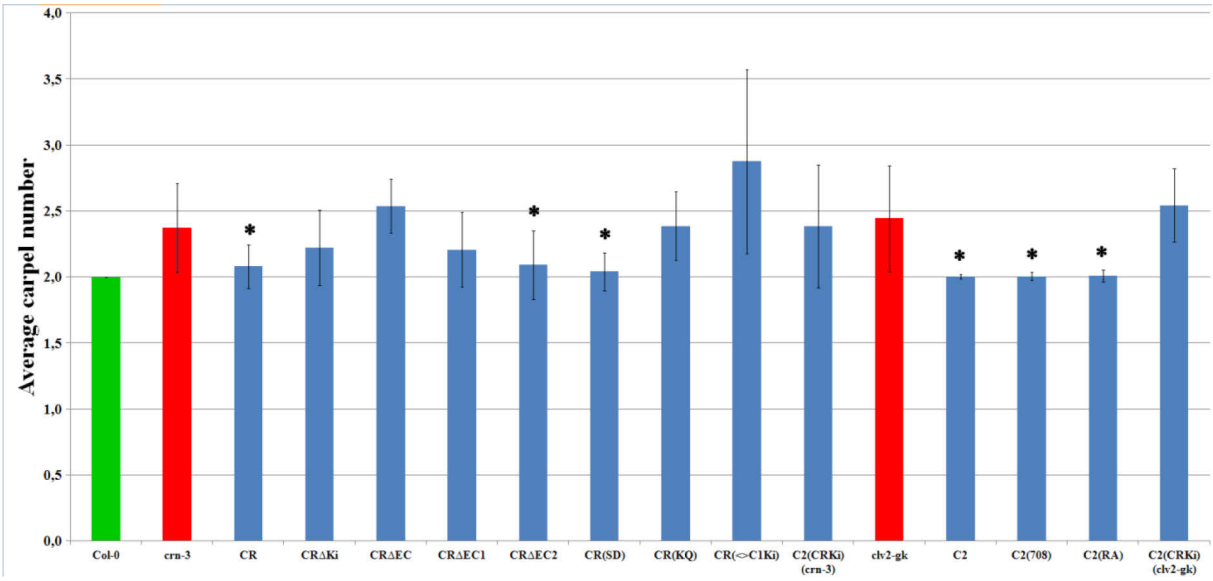

Fig. 4: Carpel numbers for the different plant lines

Average numbers of carpels for the different plant lines. The bar for wild type Columbia-*0* is green, the two bars for the two mutants, *crn-3* and *clv2-gk*, are red. The asterisk (*) indicates the lines with carpel numbers significantly different from the mutant. Error bars show the standard deviation. Between 12 and 20 carpels from 20 to 50 individual plants were analyzed for each line.

Interestingly, even if the CRN kinase appears to be a pseudokinase, the kinase is still an essential part of the protein. Deleting, mutating or replacing it does not result in a rescue of the mutant phenotype. From the kinase variations, only the CR(SD) variant was able to rescue

the mutant. This was supposed to be a constitutively active version of the kinase. Curiously, the constitutive inactive version, CR(KQ), was not able to restore the phenotype. Also, replacing the pseudokinase of CRN with the active kinase of the CLV1 protein resulted in a non-functional protein not able to rescue the mutant. On the contrary, the lines carrying the CR(<>C1Ki) variant actually exhibited a stronger phenotype, an indication that this protein might act in a dominant-negative fashion (Fig. 4 and Tab. 2).

From the different CLV2 variants, the wild type control was able to rescue the mutant, as were the two variants in which the potential RxR motif was mutated (Fig. 4 and Tab. 2). This was expected from the previous interaction- and localization studies, since removing the RxR motif did not lead to constitutive ER-export. The chimeric C2(CRKi) protein, which was supposed to resemble a full receptor kinase protein was also not able to complement the mutant, indicating that adding the kinase to the CLV2 protein somehow interferes with its functionality (Fig. 4 and Tab. 2).

Plant Line	Number of Carpels		
	#	**SD**	**p**
Col-*0*	2	0	-
crn-3	2.37	0.34	-
clv2-gk	2.44	0.4	-
Variant in *crn-3*	**Number of Carpels**		
CRN	2.08 *	0.16	0.001
CRΔEC	2.54	0.21	0.77
CRΔEC1	2.21	0.29	0.09
CRΔEC2	2.09 *	0.26	0.004
CRΔKi	2.22	0.28	0.18
CR(SD)	2.04 *	0.14	6.4×10^{-5}
CR(KQ)	2.39	0.26	0.9
CR(<>C1Ki)	2.87	0.7	0.01
C2(CRKi)	2.38	0.47	0.95
Variant in *clv2-gk*	**Number of Carpels**		
CLV2	2 *	0.02	1.8×10^{-5}
C2(RA)	2.01 *	0.05	8.7×10^{-7}
C2(708)	2.01 *	0.03	2.5×10^{-7}
C2(CRKi)	2.54	0.28	0.4

Tab. 2: Results of the mutant complementation assays

Three of each CRN and CLV2 variants are capable of rescuing the carpel phenotype of the *crn* and *clv2* mutants. These are the wild type proteins CRN and CLV2, as well as the variants CRΔEC2, CR(SD), C2(RA), C2(708). # = Average number of carpels per silique, SD = Standard deviation, p = p-value from Student's t-test. * indicates the values significantly different from the mutant value.

3. Discussion:

The aim of this experiment was to examine the function of the CRN protein in the CLV signaling pathway in closer detail, by assaying the functionality of different protein variants. This should allow us to assign specific functions to the different domains of the CRN protein.

From these experiments it can be concluded that the short extracellular tail of the CRN kinase protein most likely plays a role in protein stability. The more proximal 14 aa (CRΔEC2), separated from the TMD by three aa, can be deleted without impairing protein functionality. The 9 central aa (CRΔEC1) however seem to play an important role. Deleting these 9 aa renders the protein incapable of complementing the mutant. The CRN variant in which the entire EC is deleted (CRΔEC), along with the *crn-1* mutant which carries a point mutation in the TMD, is the only CRN variant that is no longer exported from the ER in the presence of CLV2.

From these observations, it is a possibility that a motif in the central 9 aa is essential for the function of the CRN protein. This is why this variant interacts with CLV2 and gets exported from the ER, but cannot complement the mutant. However, the EC also appears to play a role in protein stability, since removing it in its entirety results in ER-retention. A possible explanation for this could be that an extracellular tail of the CRN protein, in combination with the juxtamembrane domain of the CLV2 protein, is necessary to shield amino acids that prevent ER export when exposed. In this case, the CRΔEC variant would not be exported because these amino acids would be only partially shielded by the interacting CLV2 protein, and in the case of the *crn-1* mutant protein, in which CLV2-interation is strongly impaired, the amino acids would be partially shielded by the EC of the CRN protein, but are missing the remaining shield coming from the CLV2 protein.

Another possibility is that a motif in the TMD is responsible for ER export, just as it is for CLV2 interaction. This would explain why the *crn-1* variant with a point mutation in the TMD does not get fully exported. The CRΔEC variant however does still interact with CLV2 at least partly, and accordingly its TMD seems to be at least in part functional. Therefore, it is possible that a motif close to the extracellular domain is necessary for ER export, while a more central motif is necessary for CLV2 interaction. In this case, the removal of the EC could result in a partially incorrectly folded TMD that can still integrate into the PM and partly interact with CLV2, but only with impairments reflected in partially blocked CLV2-interaction and ER-export.

From the results of this complementation assay it appears that the kinase domain of CRN does not influence CLV2 interaction and ER export, as all kinase variants interact with CLV2 and get exported from the ER. However, the kinase still is important for the CRN protein to exert its function.

Deleting the kinase domain (CRΔKi) does not impair the interaction with CLV2 or the export from the ER to the PM, but the mutant phenotype cannot be complemented by this variant. Therefore, the kinase is probably necessary for the functionality of the CLV2/CRN complex at the PM. Interestingly, the one CRN kinase variant that does rescue the mutant is the potential phosphomimic version (CR(SD)). While this could imply that phosphorylation of the kinase is necessary for its functionality, it could also be possible that the S->D exchange has no effect at all. In this latter case the CR(SD) variant would be no different from the wild type protein and accordingly complement the mutant. Interestingly though, the CR(KQ) variant, in which the active site lysine in the kinase was replaced with a glutamine does not restore the *crn* phenotype back to wild type, even though it is just a point mutation as well. The CR(KQ) variant, just like the CR(SD) variant, interacts with CLV2 and is exported from the ER to the PM, but the mutant cannot be complemented by it. However, in a previous study the same lysine was exchanged with a glutamic acid (E), and the resulting CR(KE) variant was capable of rescuing the mutant (Nimchuk et al., 2011). One difference between glutamine and glutamic acid is the side-chain charge. While in the K->Q exchange the side-chain charge is changed from positive to neutral, it is changed from positive to negative in the K->E exchange. This could be one possible explanation for the different outcome of these experiments. It is still surprising though, that one variant can rescue the mutant and one cannot. With respect to the CR(SD) variant it would now be interesting to see if a version, in which the serine is replaced by another amino acid that cannot be phosphorylated but is no phosphomimic either, can also rescue the mutant. If so, the serine is irrelevant for CRN function and both variants would be analogous to the wild type protein. If, however, this version does not complement the mutant, the serine could actually be a target for phosphorylation and hence be essential for CRN function. This is not unlikely, and would not be incompatible with CRN being a pseudokinase. With its features, the CRN kinase is incapable of autophosphorylation, which has been shown before. But it could still be the target of transphosphorylation from an interacting kinase, e.g. the CLV1 kinase, at the serine residue. A case like this has been reported previously for the *Mycobacterium smegmatis* mvin protein (Gee et al., 2012). This pseudokinase, like the CRN kinase, has divergent sequences in the otherwise conserved HRD motif of the catalytic loop, the G-loop, and the DFG motif and

accordingly shows no autophosphorylation activity. Still, this pseudokinase was phosphorylated by the interacting PG-responsive Ser-Thr protein kinase (STPK). This possibility should be examined in closer detail for the CRN pseudokinase.

Finally, there are several indications that the kinase plays a mechanistic role as well. The two chimeric proteins used in this study, one in which the CRN kinase is exchanged with the CLV1 kinase (CR(<>C1Ki)) and one where the CRN kinase is attached to the intracellular tail of CLV2 (C2(CRKi)) do not show a difference in protein localization and CLV2-interaction, but do not complement the *crn* (CR(<>C1Ki) and C2(CRKi)) or *clv2* (C2(CRKi)) mutant either. As the C2(CRKi) variant was not exported from the ER in the absence of the CRN protein, the possibility that the spatial and mechanistic presence of the CRN kinase at the CLV2 protein alone is already enough for ER-export can be excluded. Additionally, the added kinase seems to interfere with the functionality of the CLV2 protein. In the presence of the CRN protein, the C2(CRKi) variant gets at least partially exported from the ER to the PM. However, it is not capable of rescuing the *clv2* mutant phenotype. Most likely, it interferes with other proteins already while in the ER, and possible later at the PM. This could be by spatially preventing interaction with other receptor-like proteins, such as CLV1, or by interfering with downstream components that normally interact with the CRN or CLV1 kinase and can no longer access their target site due to the additional kinase interfering. This would fit with the CR(<>C1Ki) variant also not rescuing the mutant and actually showing an enhanced phenotype. The CLV1 kinase is bigger than the CRN kinase and could have a slightly different conformation. Accordingly the CR(<>C1Ki) variant would also interfere spatially with other components of the CRN/CLV2 complex at the PM. Additionally, it is possible that downstream effectors that would normally bind to CLV1 via its kinase, now bind to the CLV1 kinase fused to the CRN protein. This way the CR(<>C1Ki) variant would interfere with CLV1 signaling, making it dominant negative. This could be a possible explanation for the enhanced phenotype.

The *crn-3* mutant has a premature stop codon in the kinase, shortening it by one third. This mutant variant of the CRN protein still interacts with CLV2 and gets partially exported, but it cannot exert its function at the PM. Again, the mutated kinase somehow seems to interfere with other components involved in the signaling pathway. In this case this interference could also come from the shortened kinase not being folded properly.

Finally, the CLV2 variants, in which the potential RxR motif is mutated (C2(RA) and C2(708)), were still retained in the ER in the absence of the CRN protein. If this was an actual ER-retention signal, as it was published for the $GABA_B$ receptor, they should have been

constitutively exported. Since both variants were also able to complement the *clv2* mutant, it appears that the inserted mutations had no effect at all. Therefore, the presumed motif does not appear to be a functional RxR motif.

4. Conclusions:

Overall, there are several conclusions regarding the function of the CRN protein and its subdomains that can be drawn from the described experiments.

First of all, the idea that the CRN protein simply is an adapter protein for CLV2, facilitating its transport to the PM and interactions with other proteins, seems to be false. Almost all CRN variants tested were able to interact with CLV2 and facilitate its export from the ER, but still weren't able to complement the mutant phenotype. Accordingly, CRN must play a bigger role in the CLV pathway than simply being an adapter for CLV2.

The extracellular domain of the CRN protein seems to play a stabilizing role for the proteins transmembrane domain. Removing the entire domain results in impaired CLV2-interaction and ER-retention. The deletion of only parts of the domain does not affect the proteins interaction with CLV2 or its localization. Interestingly, in this regard it does not matter if the central or more proximal part of the domain is deleted. However, only the variant lacking the proximal half can complement the *crn* mutant phenotype, while the variant lacking the central part cannot. Therefore, it can be assumed that a few amino acids directly adjacent to the TMD are necessary for correct folding, stabilization and/or membrane-integration of the TMD. It does, however not seem to matter which amino acids these are, as they could function more as a physical cap, not an active domain. Once in a complex with CLV2 and localized to the cells PM, some hidden motif in the central part of the EC seems to play a role for the CRN protein to function properly. To analyze this, the central part should be further subdivided to identify the critical residues rendering this protein unable to complement the mutant.

The kinase domain of CRN is essential for the proteins functionality as well. This could already be assumed from the *crn-3* mutant, which contains a premature stop codon in the kinase, truncating it by one third of its full size. Deleting it in its entirety accordingly cannot complement the mutant phenotype either. Since the kinase does appear to be a pseudokinase unable to autophosphorylate, it must act in a different way. One possibility that cannot be excluded is that the kinase gets transphosphorylated by an interacting kinase. Transphosphorylation of pseudokinases has been described before, and since the CRN kinase

does have a conserved serine in its potential phosphorylation site, this is not unlikely. Replacing this serine with an aspartic acid could mimic phosphorylation and the corresponding variant was indeed able to complement the mutant. In a next step to determine if transphosphorylation of this serine residue is essential for the CRN kinase, it should be replaced by another amino acid that would prevent phosphorylation. If this variant would not be able to complement the mutant, it must be assumed that the CRN kinase gets phosphorylated. A second plausible function of the CRN kinase is to provide mechanistic stability to the signaling active complex at the PM, or provide docking points for other proteins in that complex. This would explain why removing or manipulating the physical shape of the kinase by removing parts of it or exchanging it with another, bigger kinase cannot complement the mutant. In this regard it would be interesting to see if interaction of the CRN / CLV2 complex with the CLAVATA COMPLEX INTERACTORS 1 and 2 (CCI1 & 2), since these proteins were described to interact with the kinase domain of CLV1 in yeast two-hybrid and co-immunoprecipitation assays (Gish et al., 2013).

5. Methods:

Arabidopsis thaliana Plant Lines

Arabidopsis thaliana plants were grown at 21° C short day (8 hours light) conditions for four weeks and were then shifted to 21° C continuous light conditions for two weeks when the carpels were counted. Agrobacterium-mediated transformation was performed according to (Logemann et al., 2006).

Nicotiana benthamiana Plant Lines

Nicotiana benthamiana plants were grown in the greenhouse for four weeks prior to transient transformation. Transformation and expression were described before (Bleckmann et al., 2010).

Construction of Plasmids

The different CRN and CLV2 variants were created from cDNA using the Gateway® BP / LR Clonase® II Cloning Kits, as well as the destination vector pMDC32 described previously (Curtis et al., 2003).

The inducible CRN- and CLV2- GFP and mCherry expression vectors were described before (Bleckmann et al., 2010). The fluorophore fusions for the different CRN and CLV2 variants were created from cDNA using the Gateway® BP / LR Clonase® II Cloning Kits, as well as the destination vectors pABindGFP and pABindmCherry described previously (Bleckmann et al., 2010).

Microscopy

Imaging and FRET-APB measurements were done on a Zeiss LSM 780 confocal microscope. GFP was excited with a continuous wave 480 nm argon laser at the objective (40x water immersion, Zeiss C-Apochromat 40x/1.20 W korr M27) and emission was detected at 498 - 524 nm by 32-Channel-GaAsP-Detectors. mCherry was excited using a 561 nm continuous wave diode laser and emission detected at 578 - 639 nm. For APB measurements, a series of 12 256 x 256 pixel frames with 0.18 µM pixel size, 47 μm^2 image size and 1.27 µs pixel dwell time was recorded. After 5 frames, mCherry was photobleached in a region of interest along the PM by 80 iterations with 100 % laser power. E% was determined as GFP-intensity change after photobleaching by (GFPafter − GFPbefore)/GFPafter × 100.

This chapter is a manuscript in preparation for submission.

Authors:
Marc Somssich[1], Andrea Bleckmann[1, 3], Carin Theres[1] and Rüdiger Simon[1, 2]

[1] Institute of Developmental Genetics, Heinrich Heine University, 40225 Düsseldorf, Germany
[2] Center for Advanced Imaging, Heinrich Heine University, 40225 Düsseldorf, Germany
[3] current address: Department of Cell Biology and Plant Biochemistry, University of Regensburg, Germany

The experiment was designed by Marc Somssich, Rüdiger Simon and Andrea Bleckmann. Molecular biology and plant work was done by Marc Somssich with help from Andrea Bleckmann and Carin Theres. Microscopy was done by Marc Somssich. Data analysis was done by Marc Somssich. The manuscript was written by Marc Somssich with help from Rüdiger Simon.

6. References:

BLECKMANN, A., WEIDTKAMP-PETERS, S., SEIDEL, C. A. & SIMON, R. 2010. Stem cell signaling in Arabidopsis requires CRN to localize CLV2 to the plasma membrane. *Plant Physiol,* 152**,** 166-76.

CLARK, S. E., RUNNING, M. P. & MEYEROWITZ, E. M. 1995. CLAVATA3 Is a Specific Regulator of Shoot and Floral Meristem Development Affecting the Same Processes as CLAVATA1. *Development,* 121**,** 2057-2067.

CLARK, S. E., WILLIAMS, R. W. & MEYEROWITZ, E. M. 1997. The CLAVATA1 gene encodes a putative receptor kinase that controls shoot and floral meristem size in Arabidopsis. *Cell,* 89**,** 575-585.

CURTIS, M. D. & GROSSNIKLAUS, U. 2003. A gateway cloning vector set for high-throughput functional analysis of genes in planta. *Plant Physiology,* 133**,** 462-469.

DIEVART, A., DALAL, M., TAX, F. E., LACEY, A. D., HUTTLY, A., LI, J. M. & CLARK, S. E. 2003. CLAVATA1 dominant-negative alleles reveal functional overlap between multiple receptor kinases that regulate meristem and organ development. *Plant Cell,* 15**,** 1198-1211.

GEE, C. L., PAPAVINASASUNDARAM, K. G., BLAIR, S. R., BAER, C. E., FALICK, A. M., KING, D. S., GRIFFIN, J. E., VENGHATAKRISHNAN, H., ZUKAUSKAS, A., WEI, J. R., DHIMAN, R. K., CRICK, D. C., RUBIN, E. J., SASSETTI, C. M. & ALBER, T. 2012. A Phosphorylated Pseudokinase Complex Controls Cell Wall Synthesis in Mycobacteria. *Science Signaling,* 5.

GISH, L. A., GAGNE, J. M., HAN, L. Q., DEYOUNG, B. J. & CLARK, S. E. 2013. WUSCHEL-Responsive At5g65480 Interacts with CLAVATA Components In Vitro and in Transient Expression. *Plos One,* 8.

GUO, Y. F., HAN, L. Q., HYMES, M., DENVER, R. & CLARK, S. E. 2010. CLAVATA2 forms a distinct CLE-binding receptor complex regulating Arabidopsis stem cell specification. *Plant Journal,* 63**,** 889-900.

JEONG, S., TROTOCHAUD, A. E. & CLARK, S. E. 1999. The Arabidopsis CLAVATA2 gene encodes a receptor-like protein required for the stability of the CLAVATA1 receptor-like kinase. *Plant Cell,* 11**,** 1925-1933.

KAYES, J. M. & CLARK, S. E. 1998. CLAVATA2, a regulator of meristem and organ development in Arabidopsis. *Development,* 125**,** 3843-3851.

LAUX, T., MAYER, K. F. X., BERGER, J. & JURGENS, G. 1996. The WUSCHEL gene is required for shoot and floral meristem integrity in Arabidopsis. *Development,* 122**,** 87-96.

LOGEMANN, E., BIRKENBIHL, R. P., ÜLKER, B. & SOMSSICH, I. E. 2006. An improved method for preparing Agrobacterium cells that simplifies the Arabidopsis transformation protocol. *Plant Methods,* 2.

MAYER, K. F. X., SCHOOF, H., HAECKER, A., LENHARD, M., JURGENS, G. & LAUX, T. 1998. Role of WUSCHEL in regulating stem cell fate in the Arabidopsis shoot meristem. *Cell,* 95**,** 805-815.

MÜLLER, R., BLECKMANN, A. & SIMON, R. 2008. The receptor kinase CORYNE of Arabidopsis transmits the stem cell-limiting signal CLAVATA3 independently of CLAVATA1. *Plant Cell,* 20**,** 934-46.

NIMCHUK, Z. L., TARR, P. T. & MEYEROWITZ, E. M. 2011. An Evolutionarily Conserved Pseudokinase Mediates Stem Cell Production in Plants. *Plant Cell,* 23**,** 851-854.

OGAWA, M., SHINOHARA, H., SAKAGAMI, Y. & MATSUBAYASHI, Y. 2008. Arabidopsis CLV3 peptide directly binds CLV1 ectodomain. *Science,* 319**,** 294-294.

OKADA, K., KOMAKI, M. K. & SHIMURA, Y. 1989. Mutational Analysis of Pistil Structure and Development of Arabidopsis-Thaliana. *Cell Differentiation and Development,* 28**,** 27-38.

PAGANO, A., ROVELLI, G., MOSBACHER, J., LOHMANN, T., DUTHEY, B., STAUFFER, D., RISTIG, D., SCHULER, V., MEIGEL, I., LAMPERT, C., STEIN, T., PREZEAU, L., BLAHOS, J., PIN, J. P., FROESTL, W., KUHN, R., HEID, J., KAUPMANN, K. & BETTLER, B. 2001. C-terminal interaction is essential for surface trafficking but not for heteromeric assembly of GABA(B) receptors. *Journal of Neuroscience,* 21**,** 1189-1202.

SCHOOF, H., LENHARD, M., HAECKER, A., MAYER, K. F. X., JURGENS, G. & LAUX, T. 2000. The stem cell population of Arabidopsis shoot meristems is maintained by a regulatory loop between the CLAVATA and WUSCHEL genes. *Cell,* 100**,** 635-644.

VI. Chapter 3: The Effects of Molecular Linkers on the Functionality of Fluorescent Proteins

1. Introduction:

The construction of recombinant chimeric proteins is a common technique in molecular biology. Protein localization studies are often based on a marker being fused to the protein of interest. Most protein interaction studies involve the fusion of tags to the two proteins tested, and several assays to determine the catalytic activity of proteins or protein domains require the analyzed protein to be tagged. While these tags are necessary for the experimental procedure, they can also impair the proteins functionality by, e.g., preventing correct folding of the protein, post-translational modifications, physically hindering the binding of interacting proteins or shielding a motif critical for the proteins function. One important way to circumvent these problems, are molecular linkers in the form of amino acid peptide chains. Those can be introduced between the protein and its tag to separate these two molecules far enough to allow them to mature and function correctly.

One type of linker used successfully to separate two proteins consists of monomeric hydrophilic α-helices. These rigidly push the two molecules apart, allowing them to function without interfering with each other (Marqusee et al., 1987). This approach, however, was not suitable when designing molecular linkers for FRET-measurements. FRET primarily is a measure of distance. Here, the distance between two fluorophores is supposed to reflect the distance between the attached proteins to monitor their interaction. Accordingly, a linker between the fluorophore and the protein should be short enough to mark the proteins position and long enough to ensure protein folding and functionality (Evers et al., 2006).

A thought compromise was the introduction of long flexible linkers. These linkers, consisting of several repeats of the flexible and hydrophilic amino acids glycine and serine, were supposed to be long enough to allow for correct protein maturation, but because of their predicted flexibility, they were supposed to form a random coil, leading to a reasonable short distance between fluorophore and fused protein, which is necessary to preserve the distance relation of the interacting proteins in the range of the Förster radius (Förster, 1948). Additionally, the flexibility of the linker would allow the fluorophore to vary its orientation, which could lead to a FRET-optimized alignment of the two chromophores (Evers et al., 2006, Arai et al., 2001). A flexible linker can, however, cause new problems as well. When the time-resolved fluorescence anisotropy is measured, the orientation of a fluorophore is

determined by monitoring changes in its rotational freedom. If this fluorophore is rigidly attached to a protein of interest, anisotropy measurements of the fluorophore could indirectly provide information about the orientation of the protein of interest. If, however, a long and flexible linker is inserted between the protein of interest and the fluorophore, this would partially uncouple the fluorophore from the protein, and the measured anisotropy would then reflect the orientation of the free fluorophore, with hardly any constraints coming from the attached protein (Vogel et al., 2009).

Importantly, the results obtained from measuring the efficiencies of different linkers, are always dependent on the environment they are measured in. Therefore it is important to note, that all information described above is based on *in vitro* analysis, and that no comparable measurements have been done in living plant cells. Accordingly, at the current state, the effect that different linkers may have on the properties of fluorescent protein tags in plant cells are completely unknown.

To analyze these effects, multi-parameter fluorescence imaging spectroscopy measurements of the well-studied FRET-pair GFP / mCherry separated by different linkers were performed in living intact plant cells.

Here, the fluorescence lifetime τ is the common readout parameter for Förster resonance energy transfer (FRET), since it is strongly depending on the fluorophores distance in the nanometer range. Technically, the fluorescence lifetime is obtained using a model which assumes two populations of donor molecules. One donor population undergoes FRET and shows a reduced lifetime. But additionally a donor-only population, which doesn't show FRET, has to be taken into account, because it is known that mCherry is never 100% functional (Baird et al., 2000, Terskikh et al., 2000). Therefore, the resulting fluorescence lifetime is always an average lifetime over interacting and non-interacting molecules and is not a readout for the actual energy transfer taking place. To overcome this limitation a fit model containing the fraction of non-interacting donor-only molecules and the energy transfer rate of the interacting molecules, $k_{FRET,}$ were used as basic parameters.

2. Results:

2.1 The Different Linker Constructs used in this Study:

Three different linkers based on previously published work were designed. The shortest was a 5 amino acid linker described by Steven S. Vogel to be an effective fluorophore linker. The amino acid sequence is SGLRS and the linker will be referred to as Linker 1 (L1) (Vogel et al., 2009).

The second Linker is a supposedly flexible 10 amino acid linker consisting of glycine / serine repeats which have been reported to improve the efficiency of linkers. The amino acid sequence is GGGGSGGGGS and the linker will be referred to as Linker 2 (L2) (Alfthan et al., 1995).

The longest Linker consists of 26 aa and is mostly composed of glycine / serine repeats. This is based on the assumption that the flexible linker behaves as a Gaussian chain. In this case, the linker would always form a loose random coil with every possible conformation having the same probability. In this case, the end-to-end distance of the linker can be calculated and theoretically 26 aa would be required to make a significant difference. Furthermore, a flexible linker of 23 – 29 amino acids was shown to have the highest FRET-efficiency in a previous *in vitro* analysis. The amino acid sequence is GEGGGSGGGGSSGLRSIEGGGSGGGS and the linker will be referred to as Linker 3 (L3) (Evers et al., 2006).

The following constructs were used:

G	GFP	Free GFP. The donor-only control.
L0	GFP-mCherry	GFP and mCherry fused directly together.
L1	GFP-5aa-mCherry	GFP and mCherry separated by the 5 aa Linker 1.
L2	GFP-10aa-mCherry	GFP and mCherry separated by the 10 aa Linker 2.
L3	GFP-26aa-mCherry	GFP and mCherry separated by the 26 aa Linker 3.

To compare the effects of the different linkers GFP lifetimes (Tau), the actual FRET-rates (kFRET) and the percentages of GFP proteins in donor-only state (DO) were measured. The lifetime serves as readout for FRET taking place between the two proteins, while the actual FRET-rate can provide additional information on the distance between the proteins and the orientation of their dipoles toward each other. A high FRET-rate would indicate a short distance between them and a FRET-supporting orientation of their dipoles. The percentage of GFP proteins in donor-only state can give an indication on the folding and maturation of the

proteins connected via the different linkers. If one linker offers an improvement in protein folding and maturation, this would be reflected in a reduction of GFP proteins in donor-only state due to more mCherry proteins being matured and functional. Less GFP in donor-only state should also be corresponding with a shorter average lifetime, as donor-only GFPs increase the average lifetime.

In a second step the same parameters were determined for the different constructs (GFP, L0, L1, L2, L3) fused to three different plant proteins that localize to different cellular compartments. Doing this, provides information about influence that the intracellular environment has on the FRET-properties of the GFP-Linker-mCherry constructs. The first protein chosen for this experiment was the transmembrane receptor-like kinase CLAVATA 1 (CLV1) which would move the GFP-Linker-mCherry construct to the plasmamembrane (Clark et al., 1997). Furthermore, The homeodomain transcription factor WUSCHEL (WUS) localizes the GFP-Linker-mCherry construct to the nucleus and the ARF-GEF protein GNOM localizes to the cytoplasm, just as the free constructs do (Laux et al., 1996, Steinmann et al., 1999). So in this last case, any change would likely be due to the attached protein, not a change in environment. The following constructs were used:

C-G	CLV1-GFP	GFP fused to CLV1. The donor-only control.
C-L0	CLV1-GFP-mCherry	GFP / mCherry fused directly together fused to CLV1.
C-L1	CLV1-GFP-5aa-mCherry	GFP / mCherry separated by Linker 1 fused to CLV1.
C-L2	CLV1-GFP-10aa-mCherry	GFP / mCherry separated by Linker 2 fused to CLV1.
C-L3	CLV1-GFP-26aa-mCherry	GFP / mCherry separated by Linker 3 fused to CLV1.
W-G	WUS-GFP	GFP fused to WUS. The donor-only control.
W-L0	WUS-GFP-mCherry	GFP / mCherry fused directly together fused to WUS.
W-L1	WUS-GFP-5aa-mCherry	GFP / mCherry separated by Linker 1 fused to WUS.
W-L2	WUS-GFP-10aa-mCherry	GFP / mCherry separated by Linker 2 fused to WUS.
W-L3	WUS-GFP-26aa-mCherry	GFP / mCherry separated by Linker 3 fused to WUS.
GN-G	GNOM-GFP	GFP fused to GNOM. The donor-only control.
GN-L0	GNOM-GFP-mCherry	GFP / mCherry fused directly together fused to GNOM.
GN-L1	GNOM-GFP-5aa-mCherry	GFP / mCherry separated by Linker 1 fused to GNOM.
GN-L2	GNOM-GFP-10aa-mCherry	GFP / mCherry separated by Linker 2 fused to GNOM.
GN-L3	GNOM-GFP-26aa-mCherry	GFP / mCherry separated by Linker 3 fused to GNOM.

Note that the proteins fused to the GFP-Linker-mCherry construct are always separated from the GFP by 15 amino acids (Sequence: YPAFLYKVVDHSLIE), owed to the Gateway-Vector backbone.

In this study the different linkers were used to directly fuse two fluorophores together to determine how the linkers affect the fluorescent properties of the proteins. In a next step it will be interesting to determine the best linker to fuse a fluorophore to a protein of interest to use in FRET-interaction studies. Some preliminary measurements in that direction have already been performed. Two constructs were designed, one in which the fluorophore can be attached to the protein of interest via a 15 aa linker (Sequence: YPAFLYKVVDHSLIE), and one with a 44 aa linker that in part consistis of potentially flexible glycine / serine repeats (Sequence: YPAFLYKVVDHSLIEGEGGGSGGGGSSGLRSIEGGGSGGGSLIE). FRET was then measured between the fluorophores. As proteins of interest the transmembrane receptor-like proteins CLAVATA 2 (CLV2) and CORYNE (CRN) were used, which have been shown to interact in a strong, stable and direct fashion (Bleckmann et al., 2010).

The following constructs were used:

DO15	CRN-15aa-GFP	The donor-only control 1.
F15	CRN-15aa-GFP / CLV2-15aa-mCherry	FRET-pair 1.
DO44	CRN-44aa-GFP	The donor-only control 2.
F44	CRN-44aa-GFP / CLV2-44aa-mCherry	FRET-pair 2.

2.2 The Effects of Different Linkers separating GFP and mCherry

When comparing the average GFP lifetimes of the different constructs as a readout for FRET taking place between the GFP and mCherry, the directly fused GFP-mCherry construct exhibits the smallest shift in lifetime with only 160 ps from an average 2.58 ns for free GFP to 2.42 ns for the GFP-mCherry construct (Fig. 1). The variants, in which the GFP and mCherry are connected via the different linkers, show stronger shifts ranging from 220 ps for the construct with the 26 amino acid linker (τ = 2.36 ns), and 230 ps for the construct with the 10 amino acid linker (τ = 2.35 ns), to 270 ps for the 5 amino acid linker variant (τ = 2.31 ns) (Fig. 1).

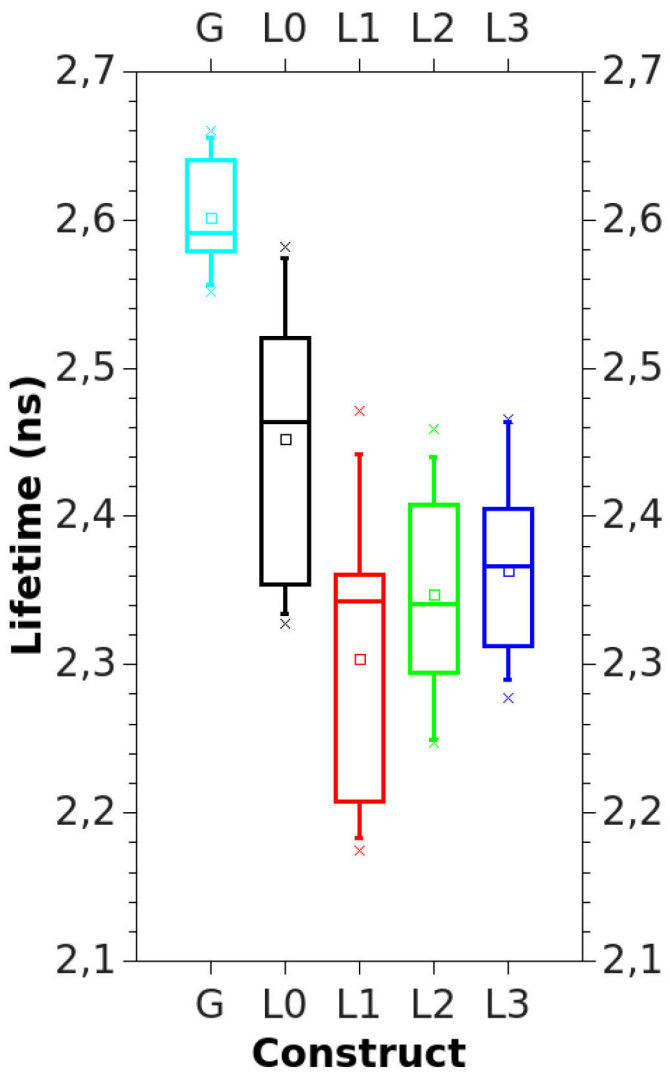

Fig. 1: GFP lifetimes of the free Constructs
Constructs are G: Free GFP (Turquoise), L0: GFP-mCherry (Black), L1: GFP-5aa-mCherry (Red), L2: GFP-10aa-mCherry (Green), L3: GFP-26aa-mCherry (Blue).

From this analysys it appears that the strongest FRET between GFP and mCherry can be measured when the two fluorophores are linked with five amino acids. This, however, does not hold true when the actual FRET-rate (kFRET) is calculated for the different constructs. In the kFRET analyses, the L0 construct exhibits the strongest FRET with a kFRET of 0.26. The different linker constructs yield rates of 0.18 (L1), 0.15 (L2) and 0.14 (L3) respectively (Fig. 2). This discrepancy between the actual FRET-rate and the lifetime readout can be explained, when the percentages of GFPs in donor-only or FRET state are calculated. For the L0 construct, 70 % of available GFP molecules are in a donor-only state, indicating a non-functional mCherry protein, possibly not folded correctly or fully matured. Because of this high amount of donor-only GFPs with a long lifetime, the average lifetime is longer, compared to the different linker constructs, even though the actual FRET-rate is higher. The situation is comparable for the L3 variant, with 68 % of GFP molecules in donor-only state. Accordingly, the L3 construct is also the variant with the second weakest drop in lifetime. For the L1 and L2 variants, the donor-only percentages are 56 and 59 % respectively, which explains why these show the strongest lifetime drops on average, even though the FRET-rate is lower than it is for the no-linker variant (Fig. 3).

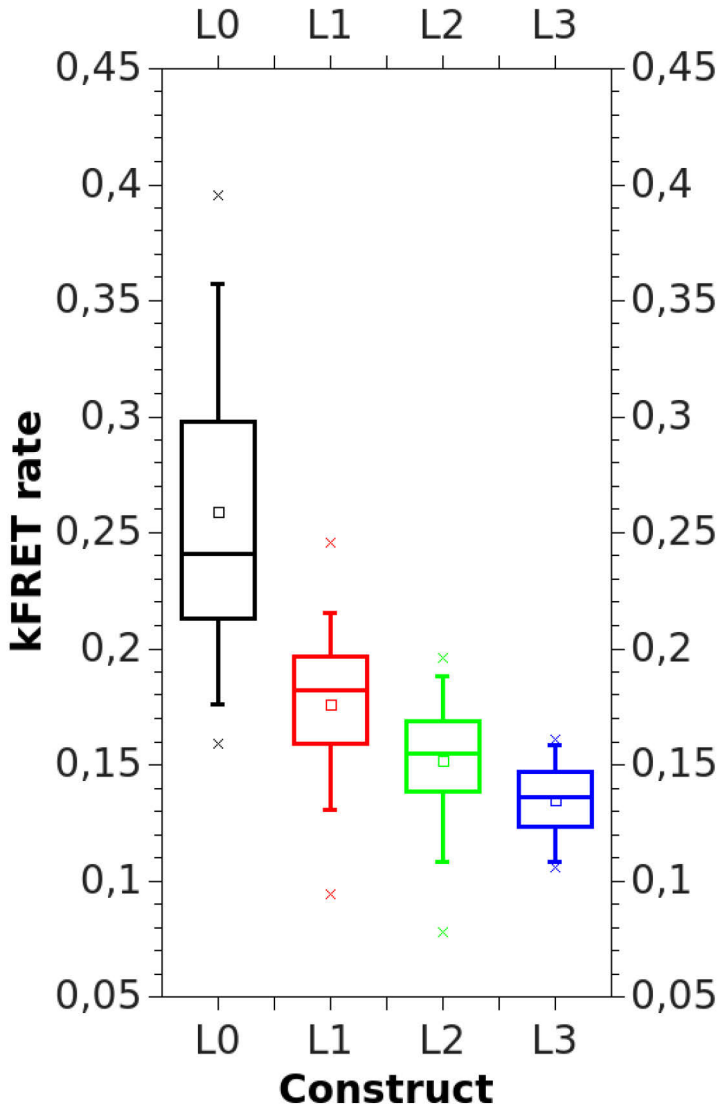

Fig. 2: kFRET rates of the free Constructs

Constructs are L0: GFP-mCherry (Black), L1: GFP-5aa-mCherry (Red), L2: GFP-10aa-mCherry (Green), L3: GFP-26aa-mCherry (Blue).

When the different constructs are fused to either CLV1, WUS or GNOM, the situation is different than it is for the free constructs.

In the case of the CLV1-GFP-Linker-mCherry constructs, the lifetime shift is comparable for all four constructs (L0 = 338 ps, L1 = 326 ps, L2 = 348 ps, L3 = 290 ps) (Fig. 4). This is in accordance with the donor-only fractions, which are comparable for all four constructs as well (L0 = 57 %, L1 = 55 %, L2 = 47 %, L3 = 58 %) (Fig. 6). For the actual FRET-rates, the directly fused GFP-mCherry pair again scores the highest rate at 0.24, while the three linker variants give comparable results (L1 = 0.2, L2 = 0.18, L3 = 0.19) (Fig. 5).

When the constructs are fused to the nuclear localized WUS, the donor-only fraction generally appeared to be very high, somewhere in the regions between 60 – 75 % (L0 = 73 %, L1 = 63 %, L2 = 66 %, L3 = 61 %) (Fig. 6). This led to the lifetime drops being relatively low (L0 = 195 ps, L1 = 239 ps, L2 = 208 ps, L3 = 262 ps) (Fig. 4). The highest donor-only fraction was again measured for the directly fused proteins, which is in accordance with the measurements of the free constructs, where it seemed that the folding / maturation was the worst without linker. The actual FRET-rate was also comparable to the rates for the free constructs (L0 = 0.26, L1 = 0.14, L2 = 0.13, L3 = 0.13) (Fig. 5). In this case, the high donor-only fractions measured are most likely due to the slow mCherry maturation. In this study, an inducible system was used for the measurements to avoid overexpression artifacts. The

measurements are normally done as soon as the proteins reach their detection limit. For bigger proteins, such as the fluorophore-tagged CLV1 and GNOM, this translates into roughly 12 hours post induction. This time frame provides the fluorophores with sufficient time to mature. For WUS, the situation is slightly different. WUS is expressed, matured and transported to the nucleus much faster. Because of this, measuring was started three to four hours post induction. This leaves enough time for GFP molecules to reach maturation, but only a few mCherry proteins are probably already fully functional at this time, resulting in a high amount of donor-only GFP molecules (Macdonald et al., 2012).

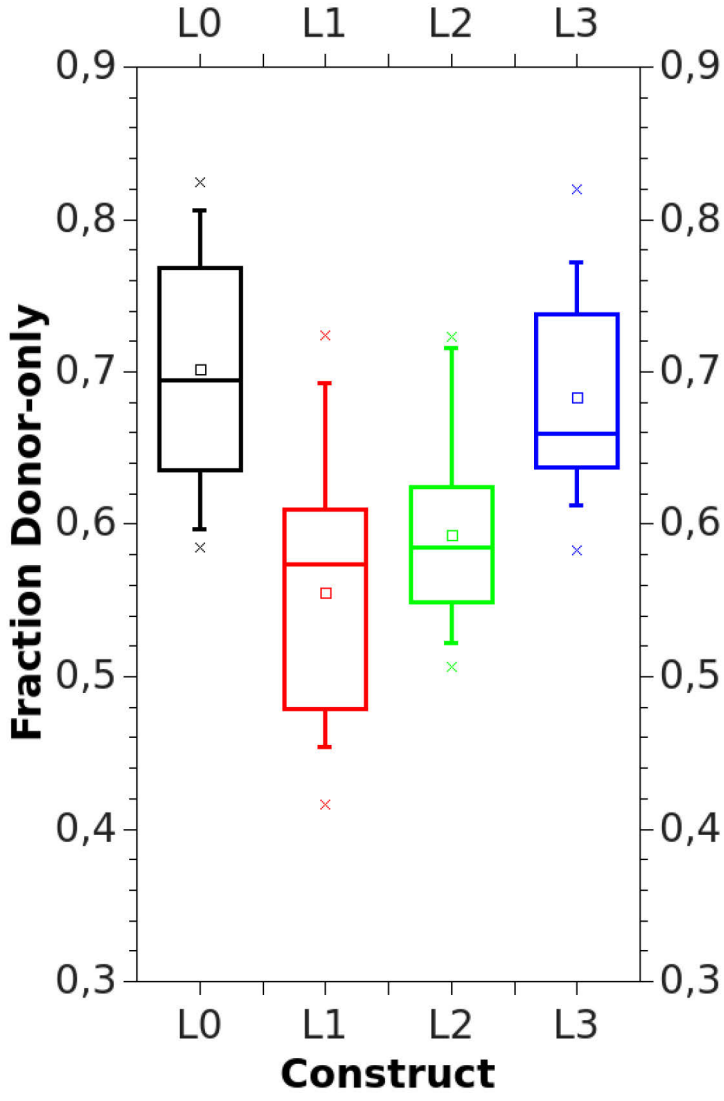

Fig. 3: Donor-only fractions for the free Constructs
Constructs are L0: GFP-mCherry (Black), L1: GFP-5aa-mCherry (Red), L2: GFP-10aa-mCherry (Green), L3: GFP-26aa-mCherry (Blue).

Finally, when the constructs where fused to GNOM, and hence localize to the cytoplasm, as they do for the free constructs, the measured values diverge the strongest from all other measurements. The highest donor-only fraction is recorded for the variants with no linker or the 10 aa linker. Interestingly, the long 26 aa linker has a low donor-only value, comparable to the short 5 aa linker (L0 = 58 %, L1 = 52 %, L2 = 58 %, L3 = 53 %) (Fig. 6). Accordingly, the lifetime shifts are biggest for the 5 aa and 26 aa linkers (L0 = 345 ps, L1 = 361 ps, L2 = 304 ps, L3 = 395 ps) (Fig. 4). The 10 aa linker exhibits the weakest lifetime drop which is due to the high donor-only fraction and, in contrast to the no-linker variant, also a very low FRET-rate (L0 = 0.22, L1 = 0.17, L2 = 0.16, L3 = 0.19) (Fig. 5). In general the FRET-rates of the three linker-variants are again comparable, even though this is

the only construct where the long linker scores the highest rate among the linker-variants (Fig. 5).

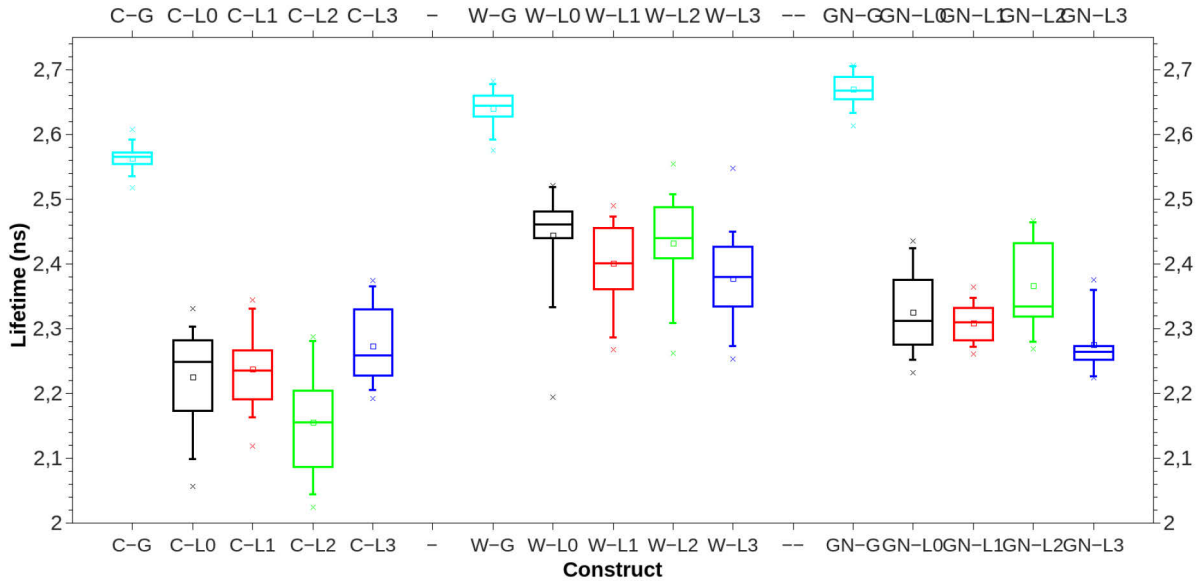

Fig. 4: GFP lifetimes of the Constructs fused to CLV1, WUS or GNOM

Constructs are C-G: CLV1-15aa-GFP (Turquoise), C-L0: CLV1-15aa-GFP-mCherry (Black), C-L1: CLV1-15aa-GFP-5aa-mCherry (Red), C-L2: CLV1-15aa-GFP-10aa-mCherry (Green), C-L3: CLV1-15aa-GFP-26aa-mCherry (Blue). W-G: CLV1-15aa-GFP (Turquoise), W-L0: WUS-15aa-GFP-mCherry (Black), W-L1: WUS-15aa-GFP-5aa-mCherry (Red), W-L2: WUS-15aa-GFP-10aa-mCherry (Green), W-L3: WUS-15aa-GFP-26aa-mCherry (Blue). GN-G: GNOM-15aa-GFP (Turquoise), GN-L0: GNOM-15aa-GFP-mCherry (Black), GN-L1: GNOM-15aa-GFP-5aa-mCherry (Red), GN-L2: GNOM-15aa-GFP-10aa-mCherry (Green), GN-L3: GNOM-15aa-GFP-26aa-mCherry (Blue).

2.3 The Effects of Different Linkers separating a Fluorophore and a Protein of Interest

To test the effects of linkers on connecting a protein of interest to a fluorophore, a CRN-Linker-GFP was co-expressed with a CLV2-Linker-mCherry fusion protein. CRN and CLV2 were shown to interact strongly and accordingly FRET can be measured between the fused fluorophores GFP and mCherry (Bleckmann et al., 2010). The different linkers could aid to align the two fluorophores optimally for FRET, or allow better fluorophore ripening. The former is specifically important in this case compared to the GFP-Linker-mCherry constructs used in the previous paragraphs, because the two fluorophores are not directly connected, but fused to different proteins this time. Accordingly, spatial freedom, provided by a linker, could help to get these proteins into close proximity.

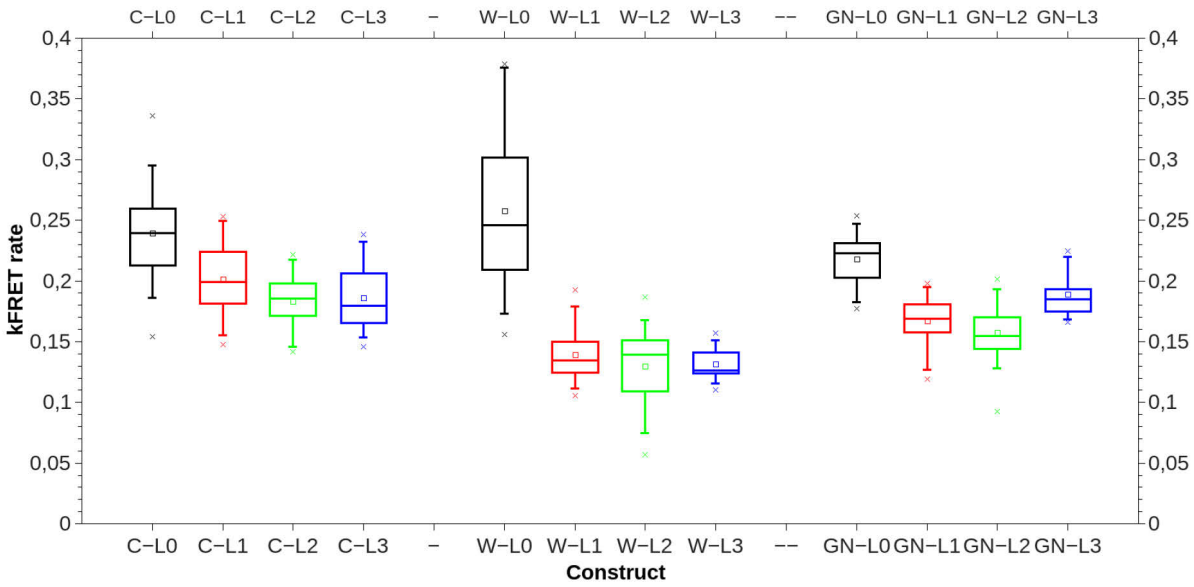

Fig. 5: kFRET rates of the Constructs fused to CLV1, WUS or GNOM

Constructs are C-L0: CLV1-15aa-GFP-mCherry (Black), C-L1: CLV1-15aa-GFP-5aa-mCherry (Red), C-L2: CLV1-15aa-GFP-10aa-mCherry (Green), C-L3: CLV1-15aa-GFP-26aa-mCherry (Blue). W-L0: WUS-15aa-GFP-mCherry (Black), W-L1: WUS-15aa-GFP-5aa-mCherry (Red), W-L2: WUS-15aa-GFP-10aa-mCherry (Green), W-L3: WUS-15aa-GFP-26aa-mCherry (Blue). GN-L0: GNOM-15aa-GFP-mCherry (Black), GN-L1: GNOM-15aa-GFP-5aa-mCherry (Red), GN-L2: GNOM-15aa-GFP-10aa-mCherry (Green), GN-L3: GNOM-15aa-GFP-26aa-mCherry (Blue).

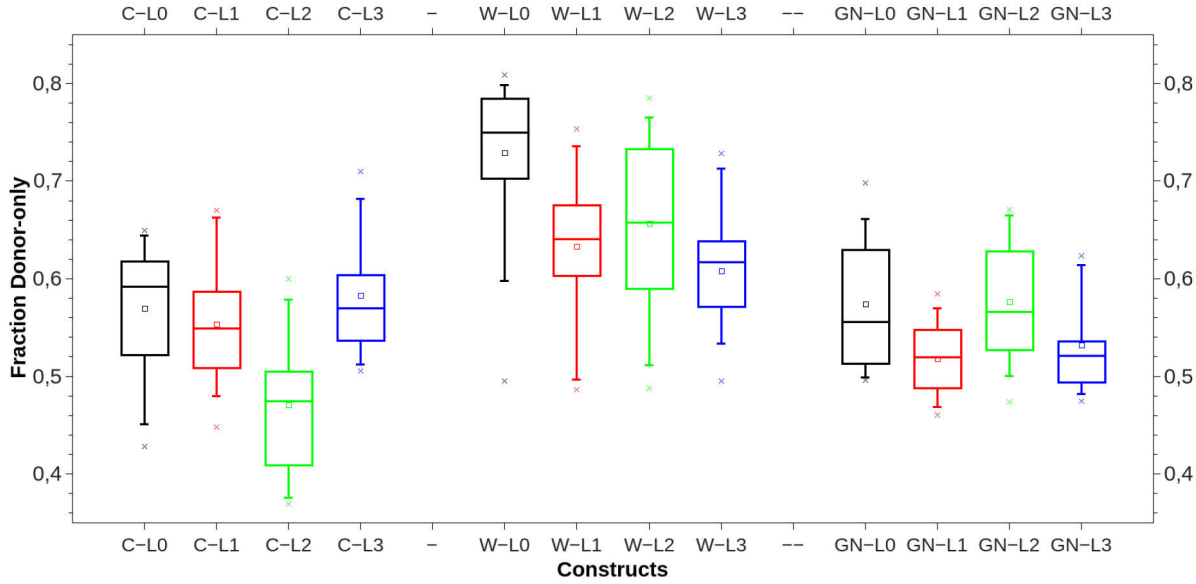

Fig. 6: Donor-only fractions for the Constructs fused to CLV1, WUS or GNOM

Constructs are C-L0: CLV1-15aa-GFP-mCherry (Black), C-L1: CLV1-15aa-GFP-5aa-mCherry (Red), C-L2: CLV1-15aa-GFP-10aa-mCherry (Green), C-L3: CLV1-15aa-GFP-26aa-mCherry (Blue). W-L0: WUS-15aa-GFP-mCherry (Black), W-L1: WUS-15aa-GFP-5aa-mCherry (Red), W-L2: WUS-15aa-GFP-10aa-mCherry (Green), W-L3: WUS-15aa-GFP-26aa-mCherry (Blue). GN-L0: GNOM-15aa-GFP-mCherry (Black), GN-L1: GNOM-15aa-GFP-5aa-mCherry (Red), GN-L2: GNOM-15aa-GFP-10aa-mCherry (Green), GN-L3: GNOM-15aa-GFP-26aa-mCherry (Blue).

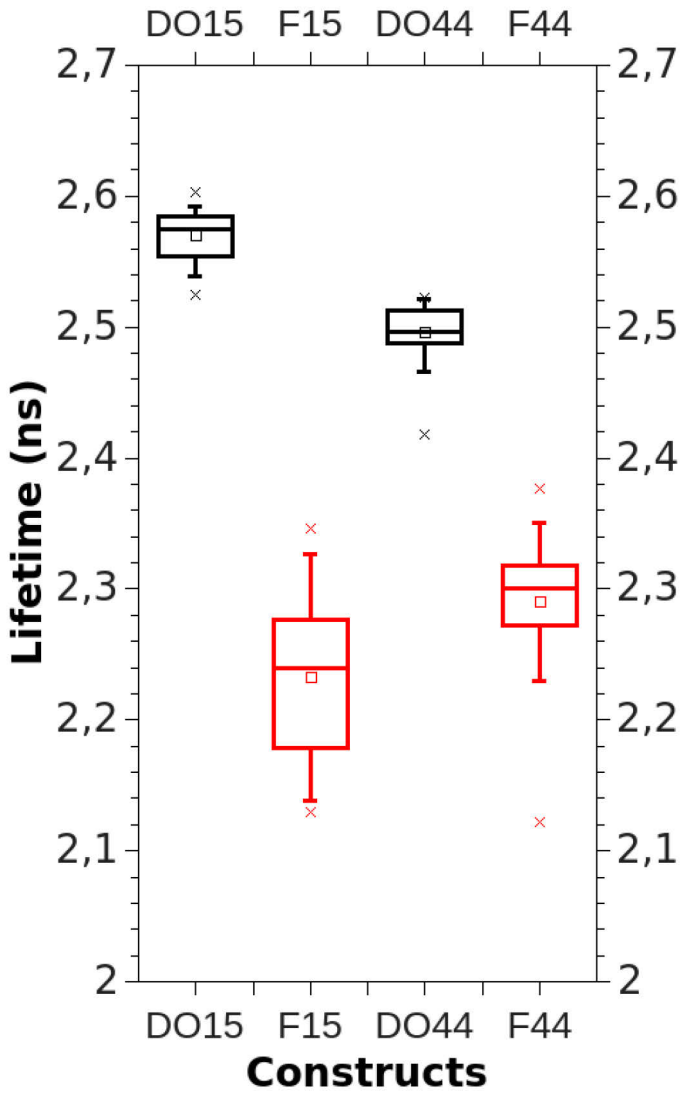

Fig. 7: CRN-GFP lifetimes with a 15 or 44 aa linker

Constructs are DO15: CRN-15aa-GFP (Black), F15: CRN-15aa-GFP / CLV2-15aa-mCherry (Red), DO44: CRN-44aa-GFP (Black), F44: CRN-44aa-GFP / CLV2-44aa-mCherry (Red)

The first readout used to determine FRET between the two fluorophores was again the average GFP lifetime. The first observation here was that the GFP connected to the CRN protein via the 44 aa linker already had a shorter lifetime in the absence of a FRET partner, compared to the CRN-15aa-GFP construct. The average lifetime of CRN-15aa-GFP was 2.57 ns, while the lifetime for the CRN-44aa-GFP variant was 2.5 ns.

When looking at the FRET samples, the CRN-44aa-GFP / CLV2-44aa-mCherry (F44) version showed a lifetime shift of 210 ps, while the CRN-15aa-GFP / CLV2-15aa-mCherry (F15) version exhibited a 340 ps drop from 2.57 to 2.23 ns (Fig. 7). This weaker FRET was also observed in the actual FRET-rate (kFRET). While the F15 FRET-pair had a FRET-rate of 0.2, the F44 variant only exhibited a rate of 0.13 (Fig. 8).

One potential advantage of a long linker is the increased spatial freedom of the proteins that could allow for improved protein folding and maturation. This improvement would be reflected in a reduced amount of non-fluorescent mCherry proteins and, accordingly, less GFP molecules in donor-only state. However, the opposite could be observed in these measurements. The donor-only percentage of GFPs in the F15 sample was 0.56, while it was 0.65 for the F44 sample (Fig. 9). This either indicates that mCherry maturation is not improved by the longer linker, or that the improved maturation cannot compensate for the increased distance between the fluorophores due to the long linker, that

would partially or temporarily move the mCherry out of the estimated maximal FRET distance of 10 nm.

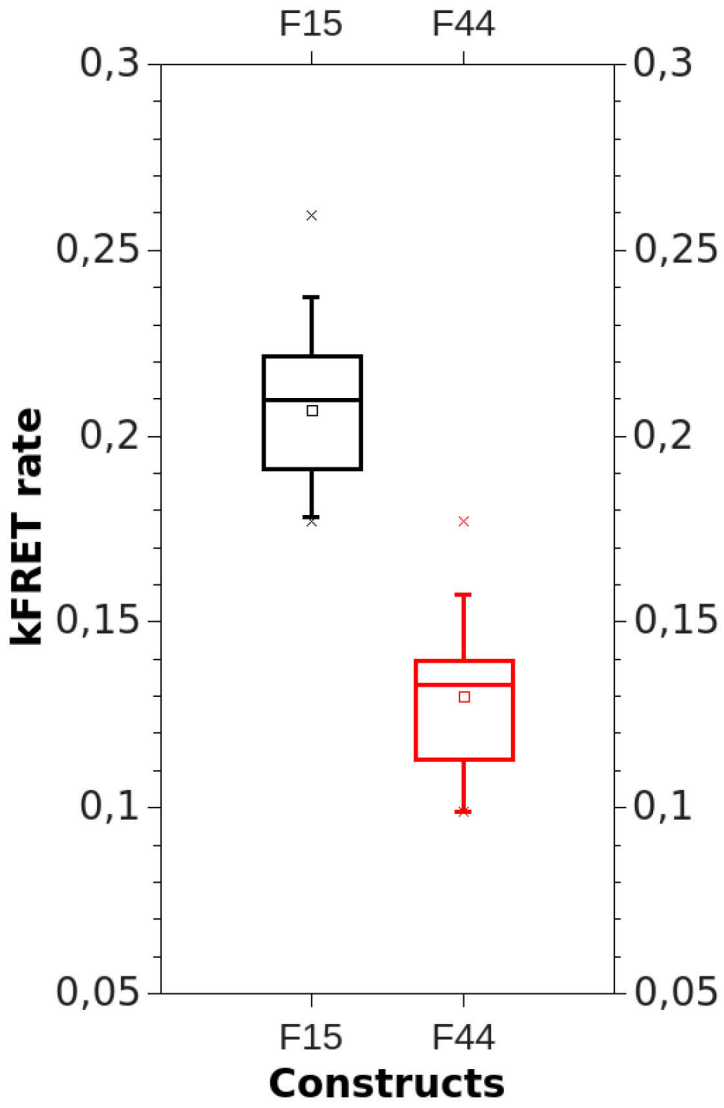

Fig. 8: kFRET rates between CRN-GFP and CLV2-mCherry
Constructs are F15: CRN-15aa-GFP / CLV2-15aa-mCherry (Black), DO44, F44: CRN-44aa-GFP / CLV2-44aa-mCherry (Red)

3. Discussion:

The aim of this study was to test different linkers for fluorescent proteins in plant cells. To design an optimal linker, there are some important points to consider: A linker has to be long enough to separate the two proteins sufficiently to allow for correct protein folding and maturation, protein interactions and not interfere with the proteins functions. On the other hand, the linker must not be so long that the fluorophore is moved beyond the maximal FRET distance of a potential FRET-partner. Also, the designed recombinant chimeric proteins behave differently in different environments. Accordingly, a study on the effects of linkers should be done in the type of cells where they are supposed to be used eventually. In this case, these are living plant cells.

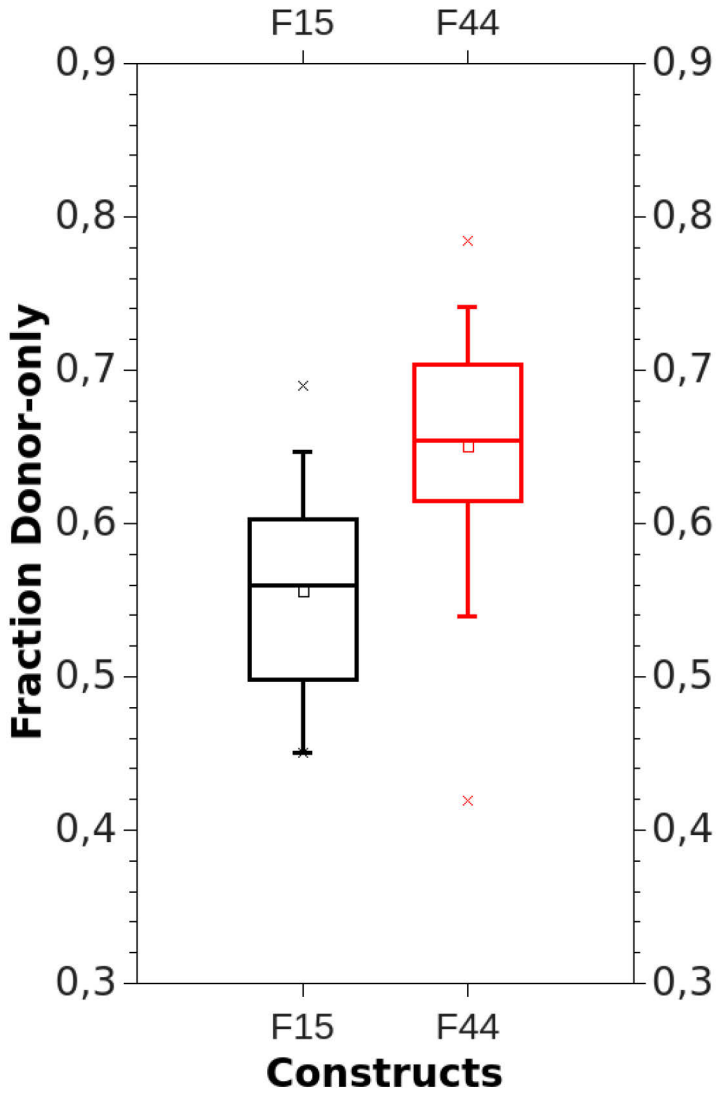

Fig. 9: Donor-only fractions for CRN-GFP with a 15 or 44 aa linker
Constructs are F15: CRN-15aa-GFP / CLV2-15aa-mCherry (Black), DO44, F44: CRN-44aa-GFP / CLV2-44aa-mCherry (Red)

Over the years, several different kinds of linkers have been designed and tested, mostly in *in vitro* studies. All of these linkers have their advantages and their disadvantages. In this study, different linkers were tested for their ability to function as an effective linker for fluorophores to use in FRET-interaction studies in living plant cells. The aim was to find a linker that allows for both, protein maturation and FRET at a high rate, in the environment of a living plant cell.

FRET is primarily a measure of distance between the donor (in this case GFP) and the acceptor (in this case mCherry) fluorophore. This is represented in the results of the kFRET

analysis. The kFRET value represents the actual rate of energy transfer between two fluorophores. In this analysis, the highest transfer rate (0.26) was obtained when the two fluorophores were fused directly together (L0 sample). With increasing linker length, the proteins get separated further and the energy transfer rates decrease (0.18 in sample L1, 0.15 in sample L2, 0.14 in sample L3) (Fig. 2).

Interestingly though, despite these measured FRET-rates, all three linker constructs tested yielded a stronger drop in the average GFP lifetime than the directly fused GFP-mCherry construct (Fig. 1). Since the average GFP lifetime is the most commonly used readout for FRET, this is a very important observation. Knowing, that the direct fusion of GFP and mCherry facilitates the strongest energy transfer rate, it appears to be counterintuitive that it yields the weakest drop in GFP lifetime and hence, seemingly the weakest FRET. This, however, is the result of the calculated lifetime being an average of all GFP lifetimes in the sample. The overall sample is a mixture of at least two populations of GFP lifetimes. One, in which the fused mCherry is a fully functional FRET-acceptor resulting in a short lifetime due to FRET, and a second one in which the fused mCherry is a non-functional FRET-acceptor and the GFP lifetime is long. When determining the percentage of GFP molecules in donor-only state, 70 % of the GFPs in the L0 sample did not have a functional FRET-acceptor, compared to only 56 or 59 % in the L1 (5 aa linker) and L2 (10 aa linker) linker samples (Fig. 3). This explains why the L0 sample, despite having the highest FRET-rate, only shows a weak drop in average lifetime.

The observation that 70 % of GFPs in the L0 sample are in donor-only state is an indication that protein folding and maturation are strongly impaired in this sample. It can be assumed, that the direct fusion of two proteins together impairs the ripening of the proteins, since the proteins have to be folded individually from one long polypeptide chain. Also, depending on their conformation, the direct fusion could result in mechanistic tension between the proteins. A linker between them would relieve this tension and could provide extra space for protein folding and maturation. This can be seen in the significantly reduced amount of GFP proteins in donor-only state in the linker samples.

The L3 linker sample probably represents a different case. Here, the FRET-rate is the weakest of all (0.14 compared to 0.26 in the L0 sample), while the average lifetime is the longest of the L1 – L3 linker samples and the percentage of donor-only is almost as high as it is in the L0 sample (68 % compared to 70 %). Theoretically, this flexible 26 aa linker is supposed to behave as a Gaussian chain, forming a loose random coil (Evers et al., 2006). Through this, the two proteins should be kept in close proximity, despite the length of the

linker. However, it is not predictable which conformation it will eventually have (in the Gaussian model, all conformations share an equal probability). In this case, it appears that the preferred conformations separate the two fluorophores at least partially beyond the maximal FRET distance. This results in a low FRET-rate (0.14) and a large amount of GFPs in an apparent donor-only state (68 %).

Partially different results were obtained, when the different constructs L0 – L3 were fused to different proteins in different cellular compartments. The actual FRET-rate was always the strongest for the L0 construct in this case as well, no matter the GFP was fused to the plasmamembrane localized CLV1, the nuclear localized WUS or the cytoplasmic GNOM (Fig. 5). The short 5 aa linker always scored very well too, normally being the second best choice, even though the 26 aa linker was as good when fused to GNOM.

There was a big difference in the percentage of GFPs in donor-only state though. In all three cases, the DO values were comparable for the non-linker L0 and the three linker constructs L1 – L3. The best results were either obtained for the 5aa and 26 aa linker (WUS and GNOM) or the 10 aa linker (CLV1), with the 5 aaa linker being the second best (Fig. 6). These results make it hard to predict the one perfect linker for all proteins and compartments. It appears that the proteins and their intracellular environments affect the fluorophores in specific ways that cannot be predicted precisely. It is to note however, that the tendency was always comparable and the linker constructs always had slightly better values than the non-linker variant. The short five amino acid linker (L1) was the best linker to directly connect the two fluorophores for the free constructs, and when tagged to the three proteins CLV1, WUS and GNOM always yielded either the best, or at least the second best results, compared to the other linkers.

The focus of this study was on linkers between two fluorophores. The next important step will be to determine the most efficient linker between a protein of interest and a fluorophore. In this case, the FRET-donor (in this case GFP) would be fused to one protein, while the FRET-acceptor (in this case mCherry) would be fused to a second protein, a potential interactor of the first protein. If the two proteins interacted, this should bring the two fluorophores into close proximity, resulting in FRET between them. It is conceivable, that a linker would be of even greater importance in this case, as the two fluorophores are fused to different proteins and it is not predictable if they would come into close proximity just by chance. Depending on how they stick out from their protein, they could stand out into

completely different directions, which would not result in FRET, even if the proteins interacted. In this case, a linker could improve the range that the fluorophores could explore in space and increase the chance of them meeting.

Some preliminary results are included here, in which the effects of two protein-to-fluorophore linkers were determined. These linkers were either 15 or 44 amino acids long, with the 44 amino acid linker additionally including flexible glycine / serine repeats. As could be expected from the previous results described here, the shorter linker gave significantly better results in all aspects (GFP lifetime, donor-only fraction, kFRET) (Fig. 7 - 9). The values for the long 44 amino acid linker were comparable to the values that were measured for the 26 amino acid L3 linker, making it likely that the linker is too long and separates the two fluorophores too far. The values of the 15 amino acid linker were comparable to the short L1 and L2 linkers.

Based on these preliminary results, it would be of great interest to determine the efficiencies of fusing the fluorophores directly to the proteins of interest and with linkers shorter than 15 amino acids. Fusing the fluorophores directly to the protein of interest would most likely interfere with the maturation of the fluorophores and decrease the chance of them getting in close proximity. Both would result in greatly decreased FRET-efficiencies. Based on the results for the free linker constructs, a five amino acid linker could give the best result. Since the fluorophores are fused to different proteins in this case, it would also be plausible if a slightly longer linker would be necessary to bring the proteins into close proximity. This needs to be determined in follow-up experiments.

4. Conclusions:

This study on the effects of different linkers for fluorophores provides several conclusions. First, the results show that the introduction of a linker between two proteins significantly improves fluorophore ripening. The constructs in which GFP and mCherry were fused directly together always exhibited the highest amount of GFP molecules in donor-only state. Furthermore, it appears that as few as five amino acids are sufficient to improve protein maturation, possibly by providing extra space for folding or relieving tension between the two proteins. The construction of longer linkers does not improve protein maturation but decreases the FRET-efficiency by increasing the distance between the two fluorophores. Also, a linker does not have to be designed from potentially flexible glycine / serine repeats, as these linkers did not give better results and a too flexible linker might actually impair the

fluorophores efficiency in more advanced spectroscopic methods, such as protein orientation measurements via fluorescence anisotropy analysis (Vogel et al., 2009).

Further studies are needed to determine the optimal linker to connect a fluorophore to a protein of interest.

5. Methods:

Nicotiana benthamiana Plant Lines

Nicotiana benthamiana plants were grown in the greenhouse for four weeks prior to transient transformation. Transformation and expression were described before (Bleckmann et al., 2010).

Construction of Plasmids

All Vectors used are based on pMDC99 and pMDC7 as described previously (Curtis et al., 2003). The CLV1, CLV2 and CRN entry clones were described previously (Bleckmann et al., 2010). The GNOM and WUS entry clones were created from cDNA using the Gateway® BP Clonase® II Cloning Kit. The destination vectors necessary to create the GFP or GFP-mCherry fusions are pABindGFP and pABindFRET as described previously (Bleckmann et al., 2010). The destination vectors necessary to create GFP-L1-mCherry, GFP-L2-mCherry and GFP-L3-mCherry were created by subsequent restriction and ligation into pMDC99 and pMDC7. All expression vectors were created using the Gateway® LR Clonase® II Cloning Kit.

Microscopy

Measurements were performed using a multiparameter fluorescence detection setup as described previously (Weidtkamp-Peters et al., 2009, Kudryavtsev et al., 2007). Experiments were performed with a confocal laser scanning microscope (FV1000 Olympus, Hamburg, Germany) additionally equipped with a single photon counting device with picosecond time-resolution (Hydra Harp 400, PicoQuant, Berlin, Germany). GFP was excited at 485 nm with a linearly polarized, pulsed (32 MHz) diode laser (LDH-D-C-485, Pico-Quant, Berlin, Germany) at 0.8 µW at the objective (60x water immersion, Olympus UPlanSApo NA 1.2, diffraction limited focus). mCherry was excited at 559 nm with a continuous-wave laser (FV1000) at 5.6 µW at the objective. The emitted light was collected in the same objective and separated into its perpendicular and parallel polarization. GFP fluorescence was then detected by MPDs (PDM50-CTC, Micro Photon Devices, Bolzano, Italy) in a narrow range of its emission spectrum (bandpass filter: HC520/35, AHF, Tübingen, Germany). mCherry fluorescence was detected by HPDs(HPMC-100-40, Becker&Hickl, Berlin, Germany), of which the detection wavelength range was set by the bandpass filters (HC 607/70, AHF). Images were taken with 20 µs pixel dwell time and a resolution of 103 nm/pixel. Series of 40

frames were merged to one image and further analyzed using custom-designed software (LabView).

Pixel-wise fluorescence-weighted lifetime analysis

The histograms presenting the decay of fluorescence intensity after the excitation pulse were built for each pixel with 128ps per bin. The fluorescence-weighted lifetime of donor molecule ($<\tau_D>_f$) in single pixel was determined using a model function containing only two variables ($<\tau_D>_f$) and scatter contribution (for details see (Stahl et al., 2013)), with maximum likelihood estimator (MLE). The instrument response function was measured with the back-reflection of the laser beam and used for iterative reconvolution in the fitting process.

Pixel-wise anisotropy analysis

The steady-state anisotropy is given by $r_G = \frac{F_{\parallel} - G \cdot F_{\perp}}{F_{\parallel} + 2 \cdot G \cdot F_{\perp}}$, where $F_{\parallel}$ and $F_{\perp}$ are the average fluorescence count rates within a pixel, with a polarization parallel and perpendicular to that of the excitation light, respectively. Both were corrected for dead time of the detection electronics (Becker, 2005) and mixing of polarization in the high numerical aperture objective (Schaffer et al., 1999) $F = F_{\parallel} + 2GF_{\perp}$ is the total fluorescence intensity. Calibration measurements with Rhodamine 110 delivered the G-factor to correct the signal for orientational sensitivity differences of the detection system.

Ensemble FRET analysis:

For each image, only the pixels with recorded fluorescence were selected. The pixels containing mainly auto-fluorescence (e.g. coming from chloroplasts) were excluded. One fluorescence lifetime decay histogram was constructed from the selected pixels for further ensemble analysis.

Fluorescent proteins in live cell usually show the bi-exponential decay feature (Suhling et al., 2002), therefore, decay histograms of donor-only samples are fitted by a bi-exponential model:

$$F_{(D,0)}(t) = \sum_m x_D^{(m)} \cdot \exp(-t \cdot k_{D0}^{(m)}) \qquad \text{Eq. 1}$$

in which m = 2. Four fit parameters were determined: two pre-exponential factors $x_D^{(m)}$, and two decay rates $k_{D0}^{(m)}$ which are the reciprocals of fluorescence lifetimes $\tau_{D0}^{(m)}$. The same procedure was repeated on every measured donor-only sample, and then the mean values of

each fit parameter were used in the following ensemble analysis of FRET samples labeled with both donor and acceptor.

The quenched donor fluorescence decay in the presence of acceptor is given by:

$$F_{(D,A)}(t) = \sum_{l} x_{FRET}^{(l)} \sum_{m} x_{D}^{(m)} \cdot \exp\left(-t \cdot \left(k_{D0}^{(m)} + k_{FRET}^{(l)}\right)\right) \qquad \text{Eq. 2}$$

where $l = 2$. Here $k_{FRET}^{(l)}$ are the FRET rates and $x_{FRET}^{(l)}$ the corresponding amplitudes.

The donor fluorescence decay recorded in FRET sample *F(t)*, is a mixture of unquenched donor-only decay (Eq. 1) weighted by its species fraction x_{Donly}, and quenched donor decay (Eq. 2) weighted by $(1- x_{Donly})$:

$$F(t) = x_{Donly} F_{(D,0)}(t) + \left(1 - x_{Donly}\right) F_{(D,A)}(t) \qquad \text{Eq. 3}$$

The decay histograms obtained from FRET samples were fitted to Eq. 3 with fixed $F_{(D,0)}(t)$ determined from donor-only samples. The fit parameters were two FRET rates with their amplitudes ($k_{FRET}^{(l)}$ and $x_{FRET}^{(l)}$) and species fraction (x_{Donly}).

This chapter is a manuscript in preparation for submission.

Authors:
Marc Somssich[1], Qijun Ma[3], Stefanie Weidtkamp-Peters[2], Claus A. M. Seidel[2, 3] and Rüdiger Simon[1, 2]

[1] Institute of Developmental Genetics
[2] Center for Advanced Imaging
[3] Institute for Molecular Physical Chemistry
Heinrich Heine University, 40225 Düsseldorf, Germany

The experiment was designed by Marc Somssich, Rüdiger Simon, Qijun Ma, Stefanie Weidtkamp-Peters and Claus Seidel. Molecular biology and plant work was done by Marc Somssich. Microscopy was done by Marc Somssich and Qijun Ma. Data analysis was done by Qijun Ma and Marc Somssich. The manuscript was written by Marc Somssich with help from Rüdiger Simon.

6. References:

ALFTHAN, K., TAKKINEN, K., SIZMANN, D., SODERLUND, H. & TERRI, T. T. 1995. Properties of a Single-Chain Antibody Containing Different Linker Peptides. *Protein Engineering,* 8**,** 725-731.

ARAI, R., UEDA, H., KITAYAMA, A., KAMIYA, N. & NAGAMUNE, T. 2001. Design of the linkers which effectively separate domains of a bifunctional fusion protein. *Protein Engineering,* 14**,** 529-532.

BAIRD, G. S., ZACHARIAS, D. A. & TSIEN, R. Y. 2000. Biochemistry, mutagenesis, and oligomerization of DsRed, a red fluorescent protein from coral. *PNAS,* 97**,** 11984-9.

BECKER, W. 2005. *Advanced time-correlated single photon counting techniques,* Berlin ; New York, Springer.

BLECKMANN, A., WEIDTKAMP-PETERS, S., SEIDEL, C. A. & SIMON, R. 2010. Stem cell signaling in Arabidopsis requires CRN to localize CLV2 to the plasma membrane. *Plant Physiol,* 152**,** 166-76.

CLARK, S. E., WILLIAMS, R. W. & MEYEROWITZ, E. M. 1997. The CLAVATA1 gene encodes a putative receptor kinase that controls shoot and floral meristem size in Arabidopsis. *Cell,* 89**,** 575-585.

CURTIS, M. D. & GROSSNIKLAUS, U. 2003. A gateway cloning vector set for high-throughput functional analysis of genes in planta. *Plant Physiology,* 133**,** 462-469.

EVERS, T. H., VAN DONGEN, E. M. W. M., FAESEN, A. C., MEIJER, E. W. & MERKX, M. 2006. Quantitative understanding of the energy transfer between fluorescent proteins connected via flexible peptide linkers. *Biochemistry,* 45**,** 13183-13192.

FÖRSTER, T. 1948. *Zwischenmolekulare Energiewanderung Und Fluoreszenz. *Annalen Der Physik,* 2**,** 55-75.

KUDRYAVTSEV, V., FELEKYAN, S., WOZNIAK, A. K., KONIG, M., SANDHAGEN, C., KUHNEMUTH, R., SEIDEL, C. A. & OESTERHELT, F. 2007. Monitoring dynamic systems with multiparameter fluorescence imaging. *Anal Bioanal Chem,* 387**,** 71-82.

LAUX, T., MAYER, K. F. X., BERGER, J. & JURGENS, G. 1996. The WUSCHEL gene is required for shoot and floral meristem integrity in Arabidopsis. *Development,* 122**,** 87-96.

MACDONALD, P. J., CHEN, Y. & MUELLER, J. D. 2012. Chromophore maturation and fluorescence fluctuation spectroscopy of fluorescent proteins in a cell-free expression system. *Analytical Biochemistry,* 421**,** 291-298.

MARQUSEE, S. & BALDWIN, R. L. 1987. Helix Stabilization by Glu- ... Lys+ Salt Bridges in Short Peptides of Denovo Design. *Proceedings of the National Academy of Sciences of the United States of America,* 84**,** 8898-8902.

SCHAFFER, J., VOLKMER, A., EGGELING, C., SUBRAMANIAM, V., STRIKER, G. & SEIDEL, C. A. M. 1999. Identification of single molecules in aqueous solution by time-resolved fluorescence anisotropy. *Journal of Physical Chemistry A,* 103**,** 331-336.

STAHL, Y., GRABOWSKI, S., BLECKMANN, A., KÜHNEMUTH, R., WEIDTKAMP-PETERS, S., PINTO, K. G., KIRSCHNER, G. K., SCHMID, J. B., WINK, R. H., HÜLSEWEDE, A., FELEKYAN, S., SEIDEL, C. A. M. & SIMON, R. 2013. Moderation of Arabidopsis Root Sternness by CLAVATA1 and ARABIDOPSIS CRINKLY4 Receptor Kinase Complexes. *Current Biology,* 23**,** 362-371.

STEINMANN, T., GELDNER, N., GREBE, M., MANGOLD, S., JACKSON, C. L., PARIS, S., GALWEILER, L., PALME, K. & JURGENS, G. 1999. Coordinated polar localization of auxin efflux carrier PIN1 by GNOM ARF GEF. *Science,* 286**,** 316-318.

SUHLING, K., SIEGEL, J., PHILLIPS, D., FRENCH, P. M. W., LEVEQUE-FORT, S., WEBB, S. E. D. & DAVIS, D. M. 2002. Imaging the environment of green fluorescent protein. *Biophysical Journal,* 83**,** 3589-3595.

TERSKIKH, A., FRADKOV, A., ERMAKOVA, G., A, Z., TAN, P., KAJAVA, A., ZHAO, X., LUKYANOV, S., MIKHAIL, M., KIM, S., WEISSMANN, I. & SIEBERT, P. 2000. "Fluorescent Timer": Protein That Changes Color with Time. *Science,* 290**,** 1585-1588.

VOGEL, S. S., THALER, C. & BLANK, P. S. A. K., SRINAGESH V. 2009. *FLIM microscopy in biology and medicine, Chaper 10: Time-resolved fluorescence anisotropy*, CRC Press Taylor and Francis Group, USA.

WEIDTKAMP-PETERS, S., FELEKYAN, S., BLECKMANN, A., SIMON, R., BECKER, W., KUHNEMUTH, R. & SEIDEL, C. A. 2009. Multiparameter fluorescence image spectroscopy to study molecular interactions. *Photochem Photobiol Sci,* 8**,** 470-80.

VII. Chapter 4: Moving towards Multi-Fluorophore FRET in Plant Cells

1. Introduction:

Protein-protein interactions are of major importance in virtually every event in the lifecycle of most organisms. Accordingly, the development, advancement and utilization of techniques that allow the detection of these interactions has always been pushed forward strongly in the scientific community. In recent years, the measurement and quantification of Förster (Fluorescence) resonance energy transfer (FRET) has emerged as an effective and precise method to detect protein interactions in living cells (Gordon et al., 1998, Bleckmann et al., 2010). FRET describes the transfer of energy by means of intermolecular long-range dipole–dipole coupling between a donor and an acceptor fluorophore (Förster, 1948). The donor fluorophore can be excited to higher electronic states by a light source with a wavelength that corresponds to its excitation spectrum. The excited donor can return to the ground state amongst others by emitting a photon (fluorescence) or by FRET.

FRET requires three prerequisites. First of all the donor's emission spectrum and the acceptor's excitation spectrum have to overlap. Second, the distance between donor and acceptor must not exceed double the Förster radius, which is usually in the range of 5 nm. Furthermore, the donor emission dipole moment has to be aligned with the acceptor absorption dipole moment. If these requirements are fulfilled, energy can be transferred from the donor to the acceptor. This will result in reduced fluorescence intensity from the donor, since the energy is released via FRET and not fluorescence (the donor is "quenched"), while acceptor fluorescence will increase due to its excitation by the transferred energy coming from the donor. To utilize this phenomenon to measure protein interactions, the two proteins that are probed for their capability to interact are each fused to either the donor or the acceptor fluorophore. If the two proteins interact, the fused fluorophores will be brought into the 10 nm maximum FRET-distance, and FRET can occur. This FRET can then be measured and quantified by a variety of different techniques (Jares-Erijman et al., 2003, Sekar et al., 2003, Jares-Erijman et al., 2006).

Of the various technical options available to determine FRET between two proteins, acceptor photobleaching (APB) has emerged as the one most commonly used. The main reason for this is that FRET-APB measurements can be done with relatively low requirements

when it comes to technical equipment, the actual procedure and subsequent data processing. In a typical FRET-APB experimental setup, the two potentially interacting proteins would each be fused to fluorescent proteins (FP) with overlapping emission and excitation spectrums. These FPs are called FRET-pairs. Typical examples of widely used FRET-pairs are the cyan fluorescent protein (CFP) and the yellow fluorescent protein (YFP) (He et al., 2003, Tramier et al., 2006), or the green fluorescent protein (GFP) and mCherry (mCh) (Tramier et al., 2006). The two fusion proteins are then co-expressed in a cell and the donor is excited by a light source, e.g. a laser. In the next step, the acceptor FP is photobleached by strong irradiation with a light source, which is specific for the acceptors excitation range, but is not affecting the donor. Once the acceptor is irreversibly photobleached, there is no more FRET between the donor and the acceptor and the excited donor will release its energy solely through fluorescence, which will increase accordingly. This dequenching of the donor following acceptor photobleaching can be quantified and used as an indicator for protein interactions (Sekar et al., 2003).

While FRET-APB is a very efficient technique to measure interactions, it has some major restrictions and drawbacks. One restriction is that with the common two fluorescent protein FRET-pairs used in plant science, only interaction between two proteins can be measured. Bigger complexes can only be assumed, when two or more proteins are all capable of interacting with each other. Probably even more problematic, at least when FRET-APB is applied in living plant cells, is the sensitivity of the system to environmental factors which results in relatively high variations in measured FRET-rates. Measurements with the same two fusion proteins can result in slightly different results when comparing different measurement days, different plants, different organs of the plant and even cells within the same tissue. This can be due to different developmental stages of the plant or the cell, changing or varying growth conditions of the plant, the expression levels of the fusion proteins and the concentration ratio between donor and acceptor. These slight variations normally should not compromise the experiment to the point where the difference between interaction and no interaction cannot be determined anymore, but it does make it difficult to discriminate between strong and weak, or stable and dynamic interactions. Because of this, very good control measurements are indispensable. However, even with very exact control measurements, even little fluctuation can make a big difference, if, for example, the measured interaction efficiency is so weak, that it is close to the measured efficiency of the negative control. In such a case, it is hard to build a strong case for either weak or no interaction.

To overcome these common problems, a double-FRET system, using three instead of the usual two fluorescent proteins in living plant cells, was designed and established. In this system mTurquoise (mTq), Venus (Ven) and mCherry (mCh) are used as fluorescent protein tags. Between these proteins, FRET is possible from mTurquoise to Venus, and from Venus to mCherry, but not from mTurquoise to mCherry. These properties enable us to measure interactions between three proteins in one big complex, if the three proteins are each tagged with one of three fluorophores and FRET can be detected between both FRET-pairs. On the other hand, it also provides the opportunity to measure an interaction and the corresponding negative control in the same compartment of the same cell with the common FRET-partner for both being tagged with the Venus, and the positive and the negative interactors tagged with either mTurquoise or mCherry. By doing this, any possible variations in the measured apparent FRET-efficiencies that are stemming from different environmental influences can be reduced to an absolute minimum.

The three fluorophores mTurquoise, Venus and mCherry were chosen for several reasons: All three can be stably expressed in plant cells and yield strong fluorescence intensities. They are photostable enough to allow imaging before the FRET-APB measurements without bleaching them before the actual APB event. The emission/excitation spectra of the three FP are separated enough to allow the precise excitation of each of them without also exciting the other two, as well as separate detection of their emitted signal without crosstalk between the channels (Woehler, 2013). Furthermore, their signals can be fully separated from the strong autofluorescence innate to plant cells.

To test this technique, the focus was directed towards the homeobox transcription factor WUSCHEL (WUS), which is involved in stem cell homeostasis in *Arabidopsis thaliana* (Laux et al., 1996). WUS promotes stem cell fate in the shoot apical meristem (SAM), where it is expressed in cells of the organizing center (OC), residing underneath the stem cell population (Mayer et al., 1998). Accordingly, the protein has to move from the cells of the OC to the stem cells to exert its function. After moving to the stem cells, further movement of WUS into neighboring cells has to be blocked to restrict stem cell fate to the small pool of cells in the center of the meristem. One possibility to regulate the mobility of WUS would be the sequestering of single WUS proteins in bigger complexes within the stem cell domain. It has been shown that adding two GFPs to the WUS protein already restricts its movement sufficiently. Since GFP and WUS are of roughly the same size (GFP is 27 kDa, WUS is 33 kDa), a WUS homotrimer would therefore be big enough already to limit the proteins movement (Yadav et al., 2011). That way, monomeric WUS protein would be able to

move a few cell layers from the OC into the stem cells, but would then form bigger complexes preventing further travel. This hypothesis relies on the assumption that WUS homomerizes in plant cells and is capable of forming larger complexes. This, however, has so far not been tested. Therefore this new multi-fluorophore FRET technique was used in this study to investigate the potential of WUS to form larger homomeric complexes in living plant cells.

2. Results:

2.1 WUSCHEL forms Homo-Dimers and Homo-Trimers

The readout for FRET in this approach was the apparent FRET, which is quantified as percentage of donor-dequenching after acceptor photobleaching (E%). To do this, the first step was to determine the background E% level for both FRET-pairs in this system. ASYMMETRIC LEAVES 2 (AS2) was used as the negative control. AS2 is an *A. thaliana* transcription factor involved in leaf development (Iwakawa et al., 2007). It is not expressed in a pattern overlapping with WUS in the meristem and there are also no other indications that it should interact with WUS.

WUS-mTurquoise, AS2-Venus and WUS-mCherry were transiently expressed in *Nicotiana benthamiana* cells and FRET was measured between mTurquoise and Venus and between Venus and mCherry (Fig. 1, A). With Venus being the central fluorophore in the FRET-chain, no FRET should be detected between mTurquoise and Venus or between Venus and mCherry in this situation. The measured E% of AS2-Venus after photobleaching WUS-mCherry was -0.1 (St. Dev. 2.0), showing no FRET between Venus and mCherry, and no interaction between WUS and AS2. The E% of WUS-mTurquoise after subsequently bleaching the AS2-Venus was 3.2 (St. Dev. 3.5). Accordingly, the background level of E% is a little higher for the mTurquoise-Venus FRET-pair, than it is for the Venus-mCherry pair in this system. The values of 0.1 (+/- 2.0) and 3.2 (+/- 3.5) are within the range commonly described as background level for FRET-APB experiments (Tab. 1, Sample 1) (Bleckmann et al., 2010).

The capability of WUSCHEL to form homomers was tested next. For this, WUS-mTurquoise, WUS-Venus and AS2-mCherry were co-expressed (Fig. 1, B). After photobleaching AS2-mCherry an E% of 1.3 (St. Dev. 1.2) was measured for WUS-Venus, verifying that WUS and AS2 do not interact. After subsequent photobleaching of WUS-Venus, the E% of WUS-mTurquoise was 18.4 (St. Dev. 7.8), indicating strong interaction between WUS-mTurquoise and WUS-Venus. This experiment shows that WUS is capable of forming homomers (Tab. 1, Sample 2).

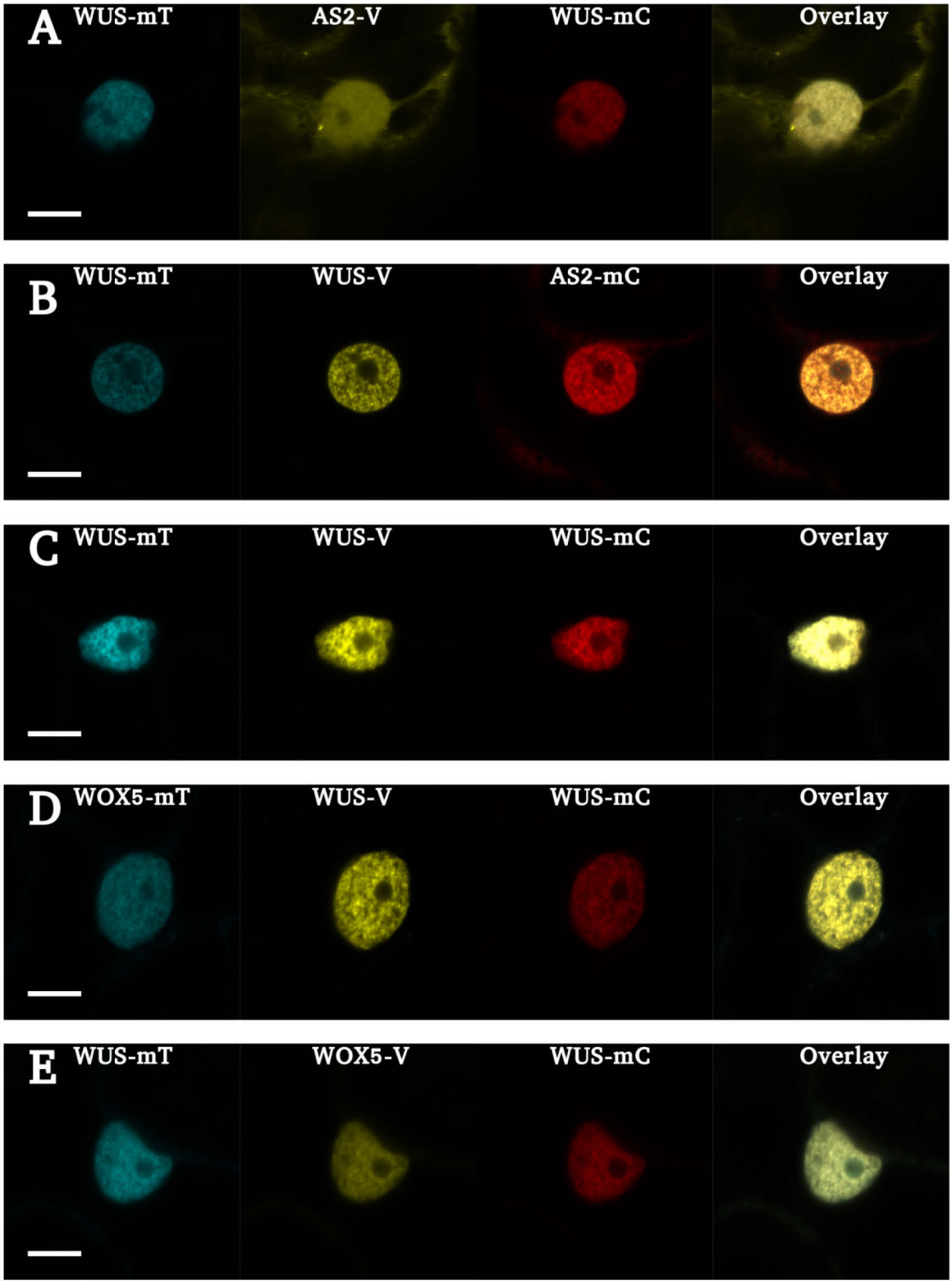

Fig. 1: Intracellular Localizations of the different Fusion Proteins

A) WUS-mT, AS2-V, WUS-mC; B) WUS-mT, WUS-V, AS2-mC; C) WUS-mT, WUS-V, WUS-mC; D) WOX5-mT, WUS-V, WUS-mC; E) WUS-mT, WOX5-V, WUS-mC. Scale bar is 10 µm.

To fully take advantage of the three-fluorophore system, it was then determined if WUSCHEL can form homo-trimeric complexes. For this WUS-mTurquoise, WUS-Venus and WUS-mCherry were co-expressed (Fig. 1, C). When the mCherry fluorophore was photobleached, an E% of 6.6 (St. Dev. 2.6) could be measured for WUS-Venus. After subsequently bleaching the Venus as well, the measured E% of WUS-mTurquoise was 20.0 (St. Dev. 7.7). Both values are well above the measured background levels, indicating interactions between all three WUS molecules. This could be an indication for homotrimers being formed, however, it is not possible to differentiate if the measured FRET between both pairs is really due to a trimeric complex being formed, or because of different sets of dimers. Furthermore, these measurements demonstrate that mTurquoise / Venus is a better FRET-pair than Venus / mCherry, with 20.0 E% compared to only 6.6 (Tab. 1, Sample 3).

Sample 1:	WUS-mT	AS2-V	WUS-mC
Average E% (St. Dev.)	3.2 (3.5)	-0.1 (2.0)	
Sample 2:	WUS-mT	WUS-V	AS2-mC
Average E% (St. Dev.)	18.4 (7,8)	1.3 (1.2)	
Sample 3:	WUS-mT	WUS-V	WUS-mC
Average E% (St. Dev.)	20.0 (7.7)	6.6 (2.6)	
Sample 4:	WOX5-mT	WUS-V	WUS-mC
Average E% (St. Dev.)	11.7 (5.8)	6.8 (4.7)	
Sample 5:	WUS-mT	WOX5-V	WUS-mC
Average E% (St. Dev.)	7.9 (4.4)	6.0 (5.7)	

Tab. 1: E% values for the different FRET-APB measurements

Sample 1 is the negative control with no interactions. Sample 2 shows interaction between WUS-mT and WUS-V, but not WUS-V and AS2-mC. Sample 3 shows interaction between all three proteins. Sample 4 shows impaired interaction between WOX5-mT and WUS-V and strong interaction between WUS-V and WUS-mC (compared to sample 3). Sample 5 shows impaired interaction of WOX5-V with both, WUS-mT and WUS-mC.

2.2 WUSCHEL and its Homolog WOX5 are able of Interacting

After observing that WUS forms homomers, the specificity of this interaction was determined. To get an idea of the specificity it was tested if WUS can interact with its closest homolog, WUSCHEL-RELATED HOMEOBOX 5 (WOX5). WOX5 is involved in stem cell

maintenance in the root meristem of *A. thaliana*, similar to the role of WUS in the SAM. To test if WUS and WOX5 are capable of forming a complex, WOX5-mTurquoise, WUS-Venus and WUS-mCherry were co-expressed (Fig. 1, D). The E% of WUS-Venus after photobleaching WUS-mCherry was 6.8 (St. Dev. 4.7), reflecting the interaction between WUS and WUS. After bleaching the Venus as well, the measured E% for WOX5-mTurquoise was 11.7 (St. Dev. 5.8). Here, it appears that WUS and WOX5 do interact, but FRET is severely weaker than it is for the WUS-WUS interaction (Tab. 1, Sample 4).

In the next step, WOX5 was expressed as the central protein of the FRET-chain, fused to Venus (Fig. 1, E). Photobleaching of WUS-mCherry resulted in an E% of 6.0 (St. Dev. 5.7) for WOX5-Venus. The E% of WUS-mTurquoise after photobleaching WOX5-Venus was 7.9 (St. Dev. 4.4), again showing weaker FRET than was measure for the WUS-WUS interaction, even if the reduction is only slightly visible for the Venus / mCherry FRET-pair (Tab. 1, Sample 5).

3. Discussion:

In this study, a three-fluorophore FRET-system for living plant cells is presented. Using this system it could be possible to detect trimeric complexes by measuring FRET between two FRET-pairs in the same cell. Furthermore, this system was successfully used to measure interaction and a negative control with a common protein in the exact same cell.

With the introduction of this system two of the biggest drawbacks of FRET-APB measurements can be overcome. For one, moving from measurements with one FRET-pair to measurements with two FRET-pairs, makes it possible to measure interactions between three different proteins in one big complex. Up to now, FRET-APB was only used to measure interactions between two proteins in living plant cells. A restriction it shared with several other widely used protein-protein interaction techniques, such as bimolecular fluorescence complementation (BiFC) assays or the split-ubiquitin and yeast two-hybrid systems (Ghosh et al., 2000, Stagljar et al., 1998, Fields et al., 1989).

Furthermore, protein interaction-measurements and their appropriate negative controls can be performed in the exact same cell. Since FRET-APB results can vary between different measurement days, different plants, different leaves and even different cells, to the point that it is difficult to discriminate between weak and strong, or very weak or dynamic and no interaction, this is a huge improvement on the way to more reliable results.

Here, this technique was used to determine the interaction properties of the WUS transcription factor. WUS is one of the central regulators in *A. thaliana* stem cell homeostasis. It is expressed in the organizing center of the shoot apical meristem of *Arabidopsis* and moves from there into the overlying stem cells, where it promotes stem cell fate (Yadav et al., 2011). The interacting state of WUS however has not been studied so far, even though knowing if WUS can form homomers would contribute to understanding how it functions. In general, it is known for other transcription factors that they function as homodimers, which could be the case for WUS as well (de Folter et al., 2005). Also, to exert its function, the WUS protein must move from the cells of the OC into the stem cell domain (Yadav et al., 2011). At the same time, its movement must be restricted to these cells. So far it is not known how WUS movement is regulated. One potential mechanism to prevent the WUS protein from moving further than just into the directly adjacent stem cell domain would be the sequestration of WUS in bigger complexes that are immobile (Yadav et al., 2011).

Utilizing three-fluorophore FRET measurements, it was possible to show that WUS is capable of forming not only homodimers, but possibly also trimeric complexes. Since it is

conceivable that two homodimers can interact with each other, it is also not unlikely that tetrameric complexes are formed. The ability to form higher order complexes is especially interesting for the sequestration model of WUS movement.

Furthermore it was shown that WUS can also interact with its homolog WOX5, but that this interaction is impaired, compared to WUS homomerization. While the homeodomain of WUS and WOX5 is strongly conserved, they are not completely identical and at least two differences are in domains of the homeobox that are important for both, protein interactions as well as DNA binding (Nardmann et al., 2009). This is also in agreement with WOX5 not being able to fully complement the *wus* mutant phenotype (Sarkar et al., 2007). In this case, it is also important to note that the mTurquoise / Venus pair appears to be more suitable for FRET-measurements than the Venus / mCherry pair. Generally, the mT / V pair yielded much higher E% values for the same interactions, e.g. 20 % for the WUS-WUS interaction, compared to 6.8 for the V / mC pair. This could be due to the slower maturation of mCherry, which can result in a lower concentration of functional acceptor molecules relative to the donor concentration. Also, it could be due to a better overlap between the emission / excitation spectra of mT and V, compared to V and mCh (Excitation / Emission maxima: mT = 433 / 480, V = 515 / 528, mC = 587 / 610). Owing to these properties, the mT / V pair appears to be better suitable to discriminate between strong and weak interactions, exhibiting a clear difference between the strong WUS-WUS interaction (E% = 20) and the weak WOX5-WUS interaction (E% = 11.7), which is only slightly visible with the V / mC pair (6.8 E% for WUS-WUS, 6.0 E% for WOX5-WUS).

4. Conclusion:

Here an improved FRET-APB interaction measurement technique for living plant cells was introduced. Utilizing a FRET-triplet instead of the usual FRET-pair it is possible to either measure interaction between three proteins or include the interaction and negative control measurement in the exact same cell, using a common central FRET-partner. Applying this technique it was shown that the plant stem cell regulator WUS can form multimeric complexes and can interact with its close homolog WOX5, but that the latter interaction is weaker, compared to WUS homomerization.

Using this improved technique will help to overcome common limitations of interaction measurement techniques in plant cells.

5. Methods:

Nicotiana benthamiana Plant Lines

Nicotiana benthamiana plants were grown in the greenhouse for four weeks prior to transient transformation. Transformation and expression were described before (Bleckmann et al., 2010).

Construction of Plasmids

The WUS and WOX5 genes were created from cDNA using the Gateway® BP / LR Clonase® II Cloning Kits, as well as the destination vector pABindmCherry described previously (Bleckmann et al., 2010) The AS2 entry clone was described previously (Rast et al., 2012). The destination vectors pABindVenus and pMASindmT were created from pMDC7 and pmTurquoise-N1, described previously (Goedhart et al., 2010, Curtis et al., 2003).

Microscopy

Imaging and FRET-APB measurements were done on a Zeiss LSM 780 confocal microscope. mTurquoise was excited with a continuous wave 405 nm diode laser at the objective (40x water immersion, Zeiss C-Apochromat 40x/1.20 W korr M27) and emission was detected at 463 - 492 nm by 32-Channel-GaAsP-Detectors. Venus was excited using a 514 nm continuous wave argon laser and emission was detected at 520 - 543 nm. mCherry was excited using a 561 nm continuous wave diode laser and emission detected at 597 - 633 nm. For APB measurements, a series of 12 256 x 256 pixel frames with 0.18 µM pixel size, 47 μm^2 image size and 1.27 µs pixel dwell time was recorded. After 5 frames, mCherry was photobleached in a region of interest encompassing the entire nucleus by 80 iterations with 100 % laser power. Immediately after the full 12 frame series was recorded, Venus was photobleached in the same region of interest, again by 80 iterations with 100 % laser power. E% was determined as donor-intensity change after photobleaching for both individual bleach series by (DONORafter − DONORbefore)/DONORafter × 100.

This chapter is a manuscript in preparation for submission.

Authors:
Marc Somssich[1] and Rüdiger Simon[1, 2]

[1] Institute of Developmental Genetics
[2] Center for Advanced Imaging
Heinrich Heine University, 40225 Düsseldorf, Germany

The experiment was designed by Marc Somssich and Rüdiger Simon. Molecular biology, plant work, microscopy and analysis were done by Marc Somssich. The manuscript was written by Marc Somssich with help from Rüdiger Simon.

6. References:

ALFTHAN, K., TAKKINEN, K., SIZMANN, D., SODERLUND, H. & TERRI, T. T. 1995. Properties of a Single-Chain Antibody Containing Different Linker Peptides. *Protein Engineering,* 8**,** 725-731. DOI 10.1093/protein/8.7.725

ALI, G. S., PRASAD, K. V. S. K., DAY, I. & REDDY, A. S. N. 2007. Ligand-dependent reduction in the membrane mobility of FLAGELLIN SENSITIVE2, an Arabidopsis receptor-like kinase. *Plant and Cell Physiology,* 48**,** 1601-1611. Doi 10.1093/Pcp/Pcm132

ARAI, R., UEDA, H., KITAYAMA, A., KAMIYA, N. & NAGAMUNE, T. 2001. Design of the linkers which effectively separate domains of a bifunctional fusion protein. *Protein Engineering,* 14**,** 529-532. DOI 10.1093/protein/14.8.529

BAIRD, G. S., ZACHARIAS, D. A. & TSIEN, R. Y. 2000. Biochemistry, mutagenesis, and oligomerization of DsRed, a red fluorescent protein from coral. *PNAS,* 97**,** 11984-9. 10.1073/pnas.97.22.11984

BECKER, W. 2005. *Advanced time-correlated single photon counting techniques,* Berlin ; New York, Springer.

BLECKMANN, A., WEIDTKAMP-PETERS, S., SEIDEL, C. A. & SIMON, R. 2010. Stem cell signaling in Arabidopsis requires CRN to localize CLV2 to the plasma membrane. *Plant Physiol,* 152**,** 166-76. DOI 10.1104/pp.109.149930

BRAND, U., FLETCHER, J. C., HOBE, M., MEYEROWITZ, E. M. & SIMON, R. 2000. Dependence of stem cell fate in Arabidopsis an a feedback loop regulated by CLV3 activity. *Science,* 289**,** 617-619. DOI 10.1126/science.289.5479.617

CHINCHILLA, D., SHAN, L., HE, P., DE VRIES, S. & KEMMERLING, B. 2009. One for all: the receptor-associated kinase BAK1. *Trends in Plant Science,* 14**,** 535-541. DOI 10.1016/j.tplants.2009.08.002

CHINCHILLA, D., ZIPFEL, C., ROBATZEK, S., KEMMERLING, B., NÜRNBERGER, T., JONES, J. D., FELIX, G. & BOLLER, T. 2007. A flagellin-induced complex of the receptor FLS2 and BAK1 initiates plant defence. *Nature,* 448**,** 497-500. 10.1038/nature05999

CLARK, S. E., RUNNING, M. P. & MEYEROWITZ, E. M. 1995. CLAVATA3 Is a Specific Regulator of Shoot and Floral Meristem Development Affecting the Same Processes as CLAVATA1. *Development,* 121**,** 2057-2067.

CLARK, S. E., WILLIAMS, R. W. & MEYEROWITZ, E. M. 1997. The CLAVATA1 gene encodes a putative receptor kinase that controls shoot and floral meristem size in Arabidopsis. *Cell,* 89**,** 575-585. Doi 10.1016/S0092-8674(00)80239-1

CLOUSE, S. D., LANGFORD, M. & MCMORRIS, T. C. 1996. A brassinosteroid-insensitive mutant in Arabidopsis thaliana exhibits multiple defects in growth and development. *Plant Physiology,* 111**,** 671-678. Doi 10.1104/Pp.111.3.671

CURTIS, M. D. & GROSSNIKLAUS, U. 2003. A gateway cloning vector set for high-throughput functional analysis of genes in planta. *Plant Physiology,* 133**,** 462-469. DOI 10.1104/pp.103.027979

DE FOLTER, S., IMMINK, R. G. H., KIEFFER, M., PARENICOVA, L., HENZ, S. R., WEIGEL, D., BUSSCHER, M., KOOIKER, M., COLOMBO, L., KATER, M. M., DAVIES, B. & ANGENENT, G. C. 2005. Comprehensive interaction map of the Arabidopsis MADS box transcription factors. *Plant Cell,* 17**,** 1424-1433. DOI 10.1105/tpc.105.031831

DIEVART, A., DALAL, M., TAX, F. E., LACEY, A. D., HUTTLY, A., LI, J. M. & CLARK, S. E. 2003. CLAVATA1 dominant-negative alleles reveal functional overlap between multiple receptor kinases that regulate meristem and organ development. *Plant Cell,* 15**,** 1198-1211. Doi 10.1105/Tpc.010504

EVERS, T. H., VAN DONGEN, E. M. W. M., FAESEN, A. C., MEIJER, E. W. & MERKX, M. 2006. Quantitative understanding of the energy transfer between fluorescent proteins connected via flexible peptide linkers. *Biochemistry,* 45**,** 13183-13192. Doi 10.1021/Bi061288t

FIELDS, S. & SONG, O. K. 1989. A Novel Genetic System to Detect Protein Protein Interactions. *Nature,* 340**,** 245-246. Doi 10.1038/340245a0

FLETCHER, L. C., BRAND, U., RUNNING, M. P., SIMON, R. & MEYEROWITZ, E. M. 1999. Signaling of cell fate decisions by CLAVATA3 in Arabidopsis shoot meristems. *Science,* 283**,** 1911-1914.

FÖRSTER, T. 1948. *Zwischenmolekulare Energiewanderung Und Fluoreszenz. *Annalen Der Physik,* 2**,** 55-75.

GEE, C. L., PAPAVINASASUNDARAM, K. G., BLAIR, S. R., BAER, C. E., FALICK, A. M., KING, D. S., GRIFFIN, J. E., VENGHATAKRISHNAN, H., ZUKAUSKAS, A., WEI, J. R., DHIMAN, R. K., CRICK, D. C., RUBIN, E. J., SASSETTI, C. M. & ALBER, T. 2012. A Phosphorylated Pseudokinase Complex Controls Cell Wall Synthesis in Mycobacteria. *Science Signaling,* 5.

GHOSH, I., HAMILTON, A. D. & REGAN, L. 2000. Antiparallel leucine zipper-directed protein reassembly: Application to the green fluorescent protein. *Journal of the American Chemical Society,* 122**,** 5658-5659. Doi 10.1021/Ja994421w

GISH, L. A., GAGNE, J. M., HAN, L. Q., DEYOUNG, B. J. & CLARK, S. E. 2013. WUSCHEL-Responsive At5g65480 Interacts with CLAVATA Components In Vitro and in Transient Expression. *Plos One,* 8. ARTN e66345. DOI 10.1371/journal.pone.0066345

GOEDHART, J., VAN WEEREN, L., HINK, M. A., VISCHER, N. O. E., JALINK, K. & GADELLA, T. W. J. 2010. Bright cyan fluorescent protein variants identified by fluorescence lifetime screening. *Nature Methods,* 7**,** 137-U74. Doi 10.1038/Nmeth.1415

GOMEZ-GOMEZ, L., BAUER, Z. & BOLLER, T. 2001. Both the extracellular leucine-rich repeat domain and the kinase activity of FLS2 are required for flagellin binding and signaling in arabidopsis. *Plant Cell,* 13**,** 1155-1163. DOI 10.1105/tpc.13.5.1155

GOMEZ-GOMEZ, L. & BOLLER, T. 2000. FLS2: An LRR receptor-like kinase involved in the perception of the bacterial elicitor flagellin in Arabidopsis. *Molecular Cell,* 5**,** 1003-1011. Doi 10.1016/S1097-2765(00)80265-8

GORDON, G. W., BERRY, G., LIANG, X. H., LEVINE, B. & HERMAN, B. 1998. Quantitative fluorescence resonance energy transfer measurements using fluorescence microscopy. *Biophysical Journal,* 74**,** 2702-2713.

GUO, Y. F., HAN, L. Q., HYMES, M., DENVER, R. & CLARK, S. E. 2010. CLAVATA2 forms a distinct CLE-binding receptor complex regulating Arabidopsis stem cell specification. *Plant Journal,* 63**,** 889-900. DOI 10.1111/j.1365-313X.2010.04295.x

HALTER, T., IMKAMPE, J., MAZZOTTA, S., WIERZBA, M., POSTEL, S., BUCHERL, C., KIEFER, C., STAHL, M., CHINCHILLA, D., WANG, X., NÜRNBERGER, T., ZIPFEL, C., CLOUSE, S., BORST, J. W., BOEREN, S., DE VRIES, S. C., TAX, F. & KEMMERLING, B. 2014. The leucine-rich repeat receptor kinase BIR2 is a negative regulator of BAK1 in plant immunity. *Curr Biol,* 24**,** 134-43. 10.1016/j.cub.2013.11.047

HE, L. S., OLSON, D. P., WU, X. L., KARPOVA, T. S., MCNALLY, J. G. & LIPSKY, P. E. 2003. A flow cytometric method to detect protein-protein interaction in living cells by directly visualizing donor fluorophore quenching during CFP -> YFP fluorescence resonance energy transfer (FRET). *Cytometry Part A,* 55A**,** 71-85. Doi 10.1002/Cyto.A.10073

IWAKAWA, H., IWASAKI, M., KOJIMA, S., UENO, Y., SOMA, T., TANAKA, H., SEMIARTI, E., MACHIDA, Y. & MACHIDA, C. 2007. Expression of the ASYMMETRIC LEAVES2 gene in the adaxial domain of Arabidopsis leaves represses cell proliferation in this domain and is critical for the development of properly expanded leaves. *Plant Journal,* 51**,** 173-184. DOI 10.1111/j.1365-313X.2007.03132.x

JARES-ERIJMAN, E. A. & JOVIN, T. M. 2003. FRET imaging. *Nature Biotechnology,* 21**,** 1387-1395. Doi 10.1038/Nbt896

JARES-ERIJMAN, E. A. & JOVIN, T. M. 2006. Imaging molecular interactions in living cells by FRET microscopy. *Current Opinion in Chemical Biology,* 10**,** 409-416. DOI 10.1016/j.cbpa.2006.08.021

JEONG, S., TROTOCHAUD, A. E. & CLARK, S. E. 1999. The Arabidopsis CLAVATA2 gene encodes a receptor-like protein required for the stability of the CLAVATA1 receptor-like kinase. *Plant Cell,* 11**,** 1925-1933. DOI 10.1105/tpc.11.10.1925

KAYES, J. M. & CLARK, S. E. 1998. CLAVATA2, a regulator of meristem and organ development in Arabidopsis. *Development,* 125**,** 3843-3851.

KINOSHITA, A., BETSUYAKU, S., OSAKABE, Y., MIZUNO, S., NAGAWA, S., STAHL, Y., SIMON, R., YAMAGUCHI-SHINOZAKI, K., FUKUDA, H. & SAWA, S. 2010. RPK2 is an essential receptor-like kinase that transmits the CLV3 signal in Arabidopsis (vol 137, pg 3911, 2010). *Development,* 137**,** 4327-4327. Doi 10.1242/Dev.061747

KINOSHITA, T., CANO-DELGADO, A. C., SETO, H., HIRANUMA, S., FUJIOKA, S., YOSHIDA, S. & CHORY, J. 2005. Binding of brassinosteroids to the extracellular domain of plant receptor kinase BRI1. *Nature,* 433**,** 167-171. Doi 10.1038/Nature03227

KOZER, N., BARUA, D., ORCHARD, S., NICE, E. C., BURGESS, A. W., HLAVACEK, W. S. & CLAYTON, A. H. A. 2013. Exploring higher-order EGFR oligomerisation and phosphorylation-a combined experimental and theoretical approach. *Molecular Biosystems,* 9**,** 1849-1863. Doi 10.1039/C3mb70073a

KUDRYAVTSEV, V., FELEKYAN, S., WOZNIAK, A. K., KÖNIG, M., SANDHAGEN, C., KÜHNEMUTH, R., SEIDEL, C. A. & OESTERHELT, F. 2007. Monitoring dynamic systems with multiparameter fluorescence imaging. *Anal Bioanal Chem,* 387**,** 71-82. 10.1007/s00216-006-0917-0

LAUX, T., MAYER, K. F. X., BERGER, J. & JÜRGENS, G. 1996. The WUSCHEL gene is required for shoot and floral meristem integrity in Arabidopsis. *Development,* 122**,** 87-96.

LI, J., WEN, J. Q., LEASE, K. A., DOKE, J. T., TAX, F. E. & WALKER, J. C. 2002. BAK1, an Arabidopsis LRR receptor-like protein kinase, interacts with BRI1 and modulates brassinosteroid signaling. *Cell,* 110**,** 213-222. Doi 10.1016/S0092-8674(02)00812-7

LIN, W. W., LI, B., LU, D. P., CHEN, S. X., ZHU, N., HE, P. & SHAN, L. B. 2014. Tyrosine phosphorylation of protein kinase complex BAK1/BIK1 mediates Arabidopsis innate immunity. *Proceedings of the National Academy of Sciences of the United States of America,* 111**,** 3632-3637. DOI 10.1073/pnas.1318817111

LOGEMANN, E., BIRKENBIHL, R. P., ÜLKER, B. & SOMSSICH, I. E. 2006. An improved method for preparing Agrobacterium cells that simplifies the Arabidopsis transformation protocol. *Plant Methods,* 2. Artn 16. Doi 10.1186/1746-4811-2-16

MACDONALD, P. J., CHEN, Y. & MUELLER, J. D. 2012. Chromophore maturation and fluorescence fluctuation spectroscopy of fluorescent proteins in a cell-free expression system. *Analytical Biochemistry,* 421**,** 291-298. Doi 10.1016/J.Ab.2011.10.040

MARQUSEE, S. & BALDWIN, R. L. 1987. Helix Stabilization by Glu- ... Lys+ Salt Bridges in Short Peptides of Denovo Design. *Proceedings of the National Academy of Sciences of the United States of America,* 84**,** 8898-8902. DOI 10.1073/pnas.84.24.8898

MAUS, M., COTLET, M., HOFKENS, J., GENSCH, T., DE SCHRYVER, F. C., SCHAFFER, J. & SEIDEL, C. A. M. 2001. An experimental comparison of the maximum likelihood estimation and nonlinear least squares fluorescence lifetime analysis of single molecules. *Analytical Chemistry,* 73**,** 2078-2086. Doi 10.1021/Ac000877g

MAYER, K. F. X., SCHOOF, H., HAECKER, A., LENHARD, M., JÜRGENS, G. & LAUX, T. 1998. Role of WUSCHEL in regulating stem cell fate in the Arabidopsis shoot meristem. *Cell,* 95**,** 805-815. Doi 10.1016/S0092-8674(00)81703-1

MÜLLER, R., BLECKMANN, A. & SIMON, R. 2008. The receptor kinase CORYNE of Arabidopsis transmits the stem cell-limiting signal CLAVATA3 independently of CLAVATA1. *Plant Cell,* 20**,** 934-46. 10.1105/tpc.107.057547

NAM, K. H. & LI, J. M. 2002. BRI1/BAK1, a receptor kinase pair mediating brassinosteroid signaling. *Cell,* 110**,** 203-212. Doi 10.1016/S0092-8674(02)00814-0

NARDMANN, J., REISEWITZ, P. & WERR, W. 2009. Discrete Shoot and Root Stem Cell-Promoting WUS/WOX5 Functions Are an Evolutionary Innovation of Angiosperms. *Molecular Biology and Evolution,* 26**,** 1745-1755. DOI 10.1093/molbev/msp084

NIMCHUK, Z. L., TARR, P. T. & MEYEROWITZ, E. M. 2011. An Evolutionarily Conserved Pseudokinase Mediates Stem Cell Production in Plants. *Plant Cell,* 23**,** 851-854. DOI 10.1105/tpc.110.075622

NÜHSE, T. S., STENSBALLE, A., JENSEN, O. N. & PECK, S. C. 2004. Phosphoproteomics of the arabidopsis plasma membrane and a new phosphorylation site database. *Plant Cell,* 16**,** 2394-2405. DOI 10.1105/tpc.104.023150

OGAWA, M., SHINOHARA, H., SAKAGAMI, Y. & MATSUBAYASHI, Y. 2008. Arabidopsis CLV3 peptide directly binds CLV1 ectodomain. *Science,* 319**,** 294-294. DOI 10.1126/science.1150083

OKADA, K., KOMAKI, M. K. & SHIMURA, Y. 1989. Mutational Analysis of Pistil Structure and Development of Arabidopsis-Thaliana. *Cell Differentiation and Development,* 28**,** 27-38. Doi 10.1016/0922-3371(89)90020-8

PAGANO, A., ROVELLI, G., MOSBACHER, J., LOHMANN, T., DUTHEY, B., STAUFFER, D., RISTIG, D., SCHULER, V., MEIGEL, I., LAMPERT, C., STEIN, T., PREZEAU, L., BLAHOS, J., PIN, J. P., FROESTL, W., KUHN, R., HEID, J., KAUPMANN, K. & BETTLER, B. 2001. C-terminal interaction is essential for surface trafficking but not for heteromeric assembly of GABA(B) receptors. *Journal of Neuroscience,* 21**,** 1189-1202.

PERRIN, F. 1929. La fluorescence des solutions. *Ann. Phys. Paris,* 12**,** 169–275.

RAST, M. I. & SIMON, R. 2012. Arabidopsis JAGGED LATERAL ORGANS Acts with ASYMMETRIC LEAVES2 to Coordinate KNOX and PIN Expression in Shoot and Root Meristems. *Plant Cell,* 24**,** 2917-2933. DOI 10.1105/tpc.112.099978

SARKAR, A. K., LUIJTEN, M., MIYASHIMA, S., LENHARD, M., HASHIMOTO, T., NAKAJIMA, K., SCHERES, B., HEIDSTRA, R. & LAUX, T. 2007. Conserved factors regulate signalling in Arabidopsis thaliana shoot and root stem cell organizers. *Nature,* 446**,** 811-814. Doi 10.1038/Nature05703

SCHAFFER, J., VOLKMER, A., EGGELING, C., SUBRAMANIAM, V., STRIKER, G. & SEIDEL, C. A. M. 1999. Identification of single molecules in aqueous solution by time-resolved fluorescence anisotropy. *Journal of Physical Chemistry A,* 103**,** 331-336. Doi 10.1021/Jp9833597

SCHOOF, H., LENHARD, M., HAECKER, A., MAYER, K. F. X., JÜRGENS, G. & LAUX, T. 2000. The stem cell population of Arabidopsis shoot meristems is maintained by a regulatory loop between the CLAVATA and WUSCHEL genes. *Cell,* 100**,** 635-644. Doi 10.1016/S0092-8674(00)80700-X

SEKAR, R. B. & PERIASAMY, A. 2003. Fluorescence resonance energy transfer (FRET) microscopy imaging of live cell protein localizations. *Journal of Cell Biology,* 160**,** 629-633. DOI 10.1083/jcb.200210140

SIMONS, K. & TOOMRE, D. 2000. Lipid rafts and signal transduction. *Nature Reviews Molecular Cell Biology,* 1**,** 31-39. Doi 10.1038/35036052

STAGLJAR, I., KOROSTENSKY, C., JOHNSSON, N. & TE HEESEN, S. 1998. A genetic system based on split-ubiquitin for the analysis of interactions between membrane proteins in vivo. *Proceedings of the National Academy of Sciences of the United States of America,* 95**,** 5187-5192. DOI 10.1073/pnas.95.9.5187

STAHL, Y., GRABOWSKI, S., BLECKMANN, A., KÜHNEMUTH, R., WEIDTKAMP-PETERS, S., PINTO, K. G., KIRSCHNER, G. K., SCHMID, J. B., WINK, R. H., HÜLSEWEDE, A., FELEKYAN, S., SEIDEL, C. A. M. & SIMON, R. 2013. Moderation of Arabidopsis Root Sternness by CLAVATA1 and ARABIDOPSIS CRINKLY4 Receptor Kinase Complexes. *Current Biology,* 23**,** 362-371. DOI 10.1016/j.cub.2013.01.045

STEINMANN, T., GELDNER, N., GREBE, M., MANGOLD, S., JACKSON, C. L., PARIS, S., GALWEILER, L., PALME, K. & JÜRGENS, G. 1999. Coordinated polar localization of auxin efflux carrier PIN1 by GNOM ARF GEF. *Science,* 286**,** 316-318. DOI 10.1126/science.286.5438.316

STONE, J. M., TROTOCHAUD, A. E., WALKER, J. C. & CLARK, S. E. 1998. Control of meristem development by CLAVATA1 receptor kinase and kinase-associated protein phosphatase interactions. *Plant Physiology,* 117**,** 1217-1225. DOI 10.1104/pp.117.4.1217

SUHLING, K., SIEGEL, J., PHILLIPS, D., FRENCH, P. M. W., LEVEQUE-FORT, S., WEBB, S. E. D. & DAVIS, D. M. 2002. Imaging the environment of green fluorescent protein. *Biophysical Journal,* 83**,** 3589-3595.

SUN, W. X., CAO, Y. R., LABBY, K. J., BITTEL, P., BOLLER, T. & BENT, A. F. 2012. Probing the Arabidopsis Flagellin Receptor: FLS2-FLS2 Association and the Contributions of Specific Domains to Signaling Function. *Plant Cell,* 24**,** 1096-1113. DOI 10.1105/tpc.112.095919

TERSKIKH, A., FRADKOV, A., ERMAKOVA, G., A, Z., TAN, P., KAJAVA, A., ZHAO, X., LUKYANOV, S., MIKHAIL, M., KIM, S., WEISSMANN, I. & SIEBERT, P. 2000. "Fluorescent Timer": Protein That Changes Color with Time. *Science,* 290**,** 1585-1588. 10.1126/science.290.5496.1585

TRAMIER, M., ZAHID, M., MEVEL, J. C., MASSE, M. J. & COPPEY-MOISAN, M. 2006. Sensitivity of CFP/YFP and GFP/mCherry pairs to donor photobleaching on FRET determination by fluorescence lifetime imaging microscopy in living cells. *Microscopy Research and Technique,* 69**,** 933-939. Doi 10.1002/Jemt.20370

VOGEL, S. S., THALER, C. & BLANK, P. S. A. K., SRINAGESH V. 2009. *FLIM microscopy in biology and medicine, Chaper 10: Time-resolved fluorescence anisotropy*, CRC Press Taylor and Francis Group, USA.

WANG, X. F., KOTA, U., HE, K., BLACKBURN, K., LI, J., GOSHE, M. B., HUBER, S. C. & CLOUSE, S. D. 2008. Sequential transphosphorylation of the BRI1/BAK1 receptor kinase complex impacts early events in brassinosteroid signaling. *Developmental Cell,* 15**,** 220-235. DOI 10.1016/j.devcel.2008.06.011

WANG, X. L., LI, X. Q., MEISENHELDER, J., HUNTER, T., YOSHIDA, S., ASAMI, T. & CHORY, J. 2005. Autoregulation and homodimerization are involved in the activation of the

plant steroid receptor BRI1. *Developmental Cell,* 8**,** 855-865. DOI 10.1016/j.devcel.2005.05.001

WEIDTKAMP-PETERS, S., FELEKYAN, S., BLECKMANN, A., SIMON, R., BECKER, W., KÜHNEMUTH, R. & SEIDEL, C. A. 2009. Multiparameter fluorescence image spectroscopy to study molecular interactions. *Photochem Photobiol Sci,* 8**,** 470-80. 10.1039/b903245m

WOEHLER, A. 2013. Simultaneous Quantitative Live Cell Imaging of Multiple FRET-Based Biosensors. *Plos One,* 8. ARTN e61096

DOI 10.1371/journal.pone.0061096

YADAV, R. K., PERALES, M., GRUEL, J., GIRKE, T., JONSSON, H. & REDDY, G. V. 2011. WUSCHEL protein movement mediates stem cell homeostasis in the Arabidopsis shoot apex. *Genes & Development,* 25**,** 2025-2030. Doi 10.1101/Gad.17258511

YU, L. P., MILLER, A. K. & CLARK, S. E. 2003. POLTERGEIST encodes a protein phosphatase 2C that regulates CLAVATA pathways controlling stem cell identity at Arabidopsis shoot and flower meristems. *Current Biology,* 13**,** 179-188. Pii S0960-9822(03)00042-3 Doi 10.1016/S0960-9822(03)00042-3

VIII. Summary:

In this study a multi-parameter fluorescent imaging spectroscopy (MFIS) setup was designed and established to facilitate the monitoring of changes in protein localizations and interaction states over time in single living plant cells. This setup was used to monitor the effects of ligand perception on the receptor proteins of the flagellin (flg) pathway involved in plant defense and the CLAVATA (CLV) pathway involved in stem cell homeostasis. Also, a functional analysis of the CORYNE (CRN) protein was performed to assign functions to the different protein domains of this putative pseudokinase. Furthermore, a study on the effects of different fluorophore linkers in plant cells was performed to determine a linker that allows for the best compromise between a high Förster (Fluorescence) Resonance Energy Transfer (FRET)-efficiency and fast protein maturation. Finally, the conventional two-fluorophore FRET Acceptor PhotoBleaching (APB) technique was developed further into a two-FRET-pair three-fluorophore technique that enables the detection of trimeric protein complexes or the measurement of a protein-protein interaction with the corresponding negative (or positive) control in the exact same cell.

The receptor-like proteins FLAGELLIN-SENSING 2 (FLS2) and BRI1-ASSOCIATED KINASE 1 (BAK1) are co-receptors involved in plant defense against bacterial pathogens. In the absence of pathogenic elicitors the two receptor-like proteins are localized to the plasmamembrane (PM) in a monomeric state. Following perception of the peptide ligand flg22, FLS2 and BAK1 form heteromeric complexes consisting of two FLS2 and BAK1 molecules each that evenly distribute along the PM.

In the CLV pathway, CLAVATA1 (CLV1) homomers and CLAVATA2 (CLV2)/CRN heteromers are evenly distributed along the PM prior to ligand binding. Additionally to that, larger multimers containing all three receptors are formed in small clusters along the PM. After the peptide ligand CLAVATA3 (CLV3) is perceived by the receptors, the CLV1 homo- and CLV2/CRN heteromers begin to aggregate into more larger multimeric complexes in clusters in specific domains along the PM. These clusters could be localized to lipid rafts and may represent the signaling active regions for the CLV receptors.

Accordingly, the flagellin and the CLAVATA pathway are two examples for different principles of signal transduction. In the flg pathway, the peptide ligand induces the formation

of its own receptor complex while the CLV3 peptide is perceived by pre-formed receptor complexes which then aggregate in specific domains of the PM.

A functional analysis of the putative pseudokinase CRN revealed that even though the kinase might not be active in signaling, it is nonetheless essential for the protein to exert its function. Also, even though the kinase does not autophosphorylate in response to ligand availability, it should not be excluded that the kinase is transphophorylated by another kinase. Furthermore, a hidden motif in the extracellular domain (EC) of CRN appears to be responsible for the proteins functionality as well, possibly by stabilizing the protein or ensuring correct membrane integration of the proteins transmembrane domain, which is directly adjacent to the EC.

The study on the effects of different fluorophore linkers in plant cells showed that a short linker, consisting of as few as five amino acids, seems to be most effective. This short linker is sufficiently long to allow for correct protein folding and maturation. Additionally, because of its shortness it keeps the fluorophore in close proximity to allow for strong FRET, if a second fluorophore is involved.

Finally, a two-FRET-pair three-fluorophore FRET-APB technique was designed and established to enable more efficient protein-protein interaction studies, allowing for the detection of trimeric complexes or the measurement of an interaction and a corresponding negative (or positive) control in the same cell. The fluorophores used are mTurquoise, Venus and mCherry. The necessary measurements can be performed on a regular laser scanning confocal microscope without additional equipment or complex post-measurement data-analysis.

IX. Zusammenfassung:

In dieser Arbeit wurde ein multiparameter Fluoreszenzabbildungsspektroskopie-Aufbau konzipiert und etabliert um Veränderungen in Proteinlokalisation und Interaktionsstatus in einzelnen lebenden Pflanzenzellen zu beobachten. Dieser Aufbau wurde dazu genutzt die Effekte von Ligandenerkennung auf die Rezeptorproteine des flagellin (flg) Signalweges, der in der pflanzlichen Schädlingsabwehr involviert ist, und des CLAVATA (CLV) Signalweges, der ein Regulator der Stammzellhomöostase ist, zu beobachten. Außerdem wurde eine Funktionsanalyse des Proteins CORYNE (CRN) vorgenommen, um den einzelnen Domänen dieser potenziellen Pseudokinase Funktionen zuzuschreiben. Zudem wurde eine Untersuchung zu den Effekten verschiedener Linker für Fluoreszierende Proteine in Pflanzen vorgenommen um einen Linker zu finden, der sowohl hohe Förster-Resonanzenergietransfer (FRET)-Effizienzen sowie die korrekte Faltung und Reifung der Proteine erlaubt. Schließlich wurde die konventionelle zwei-Protein FRET-Akzeptor-Fotozerstörung (APB) Technik in eine zwei-FRET-Paar drei-Fluorophor Technik weiterentwickelt, wodurch es möglich wird trimäre Proteinkomplexe zu detektieren oder eine Protein-Protein Interaktionsmessung mitsamt der dazugehörigen Positiv- (oder Negativ-) Kontrolle in derselben Zelle zu messen.

Die rezeptorähnlichen Proteine FLAGELLIN-SENSING 2 (FLS2) und BRI1-ASSOCIATED KINASE 1 (BRI1) sind Korezeptoren, die in der pflanzlichen Pathogenabwehr eine Rolle spielen. In der Abwesenheit von pathogenen Auslösern sind diese Proteine in monomerem Zustand an der Plasmamembran (PM) der Zelle lokalisiert. Nachdem der Ligand flg22 von den Rezeptoren erkannt wurde, formen sie heteromere Komplexe, die aus je zwei FLS2 und BAK1 Molekülen bestehen und gleichmäßig entlang der PM verteilt sind.

Im CLV-Signalweg liegen in Abwesenheit des Peptidliganden CLAVATA 3 (CLV3) CLV1-Homomere und CLV2/CRN-Heteromere gleichmäßig verteilt an der PM vor. Zudem befinden sich vereinzelt größere Multimere mit allen drei Rezeptoren in kleinen Clustern. Nachdem CLV3 von den Rezeptoren gebunden wurde, beginnen die CLV1-Homomere und die CLV2/CRN-Heteromere damit zu aggregieren und mehr Cluster in speziellen Domänen entlang der PM zu bilden. Möglicherweise liegen diese Cluster in Lipid Rafts und zeigen die Regionen der PM auf, in denen die Signalweiterleitung aktiv ist.

Demzufolge sind der flagellin- und der CLAVATA-Signalweg zwei Beispiele für unterschiedliche Prinzipien der Signalweiterleitung. Im Fall des flg-Signalweges induziert der Peptidligand die Bildung seines eigenen Rezeptorkomplexes während das CLV3 Peptid von bereits gebildeten Rezeptorkomplexen empfangen wird die daraufhin in bestimmten Bereichen zu größeren Komplexen aggregieren.

Eine Funktionsanalyse der potenziellen Pseudokinase CRN ergab, dass die Kinase zwar möglicherweise keine Rolle in der aktiven Signalweiterleitung spielt, sie aber dennoch essenziell für die Funktionalität des Proteins ist. Zudem scheint sie zwar keine Autophosphorilierungsaktivität zu besitzen, könnte jedoch von einer anderen Kinase transphosphoriliert werden. Außerdem scheint eine noch unerkannte Signalsequenz in der außerzellulären Domäne (EC) des Proteins ebenfalls wichtig für die Funktionalität des Proteins zu sein, möglicherweise indem sie zur Stabilisierung des Proteins oder die korrekte Integration der CRN-Transmembrandomäne, die unmittelbar neben der EC liegt, in die PM beiträgt.

Durch die Untersuchung verschiedener Linker für Fluoreszierende Proteine in Pflanzenzellen wurde gezeigt, dass kurze Linker aus gerade einmal fünf Aminosäuren am effektivsten sind. Diese kurzen Linker sind lang genug um eine korrekte und schnelle Proteinfaltung und Reifung zu ermöglichen. Zudem sorgen sie durch ihre Kürze dafür, dass die Fluorophore in der Nähe gehalten werden, was starken FRET zwischen ihnen und anderen Fluorophoren ermöglicht.

Schließlich wurde eine zwei-FRET-Paar drei-Fluorophor FRET-APB Technik konzipiert und etabliert die es ermöglicht, trimäre Proteinkomplexe zu detektieren oder Protein-Protein Interaktionsmessungen mitsamt einer dazugehörigen Negativ-(oder Positiv-) Kontrolle durchzuführen. Dabei wurden die fluoreszenten Proteine mTurquoise, Venus und mCherry verwendet. Die nötigen Messungen können an einem regulären konfokalen Lasermikroskop ohne zusätzliches Equipment oder komplexe Datenanalyse im Anschluss an die Messungen durchgeführt werden.

X. Appendix:

1. Abbreviations:

A. thaliana	*Arabidopsis thaliana*
aa	Amino acid(s)
APB	Acceptor Photobleaching
BAK1	BRI1-ASSOCIATED KINASE 1
BIR2	BAK1-INTERACTING RECEPTOR-LIKE KINASE 2
B1	BAK1
BR	Brassinosteroid(s)
C	CLAVATA1
CFP	Cyan Fluorescent Protein
CLV	CLAVATA
CLV1	CLAVATA1
CLV2	CLAVATA2
CLV3	CLAVATA3
CLE	CLV3/ESR-related
co-IP	co-immunoprecipitation
Col-*0*	Columbia-*0*
CR	CORYNE
CRN	CORYNE
C1	CLAVATA1
C2	CLAVATA2
DO	Donor-Only
EC	Extracellular domain
EGFR	epidermal growth factor
E%	Apparent FRET-efficiency
ER	Endoplasmic Reticulum
F	FRET
flg	flagellin
FLIM	Fluorescence Lifetime Imaging Microscopy
FLS2	FLAGELLIN-SENSING 2

FP	Fluorescent Protein
FRET	Förster (Fluorescence) Resonance Energy Transfer
F2	FLAGELLIN-SENSING 2
GFP	Green Fluorescent Protein
GN	GNOM
ICS	Image Correlation Spectroscopy
Ki	Kinase
L*er*	Landsberg *erecta*
L0	Linker0 (0 aa)
L1	Linker1 (5 aa)
L2	Linker2 (10 aa)
L3	Linker3 (26 aa)
LRR	Leucin-Rich-Repeat
mC	monomericCherry
MFIS	Multi-parameter Fluorescence Imaging Spectroscopy
mTq	monomericTurquoise
ns	nanosecond(s)
OC	Organizing Center
PM	Plasmemembrane
ps	picoseconds(s)
RLK	Receptor-Like Kinase
RPK2	LRR-RLK RECEPTOR-LIKE PROTEIN KINASE2
SAM	Shoot Apical Meristem
St.Dev.	Standard Deviation
TMD	Transmembrane Domain
Ven	Venus
W	WUSCHEL
WOX5	WUSCHEL-RELATED HOMEOBOX 5
WUS	WUSCHEL
YFP	Yellow Fluorescent Protein

2. Plasmid Maps

A)

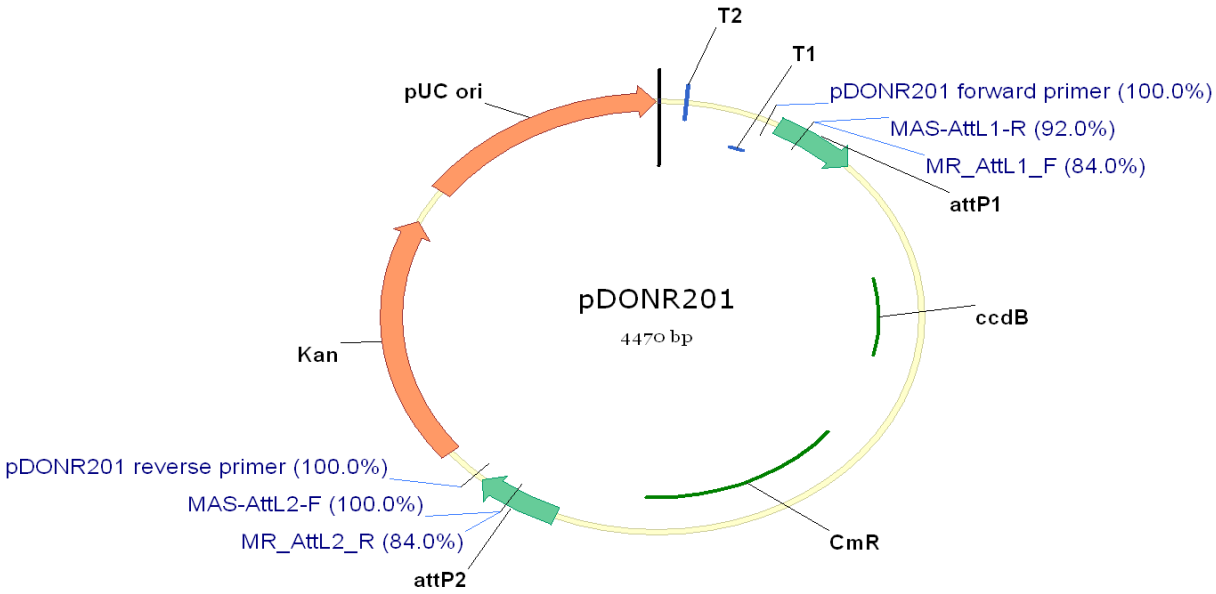

B)

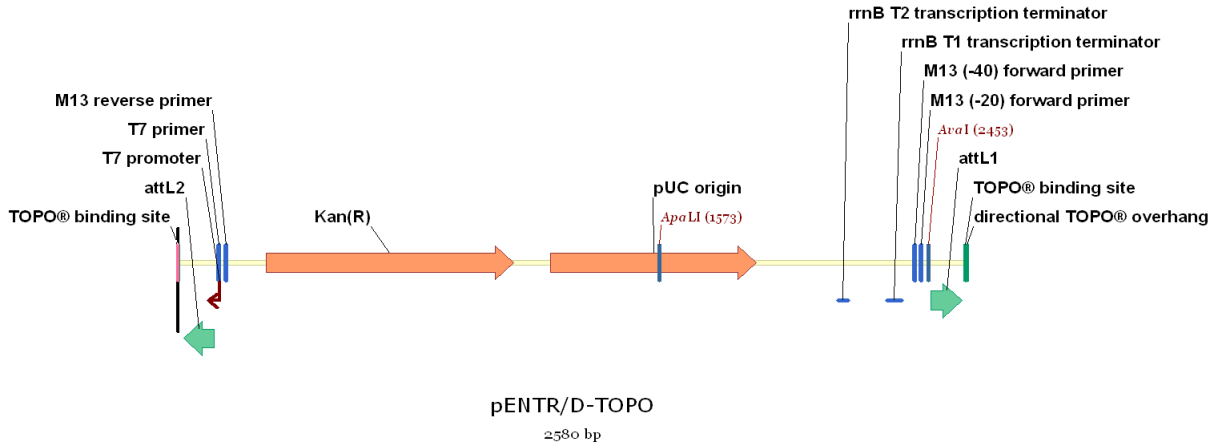

Plasmid Maps of the used Entry-Vectors

A) pDONR201: Gateway BP-Reaction Entry-Clone. attP1 and attP2 are the gateway recombination sites. ccdB is the Cytotoxic protein LynB coding region for bacterial selection. CmR is the chloramphenicole resistance gene. Kan is the kanamycin resistance gene. pUC ori is the replication starting point. T1 and T2 are transcriptional terminators.

B) pENTR/D-TOPO: Topo-Gateway Entry-Clone. attL1 and attL2 are the gateway recombination sites. TOPO binding site & directional TOPO overhang mark the site of gene insertion. T7 promoter drives the expression of the kanamycin resistance gene. Kan is the kanamycin resistance gene. pUC ori is the replication starting point. T1 and T2 are transcriptional terminators.

C)

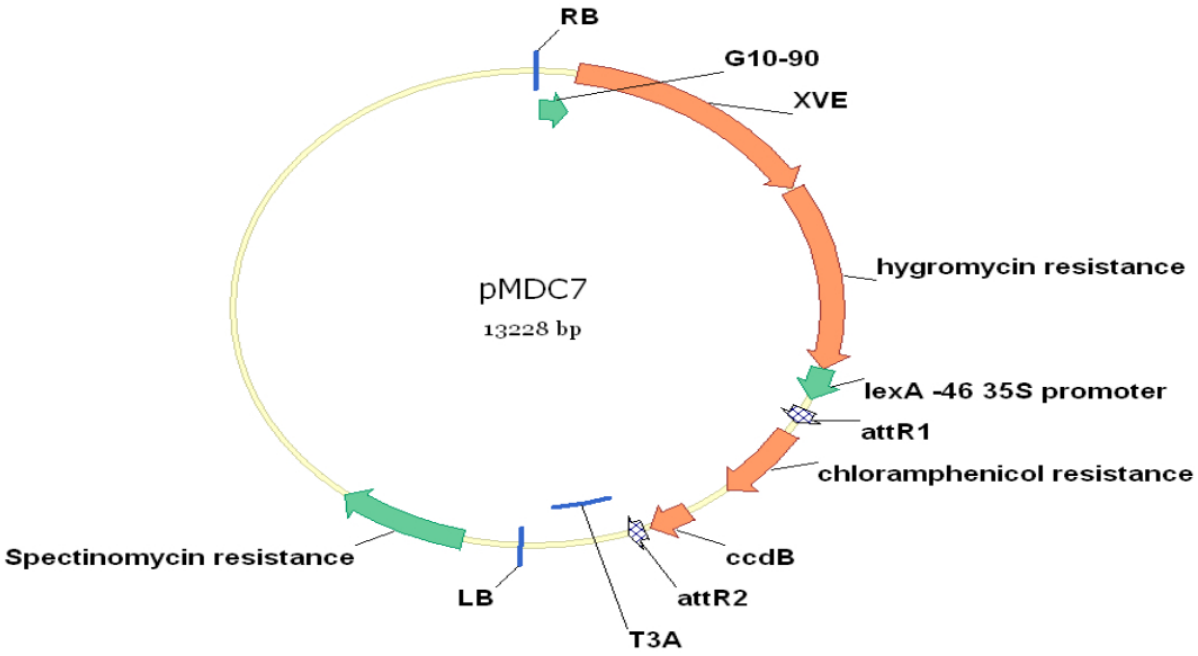
RB
G10-90
XVE
hygromycin resistance
pMDC7
13228 bp
lexA -46 35S promoter
attR1
chloramphenicol resistance
ccdB
attR2
T3A
LB
Spectinomycin resistance

D)

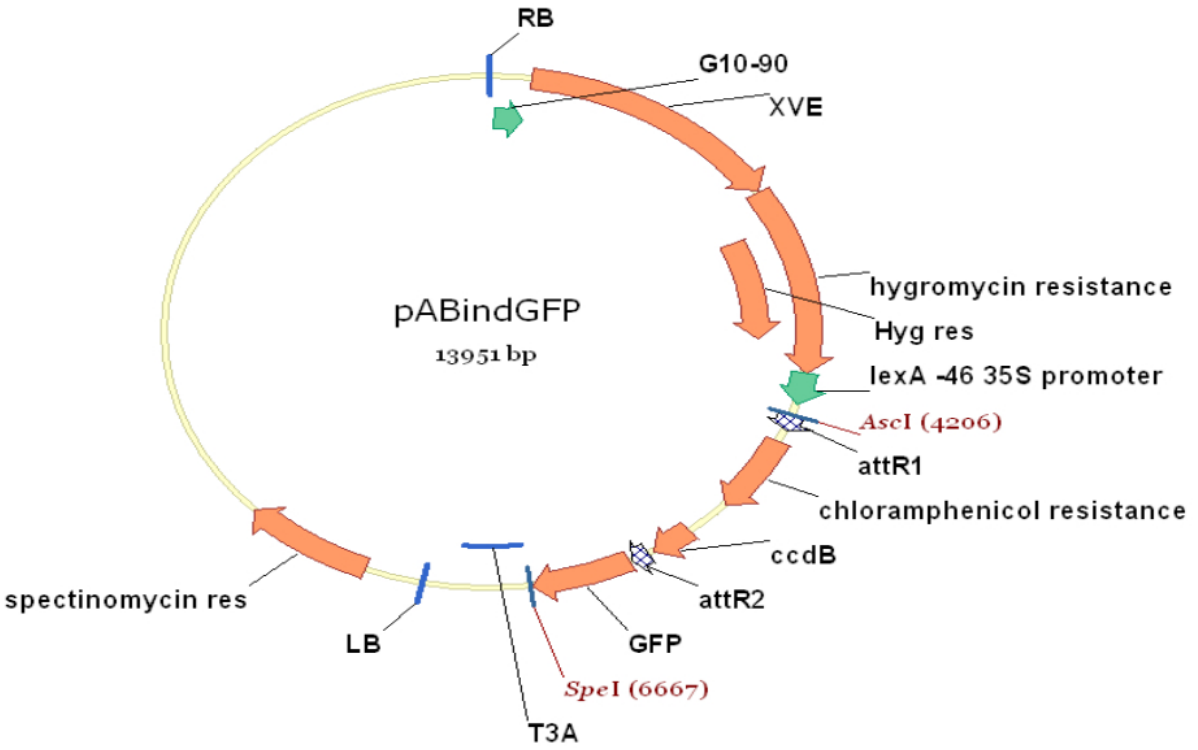
RB
G10-90
XVE
hygromycin resistance
Hyg res
pABindGFP
13951 bp
lexA -46 35S promoter
AscI (4206)
attR1
chloramphenicol resistance
ccdB
attR2
GFP
SpeI (6667)
T3A
LB
spectinomycin res

E)

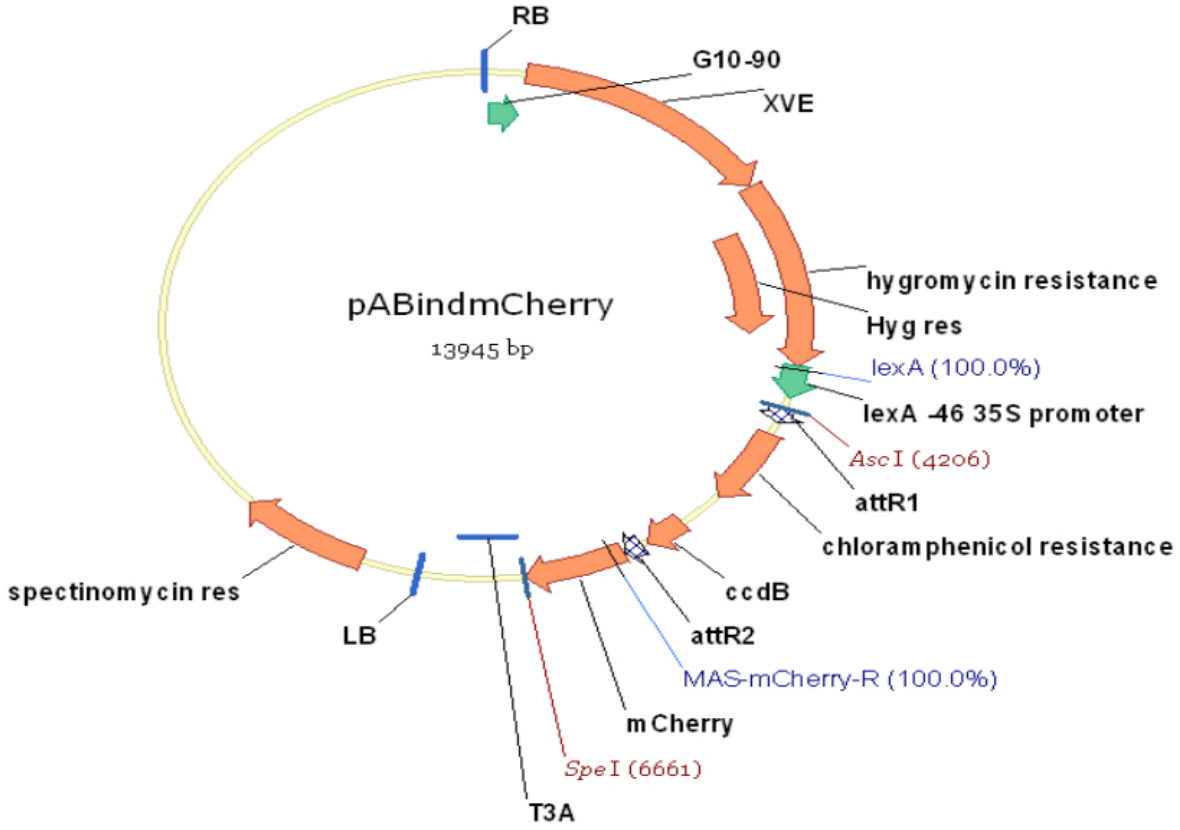
RB
G10-90
XVE
hygromycin resistance
Hyg res
pABindmCherry
13945 bp
lexA (100.0%)
lexA -46 35S promoter
AscI (4206)
attR1
chloramphenicol resistance
spectinomycin res
ccdB
LB
attR2
MAS-mCherry-R (100.0%)
mCherry
SpeI (6661)
T3A

F)

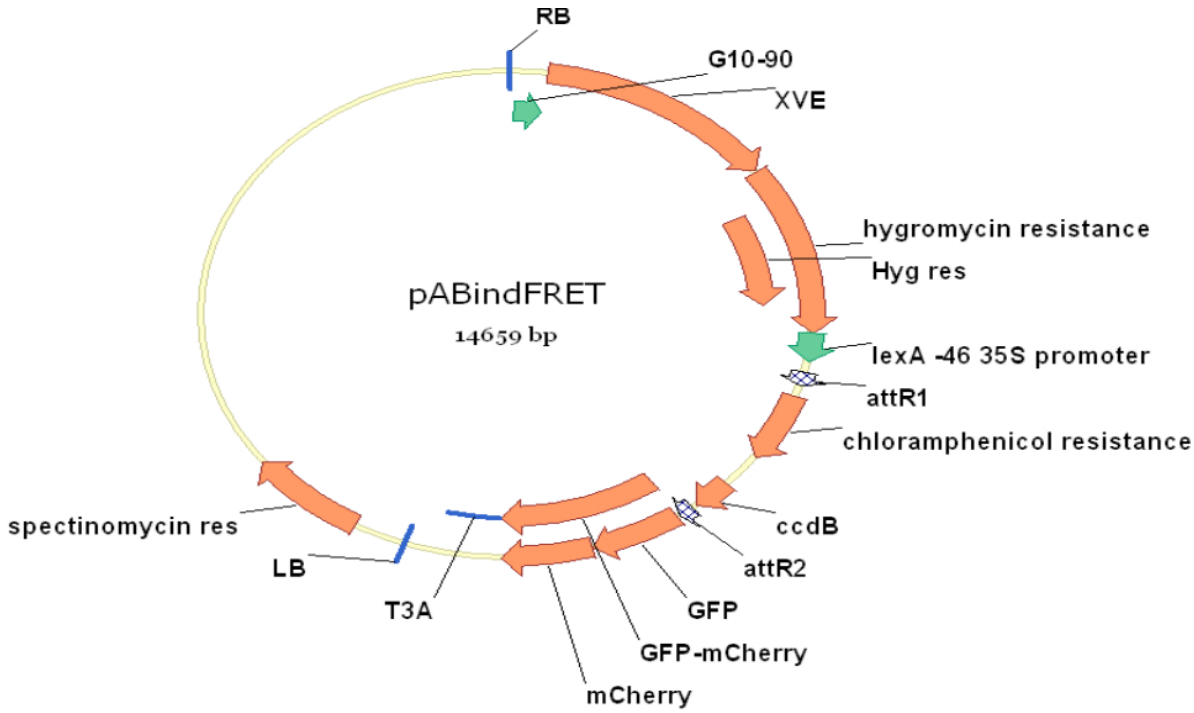
RB
G10-90
XVE
hygromycin resistance
Hyg res
pABindFRET
14659 bp
lexA -46 35S promoter
attR1
chloramphenicol resistance
spectinomycin res
ccdB
LB
attR2
T3A
GFP
GFP-mCherry
mCherry

G)

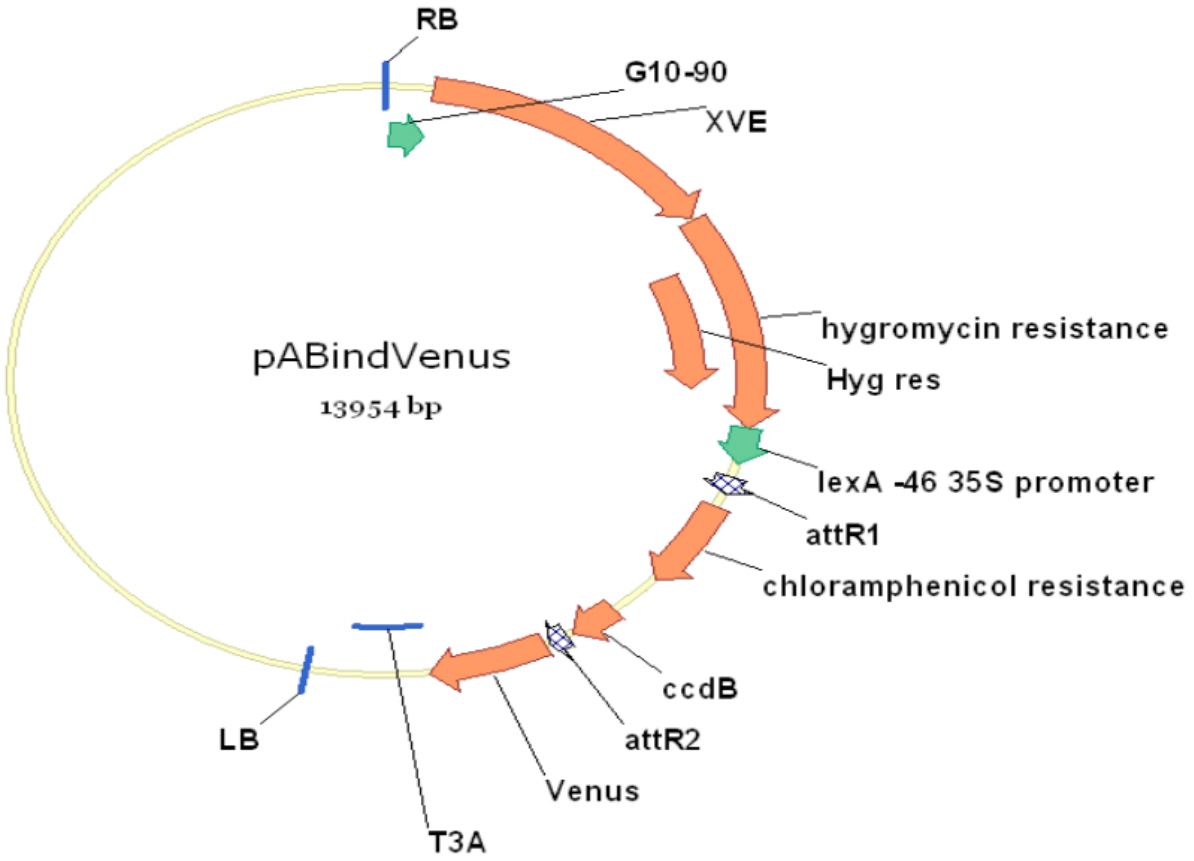
RB
G10-90
XVE
hygromycin resistance
Hyg res
pABindVenus
13954 bp
lexA -46 35S promoter
attR1
chloramphenicol resistance
ccdB
attR2
LB
Venus
T3A

H)

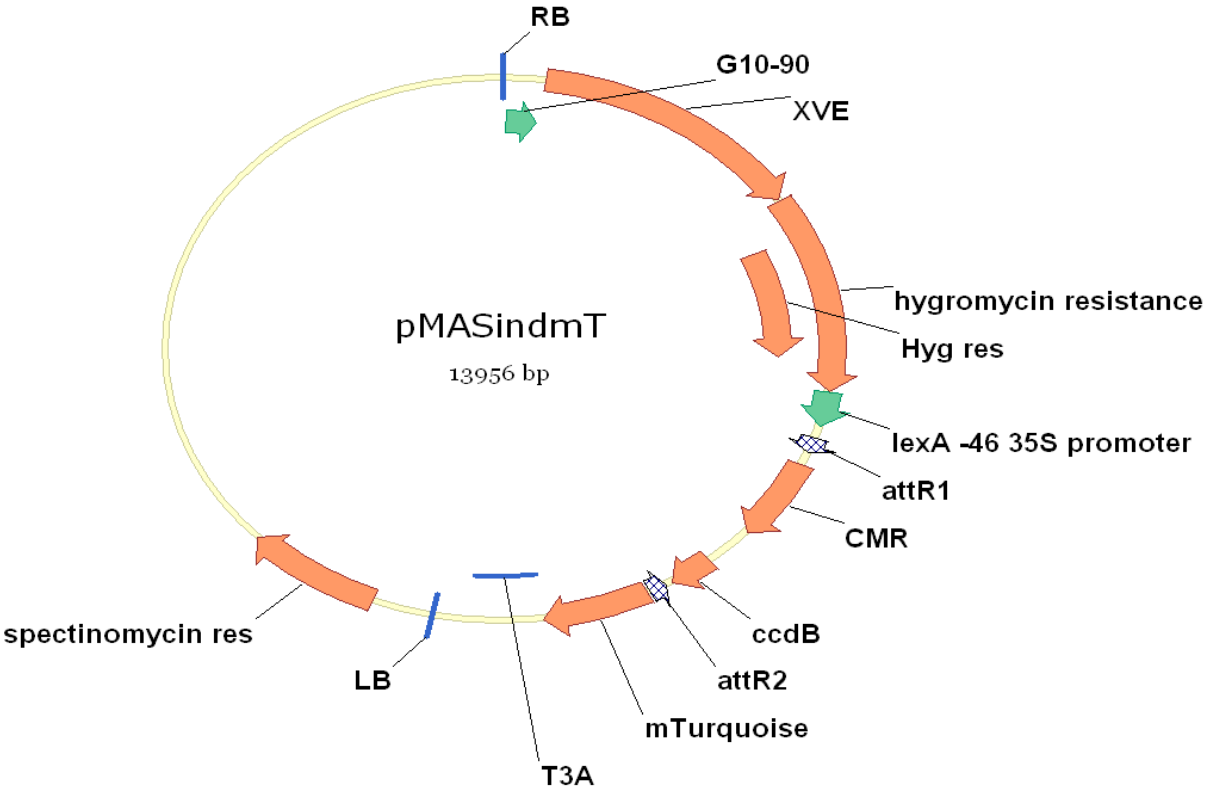
RB
G10-90
XVE
hygromycin resistance
Hyg res
pMASindmT
13956 bp
lexA -46 35S promoter
attR1
CMR
ccdB
attR2
mTurquoise
T3A
LB
spectinomycin res

I)

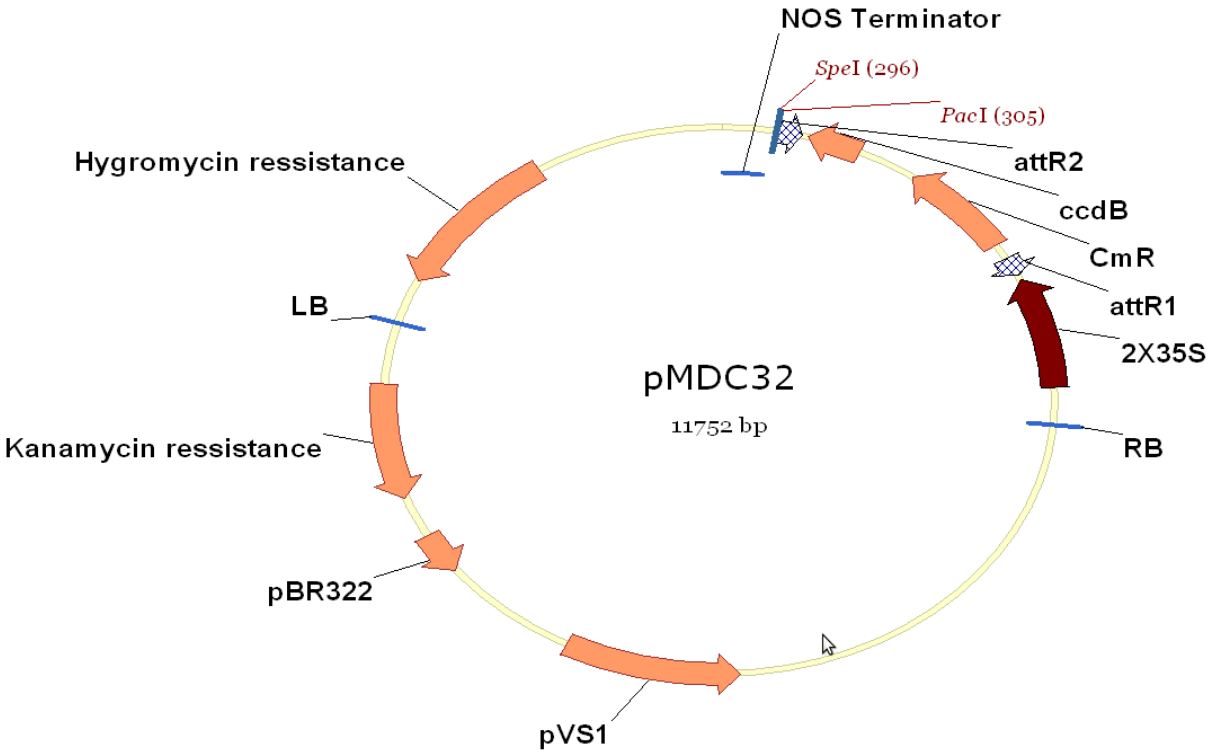
NOS Terminator
SpeI (296)
PacI (305)
attR2
ccdB
CmR
attR1
2X35S
RB
pMDC32
11752 bp
Hygromycin ressistance
LB
Kanamycin ressistance
pBR322
pVS1

J)

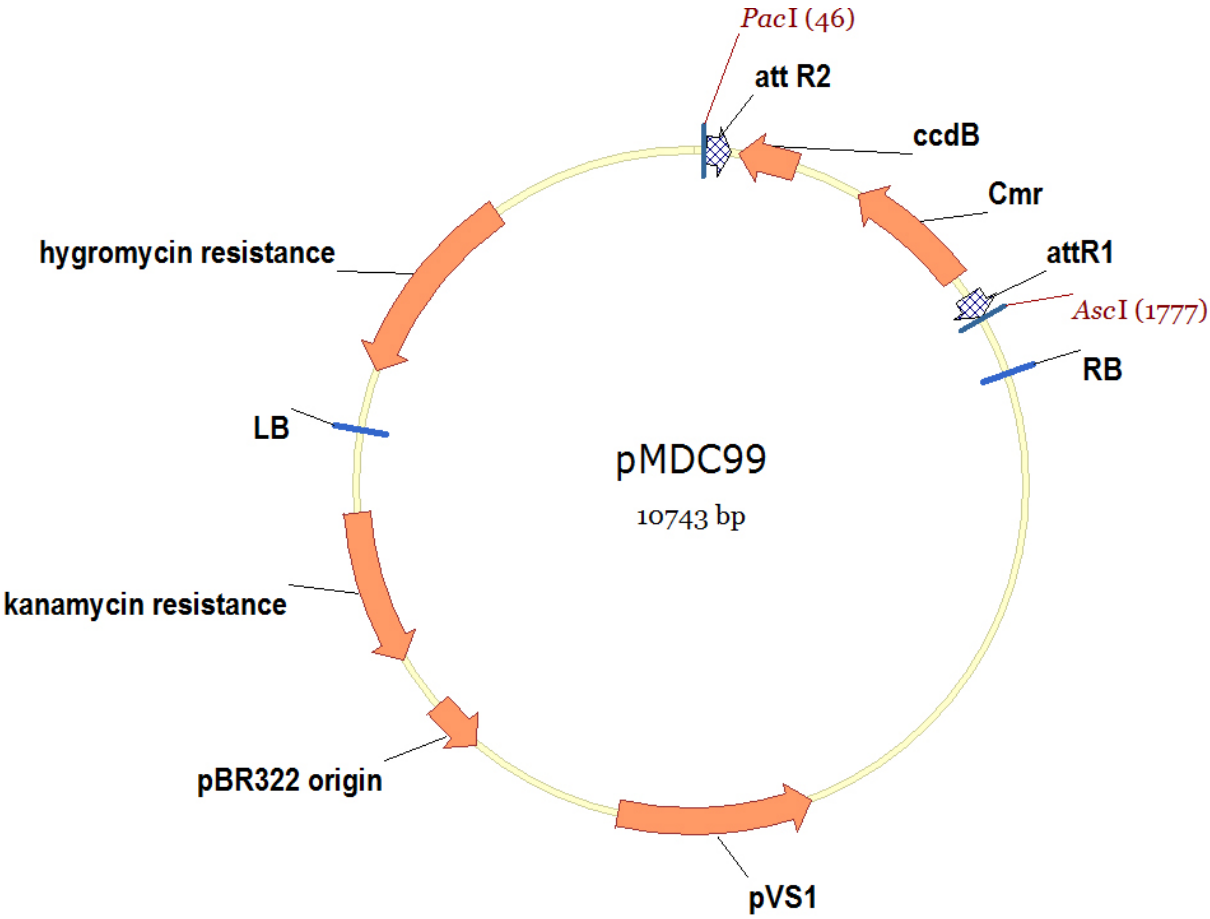
PacI (46)
att R2
ccdB
Cmr
attR1
AscI (1777)
RB
pMDC99
10743 bp
hygromycin resistance
LB
kanamycin resistance
pBR322 origin
pVS1

Plasmid Maps of the used Destination-Vectors

C) pMDC7: Gateway LR-Reaction Destination-Clone. RB & LB flank the region that will get integrated into the plant genome. G10-90 promoter drives the XVE gene. XVE: β-Estradiol inducible transcriptional activator for the lexA promoter. Hygromycin resistance gene confers resistance to hygromycin. lexA -46 35S Promotor is an XVE-inducible 35s promoter. attR1 and attR2 are the gateway recombination sites. ccdB is the Cytotoxic protein LynB coding region for bacterial selection. chloramphenicole resistance is the CmR gene and confers resistance to chloramphenicole gene. T3A is the transcriptional terminator. Spectinomycin resistance is the spectinomycin resistance gene.

D) pABindGFP: Gateway LR-Reaction Destination-Clone. Same as pMDC7, plus GFP is the GFP gene that will be fused to the gene of interest.

E) pABindmCh: Gateway LR-Reaction Destination-Clone. Same as pMDC7, plus mCherry is the mCherry gene that will be fused to the gene of interest.

F) pABindFRET: Gateway LR-Reaction Destination-Clone. Same as pMDC7, plus GFP-mCherry are the GFP and mCherry genes that will be fused to the gene of interest.

G) pABindVen: Gateway LR-Reaction Destination-Clone. Same as pMDC7, plus Venus is the Venus gene that will be fused to the gene of interest.

H) pMASindmT: Gateway LR-Reaction Destination-Clone. Same as pMDC7, plus mTurquoise is the mTurquoise gene that will be fused to the gene of interest.

I) pMDC32: Gateway LR-Reaction Destination-Clone. RB & LB flank the region that will get integrated into the plant genome. 2x35s are two 35s promoters that will drive expression of the inserted gene. attR1 and attR2 are the gateway recombination sites. ccdB is the Cytotoxic protein LynB coding region for bacterial selection. chloramphenicole resistance is the CmR gene and confers resistance to chloramphenicole gene. NOS Terminator is a transcriptional terminator. Hygromycin resistance gene confers resistance to hygromycin. Kanamycin resistance is the kanamycin resistance gene. pBR322 origin is the replication starting point. pVS1 is the minimal replicon for replication in gram negative bacteria.

J) pMDC99: Gateway LR-Reaction Destination-Clone. RB & LB flank the region that will get integrated into the plant genome. attR1 and attR2 are the gateway recombination sites. ccdB is the Cytotoxic protein LynB coding region for bacterial selection. chloramphenicole resistance is the CmR gene and confers resistance to chloramphenicole gene. Hygromycin resistance gene confers resistance to hygromycin. Kanamycin resistance is the kanamycin resistance gene. pBR322 origin is the replication starting point. pVS1 is the minimal replicon for replication in gram negative bacteria.

3. List of figures:

Chapter IV

Chapter V

Chapter VI

Chapter VII

4. List of tables:

XI. Acknowledgements

I would like to acknowledge all the people who contributed to this work in one way or another.

First off Prof. Dr. Rüdiger Simon for giving me the opportunity to work in his group, assigning these interesting topics to me and supporting me through all those years. It also helped a lot that I never had to fear running out of funding due to your promise that you will always have money for me until the very day of your retirement. I am quite happy though, that it didn't take me that long to finish this thesis.

Prof. Dr. Georg Groth for accepting to be my co-referee … again, following my diploma thesis many years ago.

Andrea for all the support as my supervisor during my early years in this group. This having a significant impact on my way of work. Also for the contributions to the work described in Chapters 1 and 2.

Steffi and Qijun for their significant contributions to everything having to do with microscopy. It is a pleasure to work with you, even when the work is frustrating. Very frustrating.

Carin for her significant contribution to the plant work described in Chapter 2.

Stephanie, Petra, Yvonne and Madlen for proof reading chapters of this thesis.

Moving on to the indirect contributions to this thesis by providing a positive and comforting environment at work every day.

René for all the good times in these last years and being one of the coolest and most funny people I have ever met.

Andrea and Nici for the good times in the early days and the friendship since then. And generally the people who were part of our group in these good old days, Marina, Vittoria, Luca – it is always nice to see you again after these years.

Yvonne for the support through all the years and all the breakfasts to discuss the state of the Union.

Stephanie for all the lunch breaks in the last years.

Jahan and Tobi for the Feierabendbeers.

Steffi and Qijun for all the fun I had talking to you. It made dealing with the problem that comes with our projects much easier.

Karine, Nadja, Petra, Gwen, Mareike, Adrian, Cansu, Jieny, Kim for your friendship during our time here.

Cornelia, Sylvia, Mehmet, Monika, Carin and Silke for ensuring that our lab is functioning, but mostly because I enjoyed being around you.

Madlen for being the perfect partner through these stressful times.

And finally, above all, my family. Foremost Mama and Papa for being the greatest parents.